Title
Identifying and characterizing genetic determinants of antibiotic sensitivity in Mycobacterium abscessus

Author
Rodriguez, Ronald

Publication Date
2022

Peer reviewed|Thesis/dissertation

Identifying and characterizing genetic determinants of antibiotic sensitivity in *Mycobacterium abscessus*

By

Ronald Rodriguez

A dissertation submitted in satisfaction of the

requirements for the degree of

Doctor of Philosophy

in

Microbiology

in the

Graduate Division

of the

University of California, Berkeley

Committee in Charge:

Professor Sarah Stanley, Chair
Professor Daniel Portnoy
Professor Arash Komeili
Professor Daniel Nomura

Fall 2022

Abstract

by

Ronald Rodriguez

Doctor of Philosophy in Microbiology

University of California, Berkeley

Professor Sarah Stanley, Chair

The work presented here focuses on identifying and characterizing genetic determinants of antibiotic sensitivity in *Mycobacterium abscessus* (*Mabs*), a non-tuberculosis mycobacterial pathogen responsible for various human infections that are notoriously difficult to treat with standard antibacterial therapy in clinical settings. Using bacterial genetics and high-throughput DNA sequencing methods, we have identified genes important for growth on amikacin and clarithromycin, two clinically relevant antibiotics used to treat *Mabs*, and ethionamide (ETH), a second-line drug currently used for treating multidrug-resistant tuberculosis infections. In chapters 1 and 2, I discuss the types of infections caused by *Mabs*, notable risk factors associated with *Mabs* infections, its epidemiology and transmission, and treatment options currently available. In chapter 3, I specifically focus on antibiotic treatment of *Mabs* infections and provide an overview on various antibiotic resistance mechanisms that are associated with treatment failure. In chapter 4, I present data that examines the antibacterial activity of ETH alone and in combination with clinically relevant antibiotics *in vitro* and *in vivo*. Furthermore, we present sequencing data on *MAB_2648c*, which encodes for a transcriptional repressor that confers ETH resistance. We demonstrate that Mab_2648c-dependent ETH resistance requires the activity of MmpSL5, a putative membrane transporter whose function remains unknown. In chapter 5, we attempt to identify the function of MmpSL5 and its potential substrates. In conclusion, we show that ETH is slightly bactericidal against *Mabs in vitro* and potentially *in vivo*, does not antagonize with clinically relevant antibiotics used to treat *Mabs* infections, and identified a biological mechanism that confers ETH resistance in *Mabs*. Future work should further examine the repurposing potential of ETH against *Mabs* and identify compounds that may reverse ETH resistance *in vitro* and *in vivo.*

Table of Contents

Acknowledgements

First, I would like to thank my parents Maria and Rafael Rodriguez for sacrificing their lives to provide, nourish, and take care of me while growing up in one of the most dangerous and impoverished neighborhoods of Brooklyn, New York during my childhood. My parents immigrated to New York City from Dominican Republic in the 1990s in search for a better quality of life. After they arrived, they immediately recognized that the education system in the United States is much more advanced and structured than what they experienced growing up in Dominican Republic. As a young kid growing up in the streets of Brownsville, my parents constantly encouraged me to go to school and find value in my educational experiences, as this was going to be the best way for me to escape my living circumstances in Brownsville and achieve financial success, and that hopefully I did not have to suffer in the same way they did while growing up in Dominican Republic. My parents told me that they would do it all over again, if necessary - to make those sacrifices again so that I could be in the position that I am currently in, and I love them for that. I would certainly not be here today without the support and sacrifices of my parents. Also, thank you to my sister and my extended family for your words of encouragement and support throughout the years.

My journey to graduate school and into science was far from a linear path, as I was never an exceptional student and I never enjoyed science during middle school and high school. I was known for being an immature student that ran around in the hallways, cracked jokes, and occasionally got into fist fights with the wrong people. I would also hangout with gang affiliates afterschool to engage in street fights, steal from convenience stores, and vandalize housing properties. When I started college, I no longer wanted to indulge in such activities, especially when I realized that hanging out with the wrong crowd of people would not allow me to advance in life, and possibly keep me in Brownsville. This represented the exact opposite of the lifestyle my parents would have wanted for me and stands against their values and beliefs as parents and educational supporters. I decided to pursue a career in science late into my college career, which helped me escape this lifestyle. Going to school in mid-town Manhattan and exploring Central Park while working in a research lab where I got a clear view of the Hudson River through one lab window, and all the bright lights of Time Square through another window became part of a recipe for success.

Participating in scientific lab research became a place of a refuge and made it easier to leave behind my immature, or rather foolish, childhood lifestyle. Despite feeling like I was a late bloomer to science relative to my peers, I was excited to do research for the first time. It presented a great opportunity for personal growth, maturity, and independence. I did not worry much about what was going on in Brownsville because I spent so much time doing research. Most of the time I would spend at home was only to eat, sleep, and shower. I felt as if I was turning over a new leaf that was going to blossom into something greater, something that I would have never imagined, something like pursuing a doctoral degree.

I would like to thank Jason Rauceo, my former undergraduate research advisor, for treating me like a graduate student since the day I began to work in your lab. Dr. Rauceo, a black scientist who also grew up in Brooklyn, trained me to be a good writer, a good presenter, encouraged me to peruse the scientific literature whenever necessary, and to always include the necessary controls in my experiments. He also taught me how to be meticulous and rigorous at scientific research. I am very proud that I was able to bring these skills into graduate school. I never knew what it was like to be heavily micromanaged as an undergraduate researcher because that opportunity was never available to me. The level of reading that was expected of me as a graduate student was no different than what was expected of me as an undergraduate researcher. I believe that I would not be here today without Dr. Rauceo's mentorship. Hopefully we can get more people that look like us and come from underprivileged backgrounds into science.

I would like to thank Mecky Pohlschroder, another former research advisor, for providing me with an opportunity to obtain more research experience and broaden my scientific skill set at the University of Pennsylvania. Before I started my PhD at UC Berkeley, Mecky told me that "being smart in science is not enough to get through graduate school, but that you also have be resilient and know how to persevere". After being a doctoral student for five and a half years, I can certainty say that you were right Mecky. This is one of the best words of advice that I have ever received in my science career. I learned to develop these qualities throughout graduate school, and it has greatly helped me survive many failed moments as a researcher. These experiences taught me that it is okay to fail in science and that all scientists should encounter failed experiences. Failed experiments, not the successful ones, present the best opportunities to be better as a researcher. Successful experiments will certainly provide us with the data that we so desperately crave, but more data acquisition does not always necessarily correlate to being a better scientist, or a better learning experience. I can go 6 months without acquiring data and it won't break me down or affect my confidence if I am learning new things during this time. I fear nothing, as I have learned to accept and embrace all challenges associated with being a research scientist. This perspective greatly helped me get through my graduate studies.

I would like to give many thanks to Sarah Stanley, my graduate research advisor, who figured out how to deal with me for so many years. Initially, I was a bit hesitant to join the lab, because although I was always interested in working with bacterial pathogens, I displayed less of an interest in doing mammalian research. I chose to join because I felt confident that you would provide me with high quality, effective mentoring that I was seeking as an early graduate student. In some ways, I feel like I sacrificed my scientific interests for the greater good of mentoring as a graduate student. Many graduate students choose labs solely based on scientific interests and I do not think this is always the best approach, as many graduate students need mentoring to be successful. I have been so satisfied and grateful all these years for the level of dedication that you have displayed in mentoring students. You put so much time and effort into mentoring me as a graduate student and I never took it for granted. I certainly would not be here without it.

Thank you so much for being there for me when experiments worked and when they didn't work. Thank you so much for being so patient with me, for being a great listener, for supporting my graduate needs, and for viewing me as more than just a scientist. Thank you much for being the wonderful person that you are and never judging my needs or my personality. You are so likeable and admirable. You deserve so much credit for my graduate success. I hope we can stay in touch beyond graduate school.

Lastly, I would like to thank many other people that have supported and helped me reach this point in my science career. I can list the names of everyone, but that might be equivalent to the length of this dissertation. Thank you to current and former members of the Stanley Lab that have greatly assisted me in my graduate research in many ways. Thank you to my thesis committee for meaningful conversations, providing valuable research and career advice. Adapting to the culture and lifestyle of the Bay Area during my graduate career, particularly in Berkeley, was a difficult challenge, so I would like to thank those that helped make graduate life a bit more adaptable and comfortable. These include faculty at Berkeley, friends in the PMB department, friends in other graduate departments, and friends that I met in other parts of the Bay Area. I would also like to thank mental health advocates and supporters that have helped me cope with social anxiety, depression, and loneliness. You all know who you are. I would like to give a big shoutout to my lifelong friends back home along the east coast, with whom I have kept in regular contact with all these years using gaming platforms, discord, and zoom. Your conversations and virtual company have gotten me through some tough times as a graduate student. You all know who you are.

I love you all.

I hope you enjoy reading this dissertation.

Peace out.

Chapter 1. Clinical significance, prevalence, epidemiology, and transmission of *Mycobacterium abscessus* (*Mabs*)

Clinical Significance, Prevalence, and Epidemiology of Mabs

Mycobacterium abscessus (*Mabs*) is an emerging bacterial pathogen associated with non-tuberculosis mycobacteria (NTM), a group of more than 200 mycobacterial species that exclude *Mycobacterium tuberculosis* (*Mtb*) and *Mycobacterium leprae*, the causative agents of tuberculosis and leprosy, respectively (1). *Mabs* naturally occupies diverse habitats, many of which include soil, aquatic environments, municipal water systems, fomites, and surgical equipment in hospital settings (2). Environmental acquisition of *Mabs* into a human host can result in a wide variety of infections, ranging from pulmonary to soft and skin tissue infections (SSTIs) (3). In rare cases, *Mabs* may also cause bacteremia and cerebral infections (4, 5). Pulmonary infections are the most common type of infections caused by *Mabs*, representing 82% of pulmonary infections caused by rapidly growing NTM species (6). Individuals suffering from bronchiectasis, chronic obstructive pulmonary disorder (COPD), prior tuberculosis infection, and cystic fibrosis (CF) are at high risk of establishing long-term infections following pulmonary exposure of *Mabs* (7, 8).

In the United States (U.S), *Mabs* represents 2.6 – 13% of all NTM infections with an estimated disease prevalence of 1.8/100,000 individuals, which is second after the *Mycobacterium avium* complex (MAC) (7, 9). Most *Mabs* infections are found in the southeast region of the U.S (3, 10, 11). The prevalence of *Mabs* infections in the U.S is likely much higher than what is currently being reported since many states are not required to report NTM infections and current diagnostics are limited in detecting *Mabs* infections (12, 13). Pulmonary *Mabs* infections often display radiographic and structural features that resemble those found in *Mtb* infections, which may further contribute to underestimated disease prevalence (14–17).

In the past decade, *Mabs* infections has been found in other parts the world, largely in the context of the cystic fibrosis (CF) population (18). CF is a hereditary condition commonly found in infants that is characterized by a defective cystic fibrosis transmembrane conductance regulator (*CFTR*) gene, resulting in a loss of chloride transport across epithelial cell membranes (19). The inability to conduct chloride transport results in an accumulation of respiratory mucus that serves as a nutritional source for many opportunistic pathogens, some of which include, but are not limited to, *Pseudomonas aeruginosa*, *Staphylococcus aureus*, MAC, and *Mabs* (18, 20).

CF represents a unique risk factor for the acquisition of *Mabs* infections, as *CTFR* plays a specific role during *Mabs* infection, but not in the context of other mycobacterial infections (18). Loss of *CFTR* leads to a reduction in neutrophilic chemotaxis, reduced intracellular production of reactive oxygen species (ROS), and macrophage killing (18). This lack of innate immunity ultimately results in an expansion of extracellular bacteria and disease progression, which largely explains the susceptibility of the CF population to

long-term pulmonary infection (18). Pulmonary *Mabs* infections among the CF population were first observed in the United Kingdom (U.K), where *Mabs* is the most common pathogen causing NTM infections, representing 51.4% and 35.3% of all NTM cases in England during 2014 and 2015, respectively (21, 22). Whole genome sequencing (WGS) of *Mabs* isolates collected from several U.K CF clinics identified bacterial clones with a high degree of genomic similarity, identified as clones sharing less than 20 single nucleotide polymorphisms (SNPs) (23, 24). These clones, termed dominant circulating clones (DCCs), have been found outside of the U.K and in other parts of the world, including Asia, South America, and Australia (25–27). The appearance of DCCs in different geographical regions has introduced controversy regarding the mechanism by which *Mabs* is acquired and transmitted (2).

Potential Modes of Mabs Transmission

While *Mabs* infections were initially thought to be acquired from environmental sources, the appearance of DCCs have introduced direct and/or indirect person-to-person transmission as an alternative, or potentially dominant mode of *Mabs* acquisition (23). DCCs initially identified among *Mabs* isolates circulating in CF populations have been found in Japan and Taiwan, where CF is rare among pulmonary *Mabs* infections, supporting the potential for person-to-person transmission (25, 28). Identifying the predominant mode of *Mabs* transmission in a particular geographical region has been challenging for several reasons. Although many studies have collected, analyzed, and compared whole genome sequences of *Mabs* isolates, very few have been able to establish the appropriate epidemiological and contact links to conclusively state that person-to-person transmission is occurring within a geographical region (29). In Germany, genomic sequences of *Mabs* isolates obtained from different CF patients were significantly more diverse than those obtained from the same patient, suggesting that person-to-person transmission in unlikely within this cohort (30). In *Mabs* isolates found throughout Asia, genomic diversity among non-CF isolates is much broader than what has been observed in CF populations, which also does not support person-to-person transmission as the exposure route, but possibly environmental (29). However, environmental sampling of *Mabs* near clinical settings where these infections have been found remain limited, making it difficult to conclude that environmental exposure of *Mabs* is the only or predominant source of transmission (31, 32). A case study in Australia was able to establish a genetic association between *Mabs* in clinical settings and those found in nearby environments, suggesting that environmental transmission is likely, although the directionally of potential transmission was not confirmed (27, 33). It is possible that *Mabs* exposure is due to a combination of environmental and patient exposure, but this may largely depend on the geographical region, genomic potential for transmission, and patient status (CF vs non-CF) (25, 30). Future case studies that equally address these distinct factors should provide a clearer picture for the predominant mode of transmission. Furthermore, this information will hopefully be critical in determining whether transmission is representative of all clinical isolates worldwide or whether it is geography specific.

Chapter 2. Treatment of *Mabs* infections: Current therapeutics and potential alternative approaches

Antibiotic Treatment of Mabs Infections

Treatment of *Mabs* infections involves combinatorial antibiotic therapy for a minimum of 12 months, which is only successful in approximately 30 – 50% of clinical cases primarily due to patient intolerance and antibiotic resistance (34). *Mabs* is resistant to most clinically relevant antibiotics, including most anti-mycobacterial agents that are used for tuberculosis treatment (35). The antibiotic resistance profile of *Mabs* is unique in that the bacteria can acquire resistance to clinically relevant drugs while also displaying innate resistance (36, 37). This extraordinary level of drug resistance greatly contributes to treatment failure and arguably makes *Mabs* one of the most dangerous multidrug-resistant pathogens encountered in clinical settings, deeming *Mabs* "an antibiotic nightmare" (37, 38).

While there is currently no standard drug-regimen used to treat *Mabs* infections, the American Thoracic Society (ATS), British Thoracic Society (BTS), and the Infectious Disease Society of America (IDSA) have recommended guidelines on what antibiotics should be prescribed for treatment (39, 40). Patient-specific drug formulations and durations will largely depend on culture conversions, antibacterial susceptibility testing of collected isolates during treatment, and patient tolerance to specific antibiotics (41–43). General recommendation guidelines include an initial treatment phase of intravenous antibiotics for a minimum of four weeks: amikacin (aminoglycoside), tigecycline (tetracycline), and imipenem (beta-lactam) in combination with either oral clarithromycin or azithromycin (macrolides) (39, 40). A continuation phase of treatment consisting of nebulized amikacin, either clarithromycin or azithromycin, and one to three additional antibiotics is then recommended. Additional antibiotics may include linezolid (oxazolidinone), clofazimine (anti-mycobacterial), minocycline (tetracycline), co-trimoxazole (anti-folate), and moxifloxacin (fluoroquinolone) (39, 40). Antimicrobial susceptibility testing is always recommended before antibiotic administration (39, 40). The goal of antibiotic treatment is to maintain negative culture conversion for a minimum of 12 months (39, 40, 42). However, this goal is rarely met (36.1% negative culture conversion rate), primarily due to drug resistance and host toxicity (44, 45). When antibiotic treatment fails, alternative therapeutic approaches must be considered (46).

Adjuvant surgery, surgical resection, and lung transplantation

Adjuvant surgery of infected sites together with combinatorial therapy may be available to patients who demonstrate relapse, drug resistance, and persistent sputum positivity (45). In the context of long-term pulmonary infections, lung transplantation is available, although this approach should be performed with caution (45, 47). It is recommended that culture negativity is achieved with confidence before lung transplantation is performed due to the possible of bacterial transmission taking place during these procedures (45). Depending on the severity of the infection, pulmonary *Mabs* infections may sometimes serve as a contraindication to lung transplantation (45, 47). Administration of

immunosuppressive drugs such as cyclosporine, sirolimus, and tacrolimus following transplantation is important to minimize allograft rejection (45, 48). However, this is often problematic, as some antibiotics that are commonly used to treat *Mabs* infections, specifically clarithromycin and azithromycin, are known to exhibit negative drug interactions with these immunosuppressive agents, which may increase allograft rejection (48). Attempting to increase the level of immunosuppression is an option, although this may not always be ideal, as immunosuppression alone is one of the major risk factors associated with long-term, disseminated *Mabs* infections (7). Transplant complications can be detrimental for the host, primarily due to disseminated *Mabs* infections and increased susceptibility to non-NTM bacterial infections, caused by pathogens such as *Pseudomonas aeruginosa*, *Aspergillus* species, and *Stenotrophomonas maltophilia* (49–52). Disseminated *Mabs* infections are very common in those infected with *Mabs* post-transplantation, causing SSTI infections (52–54). In these cases, surgical resection of the infected site is available in addition to combinatorial drug therapy (55).

Phage therapy

The use of lytic mycobacteriophages (phages), which are bacterial viruses that specifically infect mycobacteria, has received considerable attention for treating different types of *Mabs* infections (46, 56). Several case studies have demonstrated the clinical utility of using lytic phage cocktails for successfully treating pulmonary and disseminated *Mabs* infections (57–61). One case study involved the use of a three-phage cocktail for treating a 15-year-old CF patient who was suffering from a disseminated *Mabs* infection (61). Although the phage cocktail did not lead to complete bacterial clearance, clinical improvement was seen upon page administration (61). In another case study involving an 81-year-old individual suffering from non-CF associated bronchiectasis, macrolide resistant, pulmonary *Mabs* infection, treatment with the same phage cocktail decreased bacterial load in sputum samples over the treatment course but was ineffective long-term due to the patient generating antibody responses against the phages (60). Bacterial load was more effectively cleared using a nebulized phage-cocktail (59). Examining the utility of phages in a larger case study consisting of 17 *Mabs* clinical isolates demonstrated complete bacterial eradication in some infections (62). The use of phages in these combined studies are well-tolerated with minimal phage-resistance occurring (58–62). Phage therapy against *Mabs* infections provides several advantages, including providing personalized treatment, target specificity, and easy administration (46, 56). Furthermore, it has been observed that *Mabs* does not develop phage resistance to levels seen with other bacterial pathogens such as *P. aeruginosa* and *S. aureus*, suggesting that phage resistance may not be a major concern in the context of *Mabs* infections (58, 63, 64). However, the emergence of neutralizing antibodies, costs of phage formulations, and lack of clinical trials, currently impose limits on the progression and therapeutic success of phage therapy against *Mabs* and should be addressed in the future (46).

Host-targeted therapy

Targeting cellular pathways that boost the immune response to *Mabs* infection and/or inhibit the ability of the bacteria to proliferate intracellularly may represent an additional

avenue of research to generate novel, therapeutic strategies (46). While *Mabs* is primarily considered an extracellular pathogen, forming biofilms in CF patients, it is also capable of infecting innate immune cells like macrophages (65, 66). *CFTR* function negatively impacts innate immune cell function in a manner that remains largely unknown, although macrophages in the context of CF are thought to display excessive proinflammatory signaling (67, 68). Loss of *CFTR* function also results in uncontrolled *Mabs* proliferation (18). Therefore, therapeutic approaches that can boost innate immune cell function against *Mabs* in the CF population, should be highly encouraged, particularly in those who are immunocompromised (46, 69, 70). Many CF patients infected with *Mabs* are often administered CF modulators in addition to antibacterial therapy (58, 71, 72). Among the wide variety of CF modulators currently available for use in clinical settings (73), it remains unknown whether they display direct antibacterial activity against *Mabs* and/or may synergize with compounds that have been shown to improve immune function against *Mabs* and should be explored.

Previous work has identified compounds known to target multiple host-defense pathways that improve intracellular control of *Mabs* infections (46, 74–76). This is significant, as there is currently no vaccine available for treating *Mabs* infections, which limits the ability of host immune systems to control and clear these infections (46, 77). AR-12 is a celecoxib derivative known to upregulate autophagy pathways in the context of intracellular *Salmonella enterica* serovar Typhimurium and *Francisella tularensis* infections (78, 79). AR-12 exhibits bactericidal activity against *Mabs in vitro* and *in vivo* at concentrations that can be achieved therapeutically (74). More importantly, it is also active against intracellular *Mabs*, which is difficult to achieve with clinically relevant antibiotics targeting *Mabs* (74, 80). It will be interesting to determine if AR-12 can also directly influence the host-response to *Mabs* infection, making it possible to develop a "host-bacterium' dual therapy in the future.

The peroxisome proliferator-activated receptor α (PPARα) is important in controlling intracellular *Mabs* infections, as loss of PPARα in the context of *Mabs* leads to increased inflammation and lower macrophage antibacterial responses (75). PPARα has been well studied in the context of other infections, such as *P. aeruginosa* and *M. tuberculosis*, where it is required for controlling bacterial replication and excessive inflammatory responses (81, 82). Murine administration of gemfibrozil, a known PPARα agonist, improved *Mabs* clearance while lowering inflammatory responses (75, 83). The biological function of PPARα should be further evaluated for its therapeutic potential in controlling *Mabs* infections in future work.

The phagocytic ability of innate immune cells may also be used to generate dual host and bacterial-directed therapeutic approaches (84). Phagocytosis is an important innate immune mechanism that engulfs bacterial pathogens to clear and remove them from an infected host (85). Second lipid messengers are required for phagolysosome biogenesis and maturation (86, 87). The use of liposomes containing phosphatidylinositol 5-phosphate (PI5P) enhances the macrophage antibacterial response against *Mabs in vitro*

and *in vivo* by increasing phagosome acidification and ROS production (76). PI5P-containing liposomes synergized with amikacin against *Mabs* under these conditions (76). These findings may provide an avenue of therapeutic approaches aimed at simultaneous targeting of both extracellular and intracellular *Mabs*.

Drug development, repurposing, and repositioning

Developing novel drugs that display antibacterial activity against *Mabs* both *in vitro* and *in vivo* is highly desired, although this presents several challenges (88–92). Drug development is slow and costly, as it takes approximately 10-15 years of laboratory research and 0.8-2.5 billion dollars to introduce a potential drug candidate into a product that can be tested in clinical trials (93). Furthermore, the rate of drug resistance development far outpaces drug development efforts. Only 30-40 novel antibiotics are currently in clinical trials and over 75% of drugs in clinical development pipelines display novel mechanisms of action against drug-resistant bacterial pathogens (94–96). Unfortunately, the correlation between *in vitro* and *in vivo* activity of novel drug candidates is poor (97). Many of these challenges can be overcome by repurposing and repositioning of existing drug candidates (98, 99).

Drug repurposing refers to incorporating drugs that have been used in clinical settings and/or have been approved by the Food and Drug Administration (FDA) into novel drug regimens (98). Drug repositioning refers to chemical optimization of clinical and FDA approved drugs (99). These drugs have pharmacologically validated targets, which circumvents the high cost associated with developing new approval pipelines for drugs that do not have validated targets (93, 99). There are several examples of repurposed drug efforts in the context of *Mabs* infections (100). These drugs are active against *Mabs* *in vitro* and include bedaquiline (used in the treatment of multi-drug resistant *Mtb*), tedizolid (used in the treatment of bacterial skin infections), and avibactam (used in the treatment of urinary tract infections) (101–109). It remains to be determined if these drugs will be incorporated into regimens currently used for treating different types of *Mabs* infections.

Additional examples of drug repositioning efforts against *Mabs* include rifabutin (rifamycin class) and thiacetazone (anti-mycobacterial) (110–114). Rifabutin is associated with the rifamycin class of antibiotics that target the bacterial RNA polymerase (115, 116). Rifabutin is structurally similar to rifampicin, which exhibits low potency against *Mabs* (111, 117, 118). However, rifabutin, which lacks the hydroquinone group present in rifampicin, is much more active against *Mabs* (MICs: > 100 mg/L for rifampicin versus 6.3 mg/L for rifabutin) and synergizes with clinically relevant drugs currently used against *Mabs*, demonstrating repositioning potential (110, 111, 113, 119, 120). Thiacetazone, a mycolic acid inhibitor previously used to treat tuberculosis infections but has been discontinued due to host toxicity, exhibits low activity against *Mabs* (MIC: > 200 μg/ml) (114, 121–124). Derivatives of thiacetazone are more active than the parent compound (MIC: 3.1 μg/ml for the D15 derivative) in both non-CF and CF isolates of *Mabs* (114).

These data indicate that thiacetazone may provide novel drug candidates that can be used to target *Mabs* in clinical settings.

Large chemical libraries containing structurally diverse compounds have been screened against *Mabs* (125–127). Many of these compounds, which are known to target host pathways, display activity against *Mabs in vitro* (127). Future work should explore the *in vivo* activity of these candidates, potential toxicities, and whether they display any repurposing/repositioning potential.

Chapter 3. Resistance mechanisms associated with clinically relevant and non-clinically relevant antibiotics

The genome of *Mabs* contains genes encoding for antibiotic modifying and degrading enzymes, target modifying enzymes, and putative efflux pumps that are thought to confer intrinsic resistance (Fig. 3.1) (36, 128–130). *Mabs* is also capable of acquiring mutations in genes that confer high-level resistance to aminoglycosides and macrolides (Fig 3.1) (131, 132). While deletion of many of these genes alters antibiotic susceptibility, there are many other genes that may confer drug resistance, although the function of these genes remains unknown (129).

Amikacin

While *in vitro* susceptibility testing indicate that *Mabs* is sensitive to amikacin, resistance to amikacin is commonly observed in laboratory and clinical settings. Deletion of *eis2* (*MAB_4532*) confers sensitivity to amikacin (MICs: 2 μg/ml for WT *Mabs* compared to 0.25 μg/ml for Δ*eis2 Mabs*), suggesting that *eis2* is important for intrinsic resistance against amikacin (133). *eis2* (enhanced intracellular survival 2) encodes for an acetyltransferase that has been shown to modify various aminoglycoside antibiotics by transferring an acetyl moiety from acetyl coenzyme A to the amine group of an aminoglycoside, reducing the affinity of the chemically modified drug for the ribosome (134, 135). The crystal structure and biochemical function of Eis2 from *Mabs* is consistent with what has been observed with acetyltransferases in other biochemical systems, in which it can modify a wide variety of aminoglycoside antibiotics aside from amikacin (136). The genome of *Mabs* also encodes for *eis1* (*MAB_4124*), although unlike *eis2*, deletion of *eis1* does not enhance amikacin sensitivity (133). Whib7 (*MAB_3508c*) is a transcriptional factor that confers resistance to amikacin and other ribosome-targeting antibiotics, including macrolides (137). Exposure to amikacin induces transcriptional induction of *eis2* in a Whib7-dependent manner. Furthermore, deletion of *whib7* confers amikacin sensitivity (MICs: 8 μg/ml for WT *Mabs* compared to 2 μg/ml for Δ*whib7 Mabs*) (137). Finally, high-level amikacin resistance is typically associated with mutations in the 16S ribosomal RNA gene, *rrs* (*MAB_r5051*) (131). Mutations C1409T (MIC: 64 μg/ml), T1498A (MIC: 256 μg/ml), and A1408G (MIC: $>$256 μg/ml) within *rrs* have been observed in clinical isolates of *Mabs* exposed to amikacin (131).

To identify novel, genetic determinants of amikacin (AMK) sensitivity, we performed a genetic screen using a transposon library of *Mabs* exposed to amikacin (138). We identified transposon insertions in *MAB_2217* (*ssuB*), encoding the ATP-binding subunit of a sulfonate ABC transporter that resulted in AMK sensitivity (approximately 5-fold decrease in transposon reads) (Fig. 3.2 A-B). Sulfonate (SO^{3-}) is part of a larger family of ATP binding cassette (ABC) membrane proteins that transport sulfonate and sulfate esters (139). In mycobacteria, sulfate is essential for virulence, the biosynthesis of sulfur-containing amino acids (methionine and cysteine), redox homeostasis, and the generation of iron-sulfur (Fe-S) clusters (140–143). Whib7 contains a Fe-S cluster that is required for transcriptional activation of target genes (144). We hypothesized that in the

presence of amikacin, SsuB is required for transporting sulfate into cell, which is then used for Fe-S cluster production that ultimately activates Whib7 to promote growth on amikacin. Therefore, the absence of *ssuB* leads to amikacin sensitivity because Whib7 is nonfunctional. However, in contrast to our TnSeq data, clean deletion of *ssuB* did not lead to amikacin sensitivity in rich media or minimal media without sulfate supplementation (Fig. 3.2 C). The discrepancy for this remains unknown, although it is possible that loss of *ssuB* alters susceptibility to amikacin only when grown in competition with other transposon-insertion mutants (145).

Clarithromycin

Accurate assessment of clarithromycin susceptibility is critical for the outcome of drug treatment against *Mabs* infections (146). Taxonomically, *Mabs* is composed of three subspecies (*M. abscessus* subspecies *abscessus*, *M. abscessus* subspecies *massiliense*, and *M. abscessus* subspecies *bolletii*) (147, 148). Clarithromycin susceptibility differs among subspecies, in which *M. massiliens*e is more susceptible to clarithromycin compared to *Mabs*, as determined by the *erm41* (*MAB_2297*) locus, which encodes an erythromycin methylase that confers inducible resistance to clarithromycin (149, 150). It is predicted that Erm41 methylates adenine 2058 on the 23S rRNA gene (*rrl*, *MAB_r5052*), which reduces the affinity of the 23S rRNA for clarithromycin (129, 150, 151). *M. massiliense* contains a T28C sequevar in *erm41*, which produces a truncated form of *erm41* and therefore, is susceptible to clarithromycin (149). This sequevar is not present in *Mabs* and thus, *erm41* is fully functional (150). Like *Mabs*, *M. bolletii* also contains a fully functional *erm41* locus that confers clarithromycin resistance, although this is less concerning, as *M. bolletii* causes fewer infections compared to *Mabs* and *M. massiliense* (150, 152, 153).

Distinguishing between *Mabs* and *M. massiliense* in clinical settings is crucial, as this will dictate whether clarithromycin should be administered (150). In cases where infections associated with *M. massiliense* has been confirmed, clarithromycin should be administered, and is associated with improved treatment outcomes (41). However, in cases where *Mabs* is the subspecies detected, clarithromycin is associated with treatment failure, due to inducible and acquired drug resistance (41). Clarithromycin should be substituted with azithromycin in confirmed cases of *Mabs*, if possible (154). Fourteen days of clarithromycin exposure induces expression of *erm41* (inducible resistance) compared to azithromycin, which is a weaker inducer of *erm41* (154). In *Mabs* cases where clarithromycin susceptibility is observed upon initial infection, inducible resistance should always be examined after 14 days of drug treatment using clinical standards of susceptibility testing and measuring *erm41* expression levels (154).

Acquired resistance (MIC: > 512 μg/ml) to clarithromycin is commonly observed in clinical isolates of *Mabs*, which involves adenine to guanine mutations in the *rrl* sequence (A2058G or A2059G) (132). Whib7 confers cross-resistance to clarithromycin, as inhibitory clarithromycin exposure induces expression of *whib7* (137). Furthermore, Whib7 is required for transcriptional induction of *erm41* (137). These two drugs behave

antagonistically when used in combination and is thought to contribute to initial treatment failure (155).

Beta-lactams, tetracycline, doxycycline, and rifampicin

Aside from imipenem (carbapenem) and cefoxitin (second generation cephalosporin), *Mabs* is highly resistant to all other beta-lactam drugs, primarily due to a broad-spectrum beta-lactamase (*bla*, *MAB_2875*) that is capable of hydrolyzing various beta-lactam antibiotics (penicillins, monobactams, and penems sub-classes) (156). Deletion of *bla* confers sensitivity to many beta-lactams (106). Bla_Mab is also capable of hydrolyzing imipenem and cefoxitin, although the kinetics of hydrolysis is much slower compared to other beta-lactams (156). Beta-lactams irreversibly bind to transpeptidases, enzymes that catalyze the production of short peptides which ultimately become incorporated into the peptidoglycan (PG) layer (157). This binding inhibits the enzymatic activity of transpeptidases and consequently inhibits the production of PG (157). The PG layer of *Mabs* is primarily composed 3→3 L,D-transpeptides, catalyzed by L,D-transpeptidases (LDTs), which are preferentially targeted by carbapenems and cephalosporins (158, 159). Other subclasses of beta-lactams preferentially target D,D-transpeptidases (160, 161). The abundance of L,D-transpeptides in *Mabs* may explain why they are resistant to most beta-lactams. Other potential mechanisms of beta-lactam resistance in *Mabs* include low cell wall permeability and cell wall porins (37, 162, 163). Despite this extraordinary level of beta-lactam resistance, beta-lactamase inhibitors are active against *Mabs*. Avibactam, a non-beta lactam, beta-lactamase inhibitor, synergizes with many beta-lactams against *Mabs* and is currently being further evaluated for its repurposing potential (105–107, 164).

Mabs possesses TetX (*MAB_1496c*), a tetracycline-modifying monooxygenase that catalyzes the mono-oxidation of tetracycline and doxycycline, but not tigecycline, rendering these antibiotics inactive (165). Deletion of *tetX* confers sensitivity to tetracycline and doxycycline (~ 20 fold-greater sensitivity) (165). Tetracycline exposure induces expression of *tetX* through the direct binding of tetracycline to a transcriptional repressor (Mab_1497), which alleviates transcriptional repression of *tetX* (165). This transcriptional activation occurs in a Whib7-dependent manner (137, 165).

An additional example of antibiotic modification in *Mabs* has been demonstrated in rifampicin, a member of the rifamycin class of drugs that target RNA polymerase, thereby inhibiting transcription (115, 116). In *Mtb*, the acquisition of mutations (Ser531Leu) in the *rpoB* subunit of RNA polymerase confer resistance to rifampicin (166, 167). These mutations are not present in *Mabs*, suggesting that other mechanisms of resistance are present (168). It is speculated that *Mabs* inactivates rifampicin through ADP-ribosylation using Arr_Mab (*arr*, *MAB_0591*), which encodes for an ADP-ribosyl transferase (129, 130, 169). ADP-ribosylation is a chemical modification involving the addition of an ADP-ribose group to another chemical moiety and is associated with diverse cellular processes (169). In *Mabs*, deletion of *arr* confers sensitivity to rifampicin (MICs: 128 μg/ml for WT *Mabs* and 0.25 μg/ml for Δ*arr Mabs*) and other members of the rifamycin class, including rifapentine and rifaximin (168).

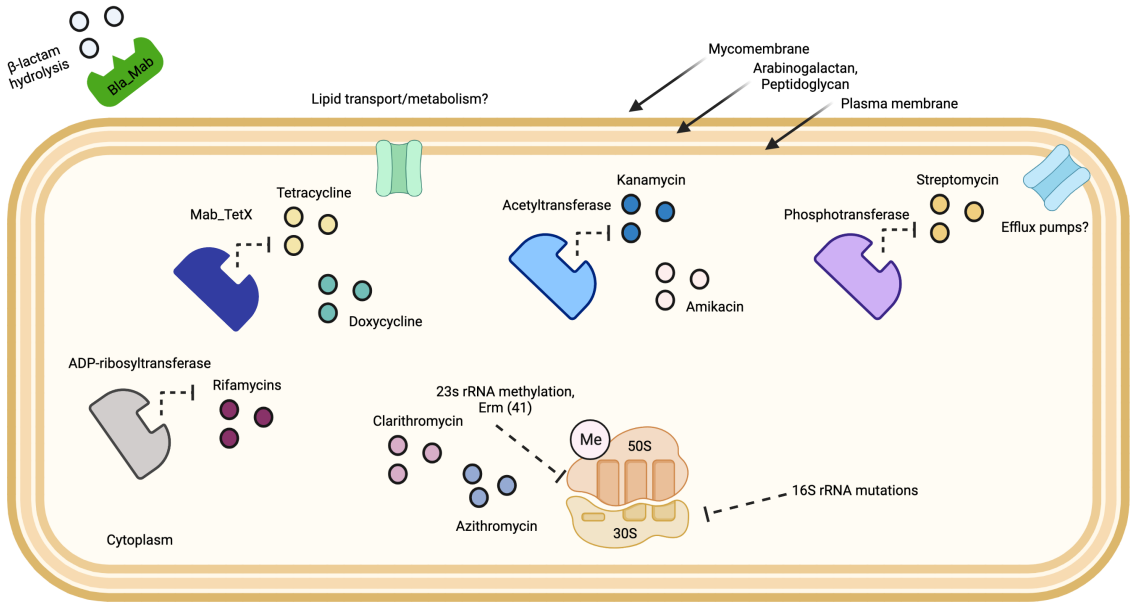

Figure 3.1. Intrinsic and acquired mechanisms of antibiotic resistance in *Mabs*.

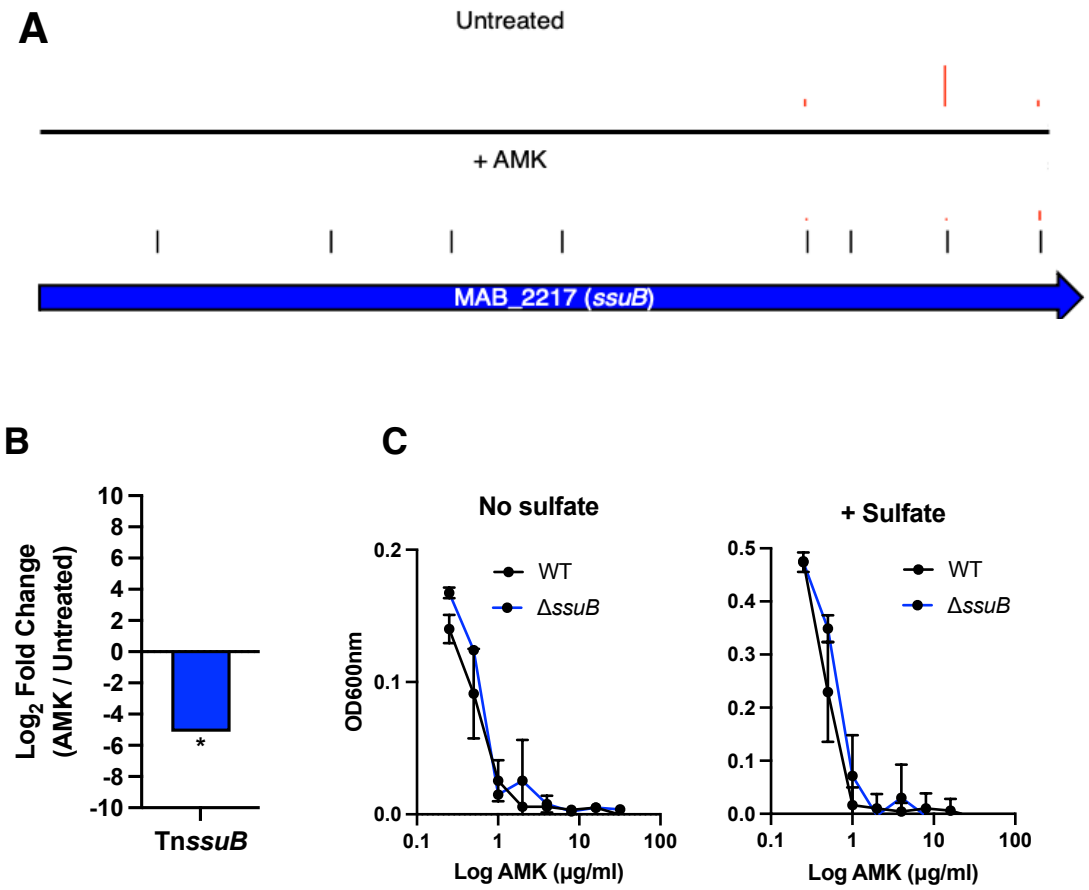

Figure 3.2. SsuB is not required for AMK resistance. (A) Transposon read densities (red lines) in *MAB_2217* (*ssuB*) with and without AMK treatment (8 μg/ml). Black lines represent all possible insertion sites (B) Fold change in the abundance of *MAB_2217* (*ssuB*) transposon (Tn) reads in the presence of AMK compared to untreated bacteria. (C) WT and Δ*ssuB Mabs* were exposed to a two-fold dilution series of AMK in PB minimal media (1.5% v/v glycerol, 0.05% Tween-80, 0.5% asparagine, 0.2% magnesium citrate, 0.5% dibasic potassium phosphate, pH 7) with and without 0.06% magnesium sulfate in 96 well plates. For sulfate starvation experiments, magnesium sulfate was substituted with 0.048% magnesium chloride Bacterial growth measured by recording optical densities at 600nm. $p \leq 0.05$ (*).

Chapter 4. *Mab_2648c-dependent transcriptional regulation of mmpSL5 contributes to ethionamide resistance in Mabs*

Abstract

Ethionamide (ETH), an inhibitor of mycolic acid biosynthesis, is currently utilized as a second-line agent for treating multidrug resistant tuberculosis infections. Here, we show that ETH displays mildly bactericidal activity against clinical strains of *Mabs* both *in vitro* and *in vivo* at concentrations that are > 100x lower than other mycolic acid targeting drugs. Using transposon mutagenesis followed by sequencing (Tn-Seq) and whole genome sequencing of spontaneous ETH-resistant mutants, we identified *MAB_2648c* as a genetic determinant of ETH sensitivity in *Mabs. MAB_2648c* encodes for a MarR transcriptional repressor associated with the TetR family of transcriptional regulators. We show that *MAB_2648c* represses expression of *MAB_2649* (*mmpS5*) and *MAB_2650* (*mmpL5*). Further, we show that de-repression of these genes in *MAB_2648c* mutants confers resistance to ETH, but not other antibiotics. To identify determinants of resistance that may be shared across antibiotics with distinct mechanisms of action, we also performed Tn-Seq during treatment with amikacin and clarithromycin, drugs currently used clinically to treat *Mabs.* We found very little overlap in genes that modulate the sensitivity of *Mabs* to all three antibiotics, suggesting a high degree of specificity for resistance mechanisms in this emerging pathogen.

Introduction

In the context of CF, *Mabs* shares its ecological niche with other bacterial pathogens, such as *Pseudomonas aeruginosa* (170). When co-cultured, amikacin treatment that inhibits *P. aeruginosa* biofilm development provides a growth advantage for *Mabs* under these conditions, highlighting the importance of considering interspecies interactions during antibiotic treatment *in vivo* (171). An attractive approach that may boost the specificity of antibiotic treatment against *Mabs* is to rationally design regimens that incorporate antimycobacterial agents, since many antibiotics that are currently used against *Mabs* in clinical settings, such as amikacin and imipenem, are not pathogen specific (172, 173). Anti-mycobacterial drugs provide the advantage of developing highly specific regimens that should be more selective at diminishing bacterial populations enriched with *Mabs*, even in polymicrobial environments (174). The potential incorporation of anti-mycobacterial agents in regimens used against *Mabs* has already received considerable attention (114, 175, 176). Clofazimine and bedaquiline, which induce the production of reactive oxygen species and inhibit ATP synthesis in mycobacteria, respectively, are active against *Mabs* when combined with other compounds (101, 177–179). These drug combinations are currently being considered for use in clinical trials against *Mabs* (175, 176, 180, 181).

Among anti-mycobacterial agents with clinical relevance, those that target mycolic acid biosynthesis should be further explored for repurposing potential against *Mabs*, since mycolic acids are unique to *Mabs* in most pulmonary infections that are ecologically shared with other phylogenetically diverse bacterial pathogens (170, 174). Mycolic acids

are known to play critical roles in the pathogenesis, virulence, and impermeability of mycobacteria (182–185). They consist of α-branched and β-hydroxylated long-chain fatty acids ranging from 60-90 carbons in length and consist of most of the mass associated with the mycobacterial outer membrane, also known as the mycomembrane (Fig 4.1) (184, 186). The alkyl chains of these fatty acids can be modified via hydroxylation, methoxylation, cycloproponation, and ketonation (184). In many mycobacterial species, the impermeability of the mycomembrane depends in large part on the presence of these modifications (184, 187–190). However, *Mabs* completely lacks these modifications and only synthesizes unmodified α- and truncated α'-mycolic acids (191).

The biosynthesis of mycolic acids relies on two distinct fatty acid synthase (FAS) systems. The first, "eukaryotic-like" system, FAS-I, produces most acyls in the cell, with chain lengths ranging from 16 to 26 carbons (184, 192, 193). To reach the extremely long chain lengths that define the meromycolate chain of a mycolic acid, these 16-26 carbon chains are elongated by the second, "prokaryotic-like" system, FAS-II (184, 194). Once the meromycolyl chain has reached its mature length (50-62 carbons), it can be functionalized through the action of a variety of enzymes (184). This meromycolyl chain is then condensed with a shorter, 26-carbon acyl-coenzyme A produced by FAS-I to produce a mycolyl-β-keto-ester, which is then reduced and covalently linked to trehalose, creating a trehalose monomycolate (TMM) (184, 195). TMMs are then transported across the inner membrane into the periplasmic space by the membrane transporter MmpL3 (184, 196). TMMs are localized to the inner leaflet of the mycomembrane by the antigen 85 complex, which transfers the mycolyl group from TMM to the periplasmic-bound arabinogalactan layer (184, 197).

The mycolic acid biosynthetic pathway has allowed for the development of anti-mycobacterial agents that target chemical reactions in both the FAS-I and FAS-II complex (184), some of which demonstrate promising potential against *Mabs*. Indole-4-Carboxamides, a subclass of anti-mycobacterial drugs that target MmpL3, are active against *Mabs* both *in vitro* and *in vivo* (198–203). Chemical derivatives of thiacetazone, an inhibitor of the HadABC dehydratase complex associated with the FAS-II complex, are active against *Mabs in vitro* (114, 124). Furthermore, PIPD1, a piperidinol derivative, is active against *Mabs in vitro* through direct targeting of Mab_4508, an MmpL3 homologue (204).

Ethionamide (ETH) is a second-line mycolic acid inhibitor currently used to treat drug-resistant infections associated with *Mtb* (205). ETH inhibits mycolic acid biosynthesis in *Mtb* by targeting the NADH-dependent enoyl ACP reductase InhA (Rv1484) (FAS-II complex) (Fig 4.2) (206). Before inhibition takes places, ETH requires activation by *ethA* (Rv3854c), a flavin-containing monooxygenase, that covalently links NAD to ETH (ETH-NAD) (Fig 4.2) (207, 208). ETH-NAD acts as a competitive inhibitor by competing with NADH for binding in the active site of InhA (Fig 4.2) (208). ETH resistance is common among *Mtb* clinical isolates (209). Mutations in the *fabG-inhA* regulatory region (g-17t and c-15t) confer resistance by upregulating *inhA* expression, thereby reducing the efficacy

of ETH (206). Furthermore, mutations in *ethA* reduce ETH bioactivation, conferring resistance (206). Mechanisms of antimycobacterial resistance against *Mabs*, including ETH, remains poorly understood.

While past studies have been able to identify genes that are important for growth on antibiotics and those that confer resistance, we still lack a completing understanding on how the products of these genes confer sensitivity or resistance. There is genetic evidence that *Mabs* can modify and efflux antibiotics using phosphotransferases, acetyltransferases, and transport proteins, although additional evidence for some of these mechanisms are necessary (114, 129, 150, 168). Furthermore, about 40% of *Mabs* genome remain unannotated and may harbor genes that are important for developing drug resistance (129, 130, 210, 211). To expand on the genetic evidence currently available and identify novel genes that can broaden our understanding on antibiotic resistance in *Mabs*, we utilized transposon mutagenesis followed by sequencing (TnSeq) to examine growth on antibiotics on a whole-genome level.

TnSeq is a powerful tool that allows for identifying genes important for bacterial growth under any condition in a high-throughput manner (212). A transposon is introduced into a desired bacterial species using a suitable DNA delivery system. Once a transposon is inserted into a gene important for growth under a specific condition, the function of that gene will be disrupted and bacteria carrying those insertions will be depleted from the mutagenized population. Conversely, insertions that confer a growth advantage will select for bacteria containing those specific insertions (213). TnSeq can also be used to help identify an essential genome, as genes that are essential for normal growth conditions will not contain transposon insertions (214, 215). To identify where the insertions are located, genomic DNA is prepared from libraries grown under specific conditions. Transposon-enriched DNA junctions are amplified on a high-throughput sequencing platform and then reads are mapped to a reference genome to identify the genomic positions of the insertions (212–215). TnSeq has been previously used to identify genes important for growth in the presence of antibiotics in *Pseudomonas aeruginosa, Staphylococcus aureus, and Mycobacterium avium* (216–218). Although a TnSeq library has been previously generated in *Mabs* (219–222), we have been able to generate a library containing approximately 80,000 unique transposon insertions in comparison to approximately 51,000 unique insertions, which allows us to identify more genes associated with antibiotic exposure (138). Further, to the best of our knowledge, we are the first to test a TnSeq library in *Mabs* in the presence of clinically relevant antibiotics (138). Here, we identified transposon mutants that display both growth defects and growth advantages when exposed to amikacin (AMK), clarithromycin (CLR), and ETH (138).

An alternative and more common approach for identifying genes associated with growth on antibiotics involves isolation of spontaneous drug-resistant mutants followed by whole genome sequencing (WGS) (223). This approach has been used to identify genes that confer resistance to a wide variety of antibiotics and their cellular targets (223–225). In *Mabs*, numerous studies have identified spontaneous mutations in genes encoding for

transcriptional regulators that confer resistance to anti-mycobacterial agents (114, 226). MmpL3, the cellular target of PIPD, a piperidinol derivative, was identified using WGS (204). In addition to TnSeq, we also utilized WGS to identify genetic determinants of ETH sensitivity (138).

Results

Construction and characterization of a transposon library in Mabs. To enable genetic screening in *Mabs* we constructed a transposon mutant library in WT *Mabs* ATCC 19977 by packaging the *Himar1* transposon in phage ΦMycoMarT7 followed by bacterial transduction (227). We chose this strain since it has a fully sequenced genome and is genetically tractable (130, 228). To determine the location and abundance of transposon insertions in the resulting library, we collected genomic DNA and sequenced the transposon junctions (229, 230). We obtained approximately 80,000 unique transposon insertions in non-essential genes. We were not able to obtain insertions in 376 genes, suggesting that these genes are essential. Of these genes, 183 overlapped with a previous study that identified essential genes in *Mabs* using TnSeq (221). Using only genes identified as essential in our study, 193 genes in *Mabs* overlaps with the essential genome of *Mtb* (Fig. 4.3B). In *Mabs*, genes associated with translation, ribosomal structure, and biogenesis was the most represented cluster of known orthologous group (COG) category among those without insertions (Fig. 4.3A). Overall, the trends in COG categories were similar when comparing *Mtb* and *Mabs* (Fig. 4.3A). As expected, genes encoding components of mycolic acid biosynthesis were predicted to be essential (Insert the data as Table 4.3).

Mycolic acid inhibitors are largely ineffective against Mabs, although ETH activity displays promising repurposing potential. To test antimicrobial activity of mycolic acid inhibitors against *Mabs*, we determined the minimum inhibitory concentration (MIC) of representative mycolic acid inhibitors: isoniazid (INH), thiacetazone (THZ), and ETH (114, 124, 206), against WT *Mabs*. We chose INH and ETH because they possess clinical relevance in the context of *Mtb* and their mechanism of action has been extensively studied (206, 209, 231). The MIC_{99} for INH (1.25 mg/ml) and THZ (> 500 μg/ml), are much higher than those commonly observed with drug sensitive *Mtb* and are above standard clinical breakpoints (Fig 4.4 A-B, Table 4.1) (232, 233). We did not observe complete growth inhibition with the THZ concentrations tested which is consistent with previous work that has reported THZ is largely ineffective against *Mabs* (114). The high-level of intrinsic resistance displayed by *Mabs* to these agents is a major reason why they are not used in clinical settings where *Mabs* infections are observed. Interestingly, the ETH MIC_{99} (8 μg/ml) suggests that this drug is at least 100x more potent than THZ or INH against *Mabs in vitro* (Fig 4.4 C) (234). Indeed, we found that ETH at this concentration displays mildly bactericidal activity against *Mabs in vitro* and *in vivo* using GM-CSF knockout mice ($GM\text{-}CSF^{-/-}$) (Fig 4.4 D-E). GM-CSF has been used as a model to examine *Mabs* growth *in vivo*, since the absence of GM-CSF results in rapid bacterial growth in comparison to WT mice (235–237). Interestingly, we did not observe ETH resistance *in vivo* after 5 days of drug treatment (Fig. 4.5).

Importantly, the ETH MIC of 9 clinical isolates tested were close to our WT ATCC 19977 strain, suggesting that relative sensitivity to ETH may not be a unique feature of a single strain (Fig. 4.4 F). This is contrast to what has been observed with other clinical isolates of *Mabs*, in which the ETH MIC ranged from 16 – 256 μg/ml (238). Therefore, the degree of ETH activity observed here against *Mabs* observed here may be not representative of all clinical isolates that may also display acquired resistance to ETH.

Whole genome sequencing of ETH-resistant bacteria identifies mutations in MAB_2648c. In *Mtb,* ETH resistance in drug-resistant clinical strains is often conferred by mutations in *ethA* or *inhA* (206). To identify mutations that confer resistance to ETH in *Mabs*, we generated spontaneous resistant mutants by plating wild-type (WT) bacteria on solid media containing 2 and 3X the agar MIC of ETH for *Mabs,* concentrations just below the maximum aqueous solubility of ETH (0.48 mg/ml) (Fig. 4.12 A) (239). Three resistant isolates (R128, R150, and R200) were selected for further analysis. First, to validate that the isolated mutants were indeed ETH resistant, we exposed WT and mutant bacteria to a two-fold dilution series of ETH in broth. We found that the mutants were approximately 8-fold more resistant (MICs: 8 μg/ml in WT and 64 μg/ml in R128, R150, and R200) to ETH than WT. To identify the genetic basis for resistance, we performed whole genome sequencing of R128, R150, and R200 (Fig. 4.12 A). Only one mutation was identified that was present in mutant bacteria but not in WT, consisting of a GC dinucleotide deletion in *MAB_2648c* at nucleotide positions 354 and 355. This deletion alters the reading frame of *MAB_2648c*, introducing a premature stop codon at amino acid position 105 (Mab_2648c ^{Asn105Stop}), which was confirmed with sanger sequencing of PCR-amplified *MAB_2648c*. *MAB_2648c* encodes for a putative *marR* (**m**ultidrug **a**ssociated **r**esistance **r**egulator) transcriptional regulator that represents a subtype of TetR transcriptional regulators, many of which have been associated with resistance to functionally diverse antibiotics in different bacteria (240). Introducing an integrative copy of WT *MAB_2648c* in the spontaneous mutants restored ETH sensitivity (Fig. 4.4 G). Many clinical isolates of *Mtb* that display acquired resistance to ETH are cross-resistant to INH due to mutations in the promoter of *inhA* (241). Our isolated *MAB_2648c* mutants do not have increased resistance to INH relative to the parental WT strain (Fig. 4.12 B-D).

Transposon insertions in MAB_2648c confer a growth advantage in the presence of ETH. To more systematically identify additional genes that modify the efficacy of ETH against *Mabs*, we screened mutants in our transposon (Tn) library for changes in growth in the presence of a subinhibitory ETH concentration (Fig. 4.6 A, 4.13 A). The Tn library was cultured in the presence of ETH for 24 hours, at which time surviving bacteria were plated on agar plates. DNA was prepared from resulting colonies and transposon gene junctions were amplified and sequenced as previously described (229, 230); changes in transposon abundance after ETH exposure were analyzed using TRANSIT (230). We identified 208 genes as potential modulators of susceptibility to ETH using a two-fold change cutoff and a *p*-value of ≤ 0.05. Among genes with annotations, those associated with transcription were the most abundant, representing approximately 9% of the

identified hits. (Fig. 4.13 B). Interestingly, mutations in two of the three *ethA* homologs in *Mabs* seemed to confer resistance in the screen (Fig. 4.6 A), suggesting that multiple monooxygenases may contribute to ETH activation in *Mabs*.

In agreement with our data from the generation of spontaneous resistant mutants, we found that bacteria carrying insertions in *MAB_2648c* were approximately five-fold more abundant in the presence of ETH (Fig. 4.6 A-B). To validate these findings, we constructed a deletion mutant of *MAB_2648c* (Δ*MAB_2648c*) and examined growth in the presence and absence of ETH. We found that Δ*MAB_2648c* was approximately 8-fold more resistant to ETH compared to WT bacteria (MICs: 8 μg/ml for WT and 64 μg/ml for Δ*MAB_2648c*) (Fig. 4.6 C). Thus, using two independent methods, we show that loss of *MAB_2648c* function leads to ETH resistance. Deletion of *MAB_2648c* did not confer resistance to any other antibiotic tested, including INH and THZ (Fig. 4.6 D-E) (Table 4.1). This result is surprising, as in other bacteria, including *E. coli* (single MarR regulator) and *P. aeruginosa* (13 MarR regulators), loss of MarR activity confers resistance to a diversity of antibiotics (242–244).

Mab_2648c negatively regulates expression of mmpS5-mmpL5 and contributes to ETH resistance. TetR regulators often negatively regulate expression of target genes that are transcribed divergently from the regulator, separated by an intergenic region of approximately < 200 base pairs (bp) (240). The genes *MAB_2649* (*mmpS5*) and *MAB_2650* (*mmpL5*) are in a putative operon located 369 bp upstream of *MAB_2648c* (Fig. 4.7 A). Mutations in TetR regulators often lead to upregulation of *mmpS* and *mmpL* genes, which contribute to clofazimine, bedaquilline, and THZ resistance in *Mabs* (114, 226). We hypothesized that *mmpS5* and *mmpL5* contribute to ETH resistance, and that in WT bacteria, their expression is repressed by Mab_2648c. To address this hypothesis, we first measured expression levels of *mmpS5* and *mmpL5* by qRT-PCR in WT and Δ*MAB_2648c* bacteria. Regardless of the presence of ETH, expression levels of *mmpS5* were upregulated > 80-fold in Δ*MAB_2648c* compared to WT bacteria (Fig. 4.7 B). A similar trend was observed for *mmpL5* (Fig. 4.7 C). The addition of ETH to bacterial cultures alone did not affect expression of *mmpS5* (Fig. 4.7 D) or *mmpL5* (Fig. 14.7 E) in WT bacteria, suggesting that Mab_2648c activity is not directly regulated by ETH. To determine whether upregulated expression of *mmpS5* and *mmpL5* in Δ*MAB_2648c* contribute to ETH resistance, we overexpressed both genes in WT bacteria under an anhydrotetracycline (ATc) inducible promoter (245) and examined bacterial growth in the presence of ETH. Overexpression of *mmpS5* and *mmpL5* increased the ETH MIC (> 16 μg/ml) compared to bacteria not induced with ATc (Fig. 4.7 F). These data suggest that upregulation of *mmpSL5* is responsible for the ETH resistance phenotype observed in the absence of Mab_2648c. To corroborate this finding, we investigated the contribution of *mmpS5* and *mmpL5* to ETH resistance in Mab_2648c^{Asn105Stop} bacteria. In agreement with our Δ*MAB_2648c* qPCR data, we also found that *mmpSL5* expression is upregulated in Mab_2648c^{Asn105Stop} bacteria compared to WT bacteria (Fig. 4.14 C-F). Deletion of *mmpSL5* (Δ*mmpSL5)* in this background sensitized bacteria to ETH at least four-fold compared to Mab_2648c^{Asn105Stop} bacteria (MICs: 4 μg/ml in Δ*mmpSL5* and > 16 μg/ml in

Mab_2648c^{Asn105Stop} bacteria) (Fig. 4.7 G). These results suggest that the loss of Mab_2648c activity leads to upregulation of *mmpSL5*, whose activity ultimately provides ETH resistance.

ETH treatment with CLR or AMK suppresses the emergence of resistant mutants. Because *Mabs* infections are never treated with sole antibiotic regimens (7), we next tested whether ETH synergizes with commonly prescribed antibacterial agents. We tested ETH in combination with three front line drugs for treating *Mabs* infections that are representative of antibiotics with different mechanisms of action: amikacin (AMK, aminoglycoside), clarithromycin (CLR, macrolide), and moxifloxacin (MFX, fluoroquinolone). We chose to test ETH in combination with these antibiotics at concentrations representative of clinically achievable levels (246–248). Treatment with ETH or MFX alone resulted in mildly bactericidal activity during the first 2 days of treatment (Fig. 4.8 A). However, after day 2 bacteria grow in the presence of either antibiotic (Fig. 4.8 A), likely due to the emergence of resistant mutants. Although we did not observe either synergy or antagonism at early timepoints of treatment with ETH and MFX after 2 days of treatment, there was extensive bacterial growth after day 2, even in the presence of both antibiotics (Fig. 4.8 A). Similar to MFX, treatment with AMK or CLR alone resulted in the rapid emergence of resistant mutants. However, the combination of ETH with either AMK or CLR prevented the outgrowth of bacteria that occurred after 2 days of treatment with single agents (Fig. 4.8 B-C). These data suggest that while synergy was not observed, ETH may have the potential to delay resistance emergence to antibiotics used against *Mabs*.

To determine if ETH can indeed suppress resistance emergence to AMK, CLR, and MFX, we measured the MIC of each antibiotic at 0, 2, 5, and 7 days of combinatorial treatment. We found that AMK and MFX resistance emerged after 5 and 2 days of ETH treatment, respectively (Fig. 4.9 A, E). Interestingly, we did not observe resistance emergence to CLR at any of time points examined (Fig. 4.9 C). ETH resistance emerged after 2 days of MFX exposure, whereas this occurred after 5 days of AMK and CLR exposure (Fig. 4.9 B, D, F). The significance of these resistance patterns remains unknown since we did not include single drug treatments in these experiments. Future experiments should specifically compare the rate of resistance emergence to CLR in the presence and absence of ETH, as our data suggest that ETH may delay or suppress CLR resistance, which may be clinically relevant.

We also tested whether ETH is capable of synergizing with small molecules that are capable of reversing ETH resistance. SMARt-420 is a spiroisoxazoline that reverses ETH resistance in *Mtb* by inactivating EthR2, a TetR-like repressor that boosts ETH activation (249). To determine if ETH resistance can be reversed in *Mabs*, we examined ETH sensitivity in the presence and absence of SMARt-420. We found that SMARt-420 did not significantly impact bacterial growth under these conditions in either WT or Δ*MAB_2648c* bacteria (Fig. 4.11), suggesting that SMARt-420 is unable to reverse Mab_2648c-dependent ETH resistance.

Δ*MAB_2648c* did not exhibit cross resistance to other antibiotics tested (Table 4.2), suggesting a unique function in mediating ETH resistance. This was surprising, as MarR homologs often confer resistance to multiple antibiotics in other bacterial species (242–244). The fact that resistant mutants fail to emerge in the combinatorial treatment of ETH with AMK and CLR suggests that there may be unique mechanisms of resistance to each of these antibiotics. To determine whether there are mediators that confer susceptibility or resistance across multiple antibiotics in *Mabs*, we performed Tn-Seq in the presence of both AMK and CLR as described for ETH. Using the same fold-change and significance cutoffs as in our ETH Tn-Seq, we found 28 significant genes in AMK and 70 genes in CLR that may modulate susceptibility to these antibiotics (Fig. 4.8 D-E, 4.15, 4.16). No genes were similarly significant in both the ETH and AMK conditions, and only 7 genes were important in both the ETH and CLR conditions. Gene hits identified in the presence of ETH and CLR are *MAB_1055* (Conserved Hypothetical Peptidase), *MAB_1915* (Probable Fatty Acid CoA Ligase FadD), *MAB_2162* (Putative AAA-family ATPase Mpa), *MAB_4059* (Hypothetical Protein), *MAB_0177* (Antigen 85-A/B/C Precursor), *MAB_4115* (Putative MmpL Membrane Protein), and *MAB_0577* (Putative ABC Transporter Solute Binding Protein). Insertions in three of these genes conferred a growth defect in both conditions, while insertions in only one gene conferred a growth advantage in both conditions (Fig. 4.8 E). Insertions in the remaining three genes had differential effects in the two conditions. In contrast to our Tn-Seq data, deletion of *MAB_4059c* (Δ*MAB_4059c*) did not alter susceptibility to ETH or CLR individually (Fig. 4.10). The discrepancy for this remains unknown, although it is possible that loss of Mab_4059c function alters susceptibility to ETH and CLR only when grown in competition with other Tn-insertion mutants (145).

Discussion

Mabs is remarkable among drug-resistant bacterial pathogens in that resistance is intrinsic but can also be acquired to functionally diverse antibiotics (36). Unlike most antibiotics that target mycolic acid biosynthesis, we show here that ETH is mildly bactericidal against *Mabs in vitro*. Using a combination of bacterial genetics, whole genome sequencing, and transposon mutagenesis, we identified Mab_2648c as an important determinant of ETH sensitivity in *Mabs*, as loss of Mab_2648c leads to ETH resistance. This loss is associated with upregulation of *mmpSL5*, which contributes to ETH resistance in a Mab_2648c-dependent manner. Our findings expand on the current knowledge regarding the role of *mmpSL* genes in conferring antibiotic resistance in *Mabs*. In line with what we have reported here, the loss of other TetR regulators in *Mabs* leads to upregulation of other *mmpSL* genes that confer resistance to bedaquiline, clofazimine, and THZ (114, 226). It is speculated that many of the *mmpSL* genes in *Mabs* encode for transporters that efflux these antibiotics into the extracellular space (128), although this requires further evaluation. Whether ETH is being transported by MmpSL5 remains unknown. Interestingly, the TetR regulator Mab_2299c negatively regulates two, genetically distant *mmpSL* couples (*MAB_2300-2301* and *MAB_1135c-1134c*) that confers cross-resistance to bedaquiline and clofazimine (226). We did not find any differences in bedaquiline and clofazimine susceptibility in the absence of Mab_2648c

(Table 4.1). TetR regulators represents the largest class of transcriptional regulators in *Mabs*, a feature that is characteristic of saprophytic mycobacteria (240). Of the 139 TetR regulators found in the *Mabs* genome, 21 of these are annotated as MarR (129). It is possible that other MarR regulators confer resistance to antibiotics with diverse modes of action, although this remains to be explored.

We now have several examples of TetR regulators conferring drug resistance in *Mabs*, highlighting the importance of deciphering the roles of those that have yet to be studied in the context of drug resistance (114, 226). Many of these findings have been obtained through the generation of laboratory, drug-resistant strains and have yet to be extended to clinical isolates (114, 226). Sequencing of TetR regulators in drug-resistant clinical isolates could help us identify novel genetic determinants of drug resistance. In our ETH Tn-Seq screen, we identified Tn mutants with insertions in 17 TetR regulators. Tn mutants with insertions in three other genes besides *MAB_2648c* (*MAB_2885*, *MAB_2731*, and *MAB_0979*) displayed a growth advantage in the presence of ETH while mutants with insertions in the other 13 TetRs displayed a growth defect. In our Tn-Seq screen with AMK, we identified Tn insertions in 2 TetR regulators: *MAB_2061c* (growth defect) and *MAB_4026c* (growth advantage). Mutants with Tn insertions in two additional TetR regulators (*MAB_1881c* and *MAB_2952c*) displayed growth defects in our Tn-Seq screen with CLR. These Tn-Seq hits can be utilized to expand our knowledge on the contribution of TetR regulators as being important genetic determinants for growth on clinically relevant antibiotics.

Questions regarding the role of Mab_2648c in ETH resistance remain. TetR regulators can be dissociated from DNA through direct binding of small ligands (240). For MarR regulators, many of these ligands are aromatic compounds (240, 250). It remains unknown what biological conditions lead to transcriptional de-repression of Mab_2648c targets, leading to upregulation of *mmpSL5* and possibly other genes. We speculate that these conditions are associated with ETH resistance, given that ETH exposure alone does not induce expression of either *MAB_2648c* or *mmpSL5* (Fig. 4.7 B-E, Fig. 4.14 A-B), suggesting that Mab_2648c may be associated with functions unrelated to drug resistance (240, 250, 251). The closest protein homologues of Mab_2649 and Mab_2650 in *Mtb* H37Rv are MmpS5 (Rv0677c, 38.57%) and MmpL5 (Rv0676c, 48.56%), respectively (252). MmpSL transporters are known to transport many lipids, some of which include TMM (MmpL3), PDIM (MmpL7), and sulfolipids (MmpL8) (253). MmpS/L4 and MmpL5 are associated with mycobactin and carboxymycobactin export, which are two of the major mycobacterial siderophores that allow for iron acquisition (253, 254). *Mtb* mutants defective in these transporters are unable to grow in low-iron environments (254). Although there are two MarR regulators in *Mtb* (Rv0042c and Rv0880), these do not share any homology with the MarR regulator identified in this work, suggesting that the mechanism by which Mab_2648c contributes to ETH resistance may be distinct from what is currently known in *Mtb* (129, 252).

It remains unknown as to whether spontaneous ETH resistance in *Mabs* is solely mediated by mutations in Mab_2648c. We examined three independent resistant clones, each obtained from a distinct ETH concentration (128, 150, and 200 μg/ml). We were limited in being able to screen for spontaneous mutants at higher concentrations, due to the poor aqueous solubility of ETH (0.48 mg/mL) (239). It is possible that spontaneous resistance to ETH may be associated with other genetic determinants, such as mutations in the promoter region of *inhA* (*MAB_2722c*) or mutations in potential bio-activators of ETH (*MAB_0103*, *MAB_0985*, *MAB_3967*) (138, 206). The identification of 96 genes with insertions that conferred a growth advantage in the presence of ETH (138) suggests that it is possible to obtain spontaneous mutations in genes independent of *MAB_2648c*.

Identifying few overlapping hits in our Tn-Seq screens with CLR and ETH was surprising (138). While ETH is known to target cell envelope metabolism in *Mtb* (206), this remains to be determined in *Mabs*. CLR synergizes with the cell wall targeting antibiotic vancomycin against *Mabs in vitro* (255), although the mechanisms responsible for this synergy remain unknown. We found that a combination of CLR and ETH was indifferent against *Mabs* (Table 4.2) (138). Interestingly, Tn insertions in genes that conferred a growth disadvantage in the presence of CLR and ETH independently (*MAB_1055* and *MAB_0177*) encode for proteins that are predicted to localize to the cell envelope (Fig. 4.8 F) (129, 138). It is possible that a combinatorial action of CLR and ETH can lead to cell surface changes that makes the mycobacterial envelope more permeable to antibiotic entry. Although we did not observe synergy between CLR and ETH against WT *Mabs* (138), examining this combinatorial action in the absence of *MAB_1055* and *MAB_0177* may display a synergistic effect. Our collective findings in this work can be used to broaden our knowledge on identifying genetic determinants of ETH and other clinically relevant antibiotics. Identifying a gene that seems to uniquely confer resistance to ETH, but not other unrelated antibiotics, suggest that intrinsic drug resistance in *Mabs* may result from a multitude of genetic mechanisms.

Materials & Methods

Construction of bacterial strains and growth conditions. *Mabs* strain ATCC 19977 was grown in Middlebrook 7H9 (BD) media supplemented with albumin-dextrose-saline (ADS). For growth on solid media, *Mabs* was cultured on LB agar (BD) or Middlebrook 7H10 (BD) where indicated. Clinical strains were obtained from Chao Qi (Northwestern University). The following antibiotics were supplemented when appropriate for *Mabs*: hygromycin B (Invitrogen, 125 μg/ml for liquid media; 1 mg/ml for solid media), zeocin (InvivoGen, 50 μg/ml), and kanamycin (Sigma, 150 μg/ml for liquid media; 100 μg/ml for solid media). To favor the generation of S morphotype *Mab*s, both liquid and solid media were supplemented with Tween-80 (Sigma, 0.05% v/v). *E. coli* was grown in LB supplemented with the following antibiotics when appropriate: hygromycin B (125 μg/ml), zeocin (50 μg/ml), and kanamycin (50 μg/ml). Deletion of *MAB_2648c* and *MAB_2649-2650* was achieved using Oligonucleotide-Mediated Recombineering followed by Bxb1 Integrase Targeting (ORBIT) as previously described (256). We adapted the original ORBIT protocol for utilization in *Mabs*. Briefly, for each target gene, an oligonucleotide

containing an *attP* site flanked by 60-80 base pairs of sequence homology surrounding each target gene was constructed and co-electroporated (2.5 kV, 25 μF, and 1000 Ω) with the payload plasmid pKM496 into bacteria expressing genes from the plasmid pKM444 (256). All electroporations were conducted with 385 μl of bacteria washed three times with 10% glycerol at an optical density of 600 nanometers (OD600nm) of 0.1-0.3. Approximately 67 ng of target oligonucleotides (Integrated DNA Technologies) were used with and without 100 ng of pKM496 for electroporations using cuvettes containing 0.2 cm gaps (Bio-Rad). Following electroporation, bacteria were rinsed with 2 ml of 7H9 and allowed to recover at 37°C with shaking for 16 hours before plating on LB supplemented with zeocin (50 μg/ml) to select for deletion mutants. PCR amplification was used to check for the correct recombination event, which was confirmed with Sanger sequencing.

Mouse infections to assess ETH efficacy

Fifteen GM-CSF knockout mice (GM-CSF$^{-/-}$) of mixed sexes (8 female and 7 male mice) (Jackson Laboratories) were infected intranasally with *Mabs* (1 x 10^6 in 40 μL). Eight hours post-infection, mice were treated with 100 mg/kg of ETH (TCI Chemicals) prepared in a formulation consisting of 20% DMSO, 20% Ethanol, and 60% water. Untreated and vehicle-treated mice were also included. Five days post-ETH treatment, lungs were harvested, homogenized, and then serial dilutions were prepared and plated on Middlebrook 7H11 agar (BD). *Mabs* CFUs were enumerated after 3 days of incubation at 37°C. All mouse procedures were approved by the Office of Laboratory and Animal Care (OLAC) at the University of California, Berkeley.

Tn-Seq screening, gene essentially calls, and statistical analyses. The transposon (Tn) library for *Mabs* was constructed as previously described for other mycobacterial species (227). For screening, an aliquot of the *Mabs* Tn library was grown in 150 ml of 7H9 broth until log phase (OD600nm 0.5-1.0). The Tn library was diluted to an OD_{600} of 0.01 (~ 5 x 10^6 CFU/ml) in 10 ml of 7H9 with and without ETH (16 μg/ml), CLR (Ambeed, 1 μg/ml), and AMK (Ambeed, 8 μg/ml). All cultures were prepared in triplicate. Bacteria were grown at 37°C for 24 hours, harvested by centrifugation, and washed twice with fresh 7H9 broth. 2 ml of bacteria containing 1.5 x 10^4 CFU/ml were plated on LB agar supplemented with kanamycin (100 μg/ml) and Tween-80 (0.05 %) on 245 mm square bioassay dishes (Corning). Plates were incubated at 37°C for 5 days and then colonies were scraped into 35 ml of 7H9 broth. Genomic DNA was extracted from the collected mixture as previously described. Genomic DNA was submitted to the UC Davis DNA Technologies Core and sequences enriched for the *Himar1* transposon were amplified on a HiSeq illumina platform (229). Sequence reads were mapped to the *Mabs* ATCC 19977 genome. Transposon-enriched sequence reads were then analyzed using TRANSIT software (230). Calls of essentiality were made by TRANSIT using the Gumbel method with the following settings: 10,000 samples, trim setting=1, minimum read set to 1, replicates averaged. For conditional essentiality, the calls were made by TRANSIT using the resampling method with the following settings: 10,000 resampling, TTR normalization, included zeros, trimming the first and last 5% of genes, winzorized resampling and site restricted resampling (230).

Determination of Minimum Inhibitory Concentrations (MIC) and synergy testing. *Mabs* strains were grown to an OD600nm of 0.2-1.0 in 7H9 and diluted to an OD600nm of 0.01 with and without a two-fold dilution series of antibiotics to be tested in 96 well, TC-treated plates in a final volume of 100 μl. Plates were incubated at 37°C for four days without shaking in tightly sealed, moist Tupperware containers to prevent evaporation. After 4 days, bacteria were fixed with an equal volume of 5% Formalin (Sigma) for safety reasons. Optical densities were then recorded at 600 nm using a SpectraMax M3 Microplate Reader (Molecular Devices). The MIC here is defined as the lowest concentration of antibiotic that inhibits 99% of bacterial growth. For synergy experiments, ETH MIC was determined as described above with and without the highest concentration of each antibiotic tested that has no effect on bacterial growth. For colony forming unit (CFU) enumeration, bacteria were washed twice in antibiotic-free growth media and then ten-fold serial dilutions were prepared followed by plating on LB agar. CFU/ml was enumerated after 5 days of incubation at 37°C.

Selection of spontaneous ETH resistant mutants followed by whole genome sequencing. To select for spontaneous resistant mutants, WT *Mabs* (1×10^8 CFU) was plated on LB agar supplemented with three different inhibitory concentrations of ETH (128, 150, and 200 μg/ml), which represents 2-, 2.3-, and 3.1-times MIC. Plates were incubated at 37°C for at least 7 days before inspection of the plates. Spontaneous resistant clones were picked and grown in 7H9 broth. ETH resistance was validated in the selected clones using the MIC protocol described above. Genomic DNA was extracted from the clones and submitted to the UC Davis DNA Technologies Core for whole genome sequencing on a NovaSeq platform. Sequence reads were mapped to the *Mabs* ATCC 19977 genome (130).

Quantitative PCR (qPCR). Bacteria at an OD600nm of 0.1 were treated with and without ETH (16 μg/ml). At 3- and 11-hours post-treatment, bacteria were harvested at 3500 rpm for 10 minutes and RNA was extracted using TRIzol (Invitrogen) and purified using the RNeasy Mini Kit (Qiagen) following the manufacturer's protocol. Total RNA was reversed transcribed to cDNA using the Superscript™ III First-Strand Synthesis System (Invitrogen) following the manufacturer's protocol. For each primer pair, ten-fold serial dilutions of cDNA were prepared for generation of standard amplification curves on a CFX Connect-Real Time PCR Detection System (Bio-Rad). Fluorescence was detected using the SsoAdvanced Universal SYBR Green Supermix (Bio-Rad). cDNA synthesis reactions without RT were included in parallel to control for genomic DNA contamination. Expression levels were normalized to *sigA* (MAB_3009) before calculating relative expression levels using the delta-delta C_T method ($2^{-\Delta\Delta C_T}$).

Plasmids. 1000bp upstream of *MAB_2648c*, the *MAB_2648c* coding sequence, and 200 bp downstream of *MAB_2648c* were PCR amplified using Q5 DNA Polymerase (New England Biolabs) and cloned into the DraI and HindIII sites of the integrative vector pMV306 (257), generating pRR107. pRR107 was electroporated into Δ*MAB_2648c* as

described above and selected using kanamycin. The *mmpS5-L5* coding sequence along with 200 bp downstream of *mmpL5* were PCR amplified using Q5 DNA Polymerase and cloned into the anhydrotetracycline (ATc) inducible promoter of pUV15LD (245), generating pRR115. pRR115 was electroporated into both WT and Δ*MAB_2648c* bacteria and selected using Hygromycin B. To check for mycobacterial clones carrying desired plasmids, individual colonies were picked into 10 μl of sterile, nuclease-free water and heat-killed at 80°C for 1 hour. 2 μl of heat-killed bacteria was used as a template for PCR using plasmid-specific primers.

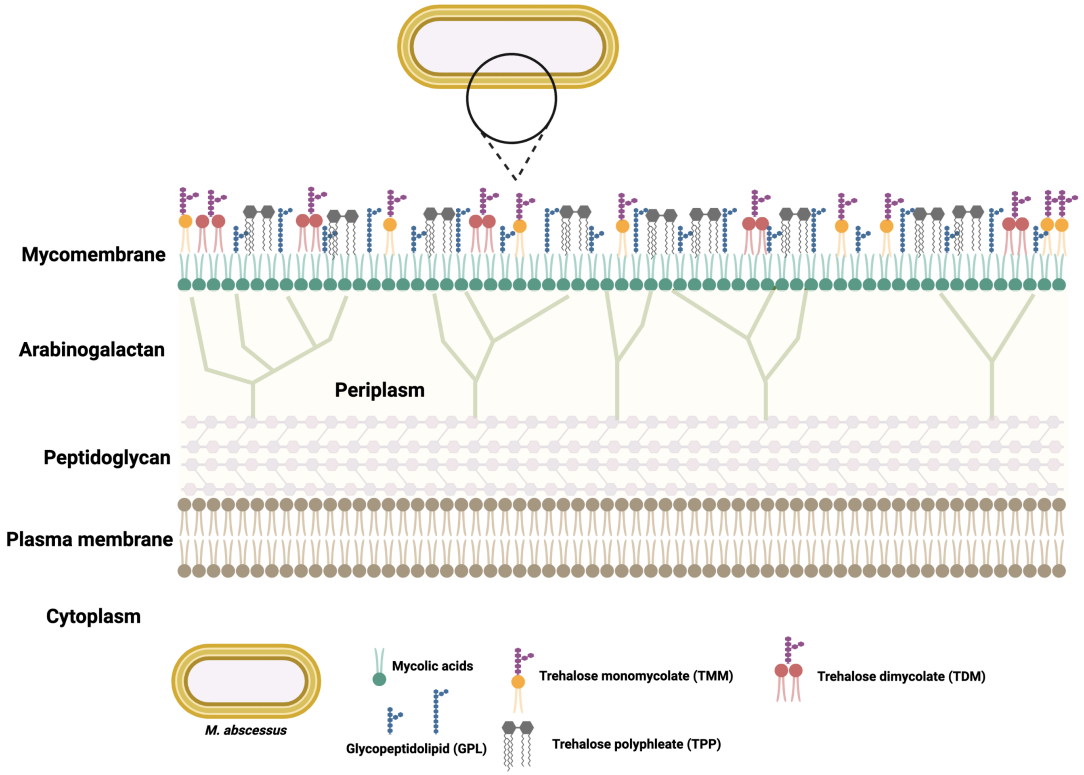

Figure 4.1. The cell surface architecture of *Mabs*, displaying the mycomembrane and their associated mycolic acids.

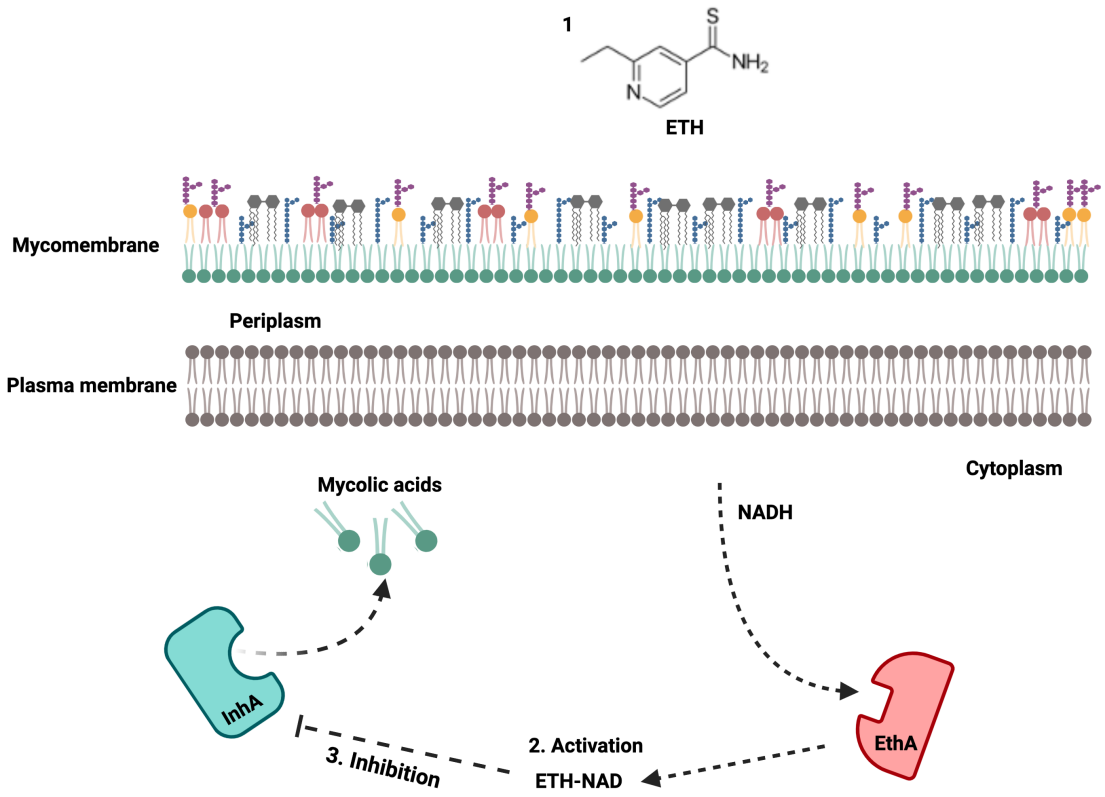

Figure 4.2. ETH target and mechanism of action in *Mtb*. Membrane permeable ETH (1) is activated by the flavin-binding monooxygenase EthA (2). Activated ETH directly binds to InhA (3), inhibiting mycolic acid transport and biosynthesis.

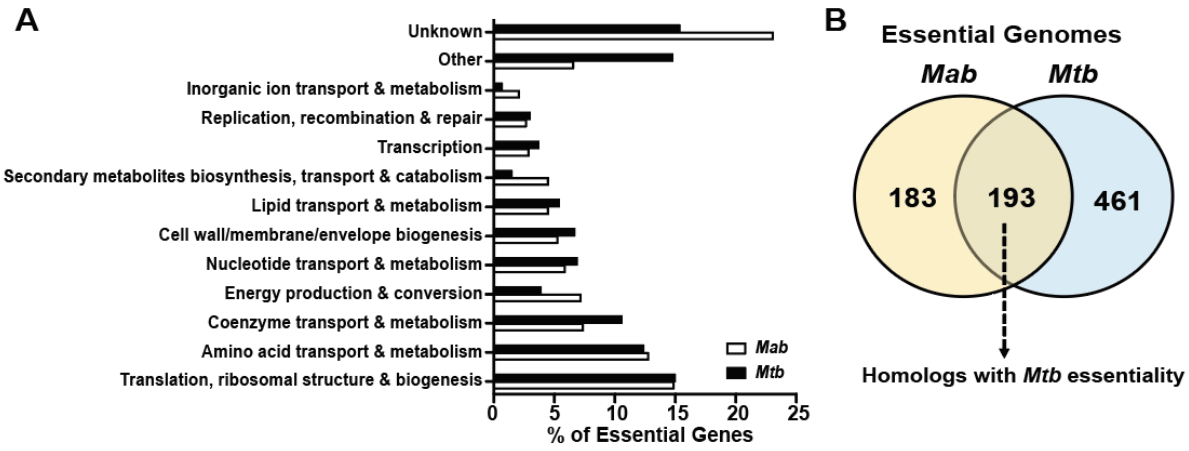

Figure 4.3. Tn-Seq analyses of the essential genome in *Mabs*. (A) Essential genes in *Mabs* were grouped in cluster of orthologous groups (COG) and then compared to the essential genome in *Mtb*. 'Other' represents COG categories representing less than 2% of the essential genome. 'Unknown' represents genes without any COG annotations. (B) Venn diagram displaying essential gene homologs in *Mabs* and *Mtb*.

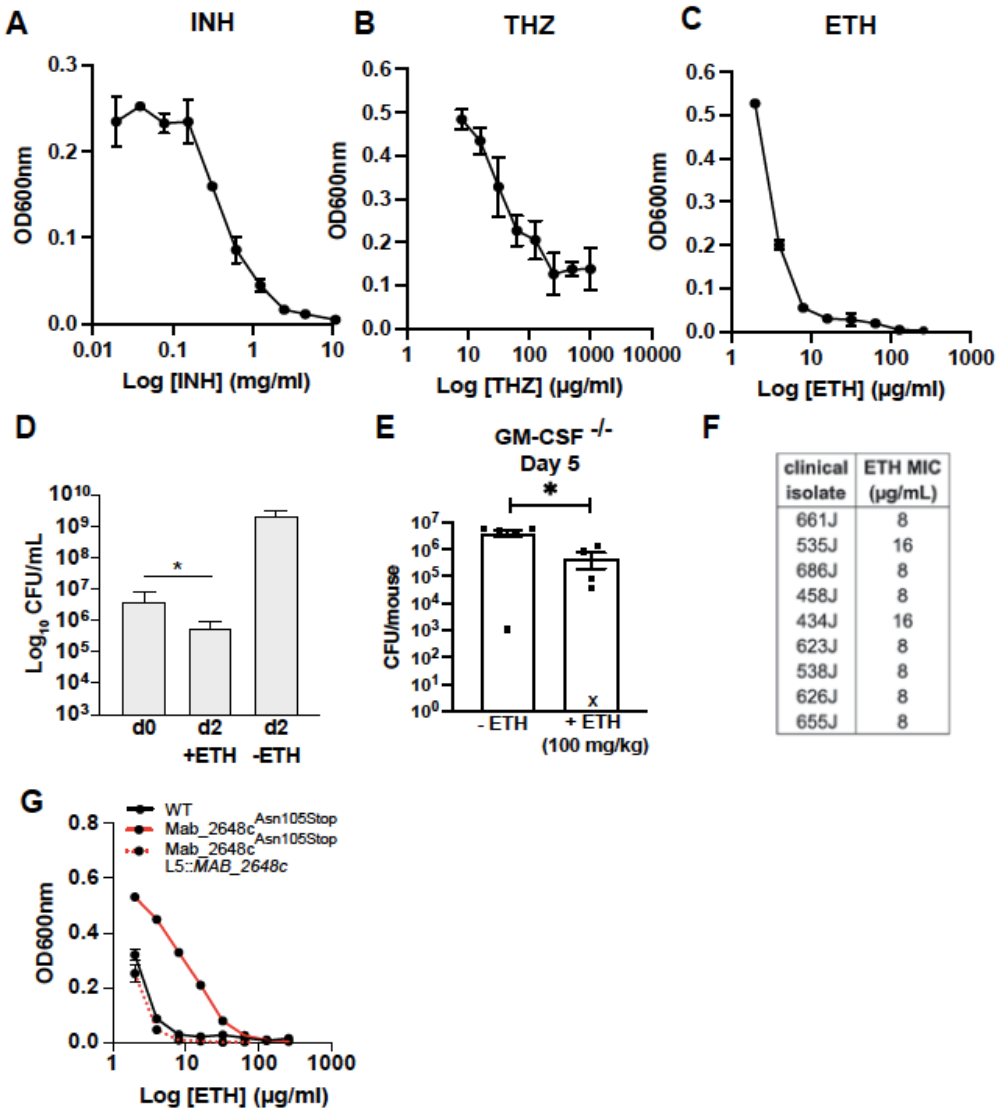

clinical isolate	ETH MIC (µg/mL)
661J	8
535J	16
686J	8
458J	8
434J	16
623J	8
538J	8
626J	8
655J	8

Figure 4.4. ETH displays mild bactericidal activity against *Mabs*. Dose-response curves for (A) INH, (B) THZ, and (C) ETH against WT *Mabs*. (D) WT *Mabs* was treated with and without ETH (20 µg/ml) for 2 days and viable bacteria were enumerated by CFU. (E). GM-CSF$^{-/-}$ mice were treated with and without 100 mg/kg of ETH, mouse lungs harvested 5 days after treatment, and then bacterial burden determined by CFU. 'X' represents a mouse that did not survive ETH treatment. (F) ETH MIC values for clinical isolates of *Mabs*. (G) ETH dose-response curves for WT, Mab_2648c^{Asn105Stop}, and Mab_2648c^{Asn105Stop} complement (Mab_2648c^{Asn105Stop} L5::*MAB_2648c*) strains. All experiments are representative of at least three biological replicates except for (E), which is representative of two biological replicates. Error bars represent standard deviation, $p \leq 0.05$ (*).

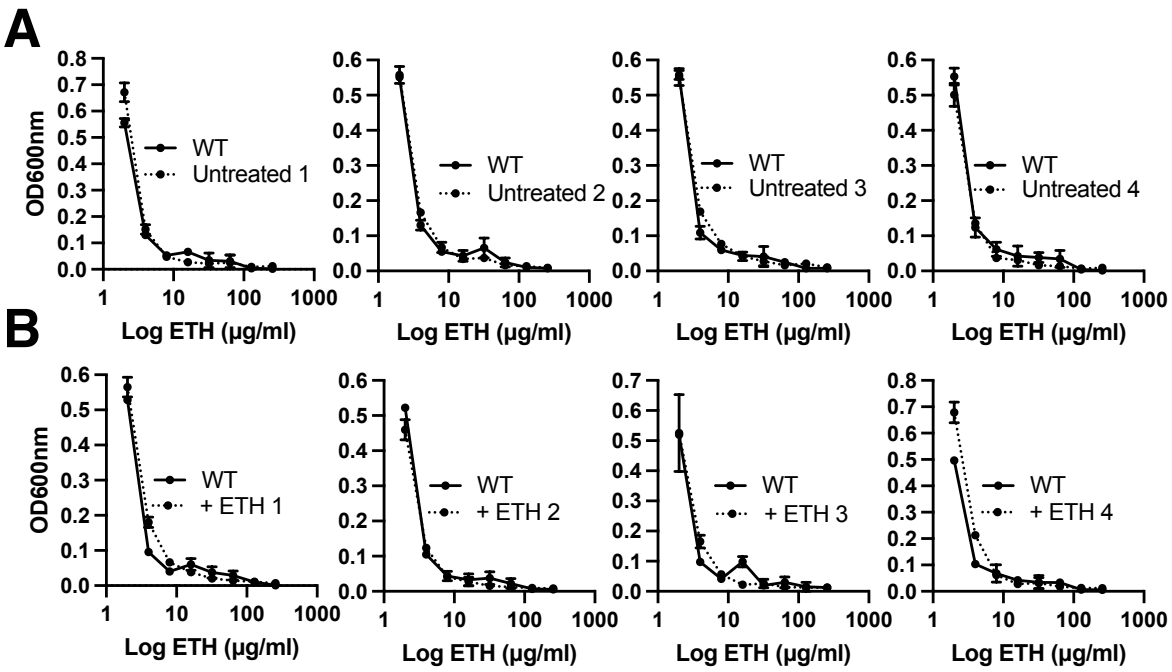

Figure 4.5. Five days of ETH exposure in mice does not lead to *in vivo* resistance. *Mabs* collected from the lungs of GM-CSF$^{-/-}$ mice treated in the absence (A) or presence of ETH (100 mg/kg) were exposed to a two-fold dilution series of ETH and bacterial growth examined as described in materials and methods. WT *Mabs* was included in parallel. 1-4 represent bacterial samples collected from separate mice in each experimental group.

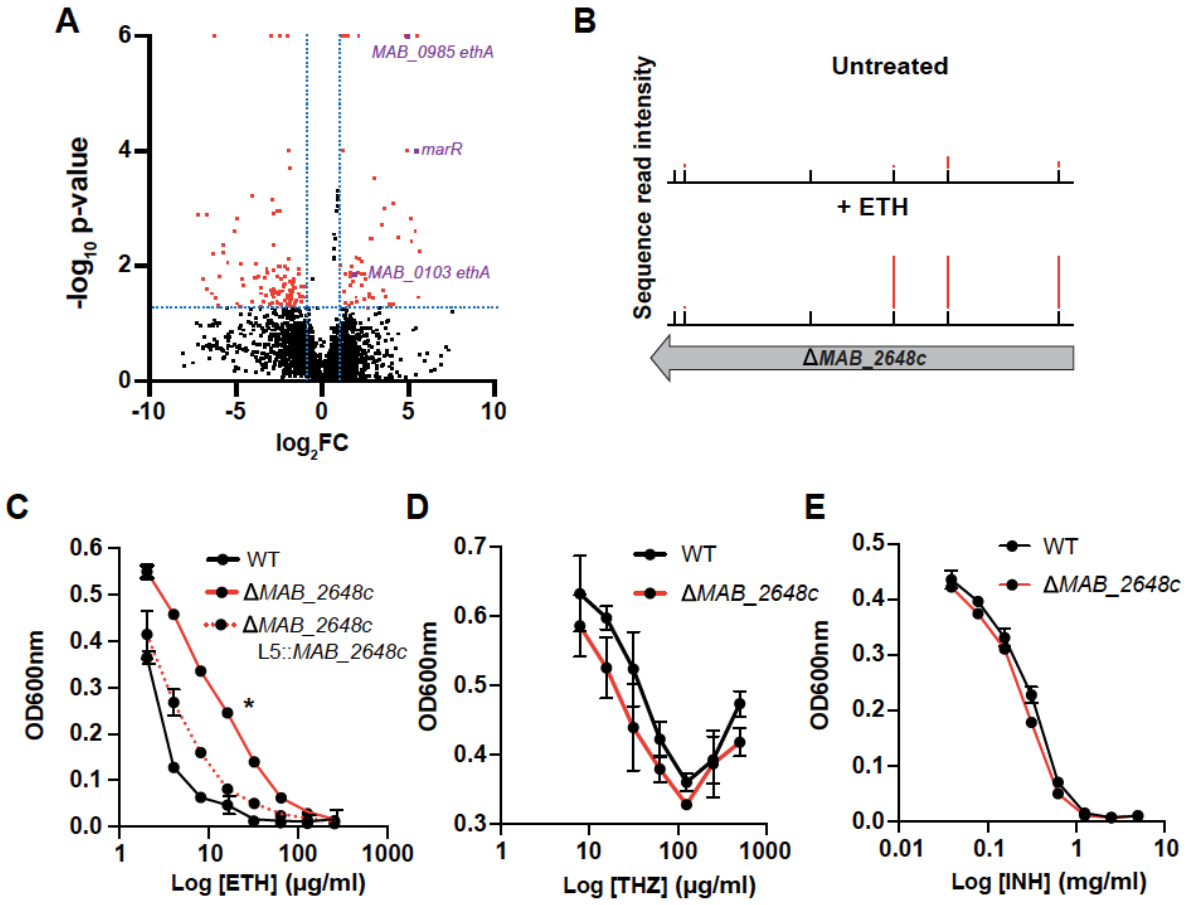

Figure 4.6. *MAB_2648c* is a determinant of ETH susceptibility. (A) Volcano plot displaying all transposon insertion mutants from a Tn-Seq screen in the presence of ETH. Red dots represent mutants with log fold change > 2 and $p \leq 0.05$ (B) Transposon sequence read densities for *MAB_2648c* in the presence and absence of ETH. Black tick marks represent all possible insertion sites. (C-E) Dose-response curves for WT, Δ*MAB_2648c*, and Δ*MAB_2648c* complement (Δ*MAB_2648c* L5::*MAB_2648c*) strains in the presence of ETH (C), THZ (D), and INH (E). All experiments are representative of at least three biological replicates. Error bars represent standard deviation. $p \leq 0.05$ (*) for Δ*MAB_2648c* vs complemented strain.

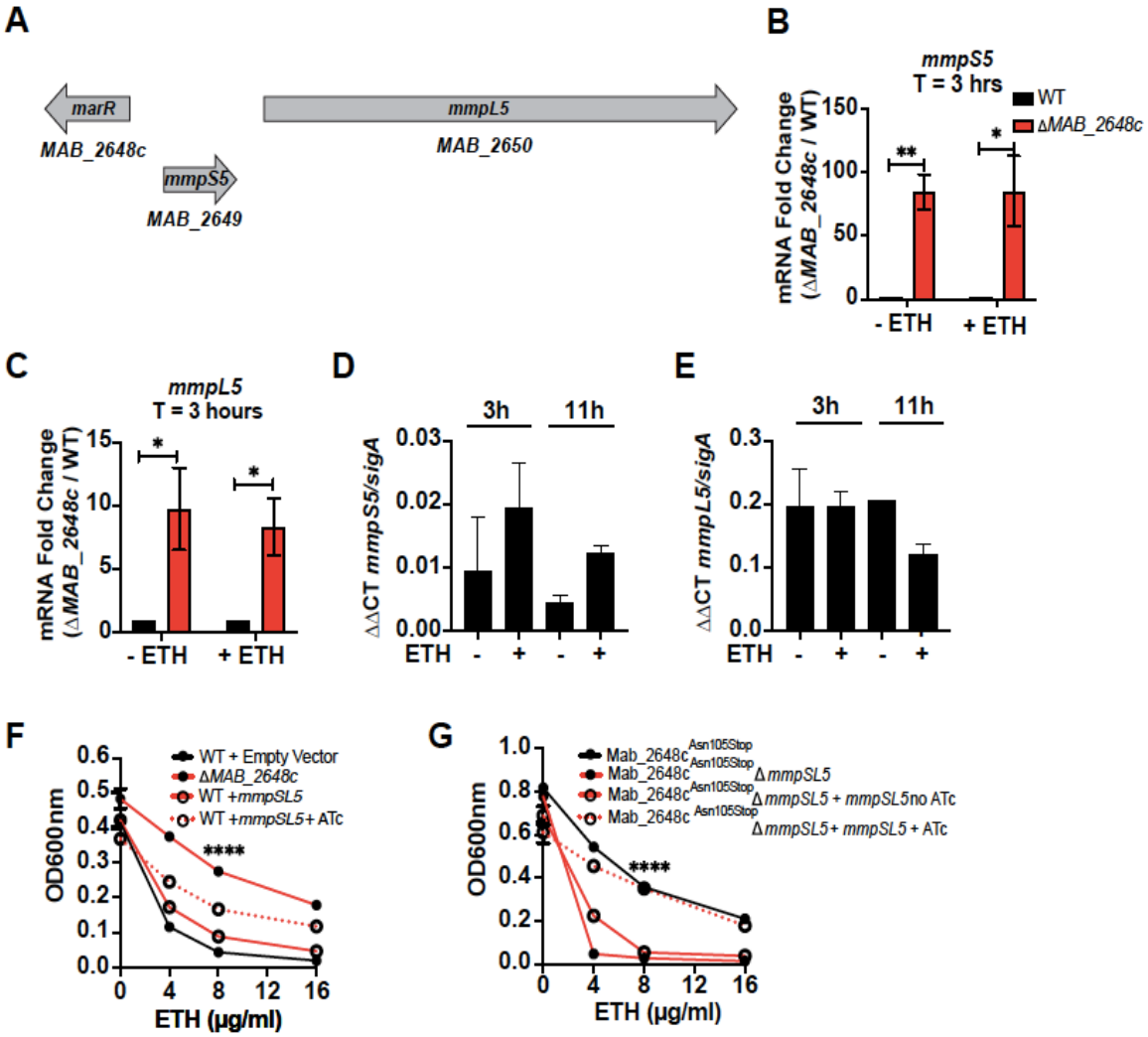

Figure 4.7. *mmpS5* and *mmpL5* are negatively regulated by Mab_2648c and contribute to ETH resistance. (A) Schematic representation of the genetic organization of *MAB_2648c*, *mmpS5*, and *mmpL5*. (B-E) Gene expression levels of *mmpS5* and *mmpL5* in WT and Δ*MAB_2648c* bacteria in the presence and absence of ETH at the indicated time points. (F-G) ETH dose-response curves for the indicated strains. ATc (100 ng/ml) was included where appropriate. All experiments were performed at least in biological duplicates. Error bars represent standard deviation. $p \leq 0.05$ (*); $p \leq 0.01$ (**); $p \leq 0.0001$ (****) comparing the *mmpSL5* mutant with and without ATc.

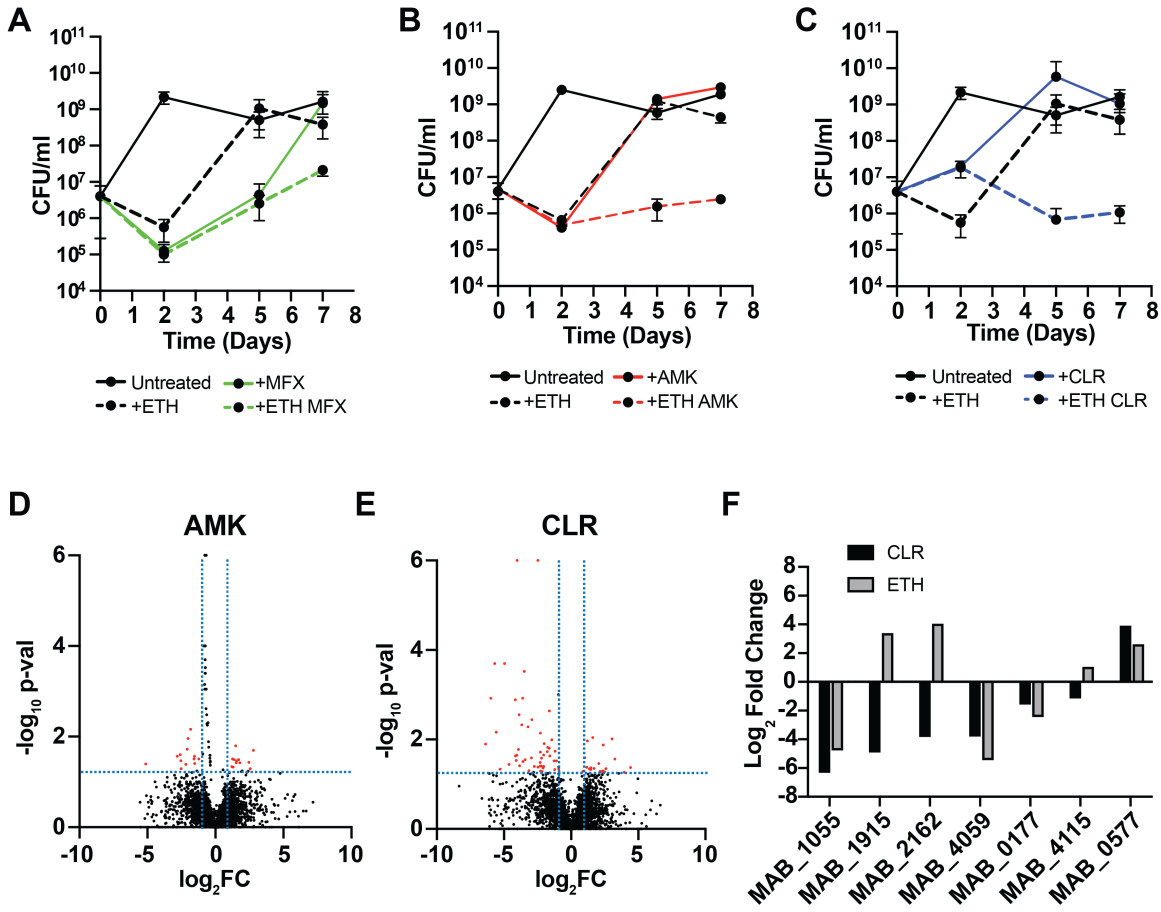

Figure 4.8. Prolonged ETH treatment suppresses emergence of drug resistance to some clinically relevant antibiotics. (A-C) WT *Mabs* was treated with and without ETH (20 μg/ml) in the presence of moxifloxacin (MFX, 3 μg/ml), amikacin (AMK, 25 μg/ml), and clarithromycin (CLR, 3 μg/ml) or in combination with ETH. At the indicated time points, bacteria were collected, washed, and then ten-fold serial dilutions were plated on LB agar for CFU/ml enumeration. (D-E) Volcano plots displaying all gene hits from a Tn-Seq screen in the presence of AMK (D) and CLR (E). Red dots represent mutants that display growth advantages while black dots represent mutants that display growth defects in the presence of the indicated drug. (F) Fold changes in the transposon read intensities of select mutants from our Tn-Seq screen with ETH and CLR. All experiments were performed in biological duplicates. Error bars represent standard deviation.

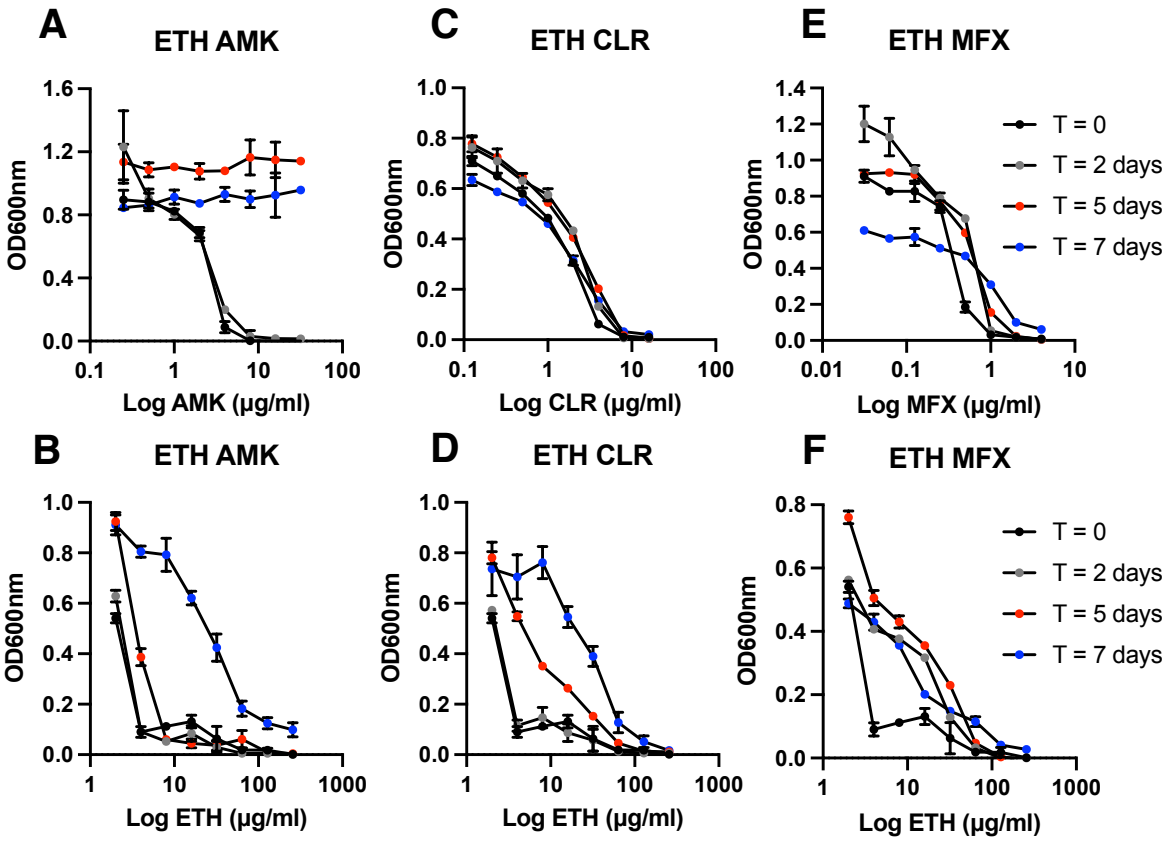

Figure 4.9. Two days of ETH treatment may suppress the emergence of CLR resistance, but not AMK and MFX. WT *Mabs* was treated with ETH (20 μg/ml) in the presence and absence of amikacin (AMK, 25 μg/ml) (A-B), clarithromycin (CLR, 3 μg/ml) (C-D), and moxifloxacin (3 μg/ml) (E-F). 1 mL of bacteria was collected at the indicated time points, washed with 7H9, and then recovered in 7H9. Recovered bacteria were then exposed to a two-fold dilution series of each indicated antibiotic and growth was measured as described in materials and methods.

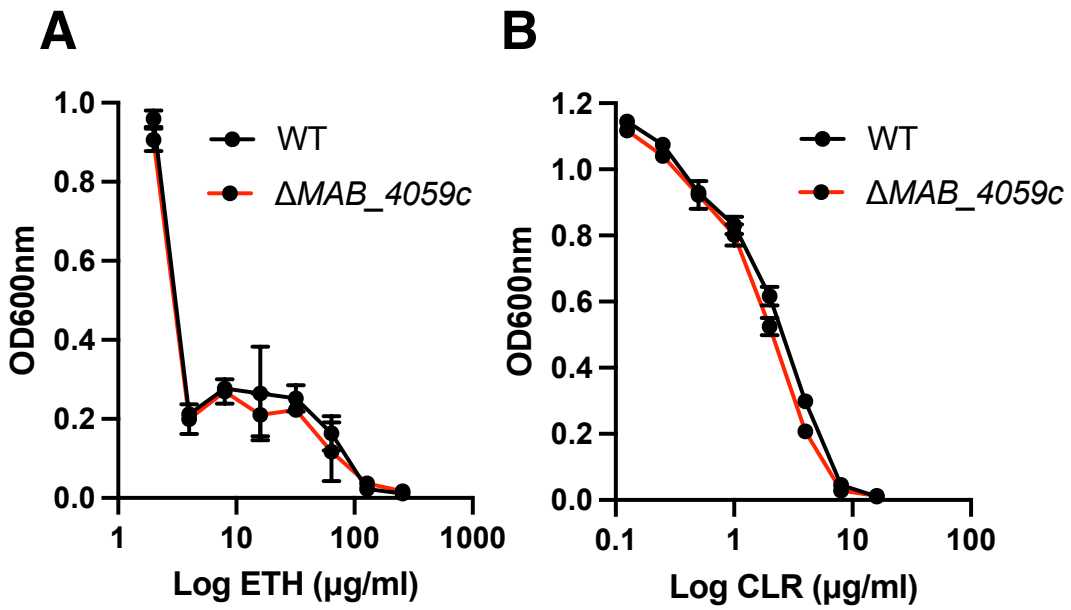

Figure 4.10. Mab_4059c is not required for grown in the presence of ETH and CLR. WT and Δ*MAB_4059 Mabs* were exposed to a two-fold dilution series of ETH (A) and CLR (B) and growth was measured as described in materials & methods.

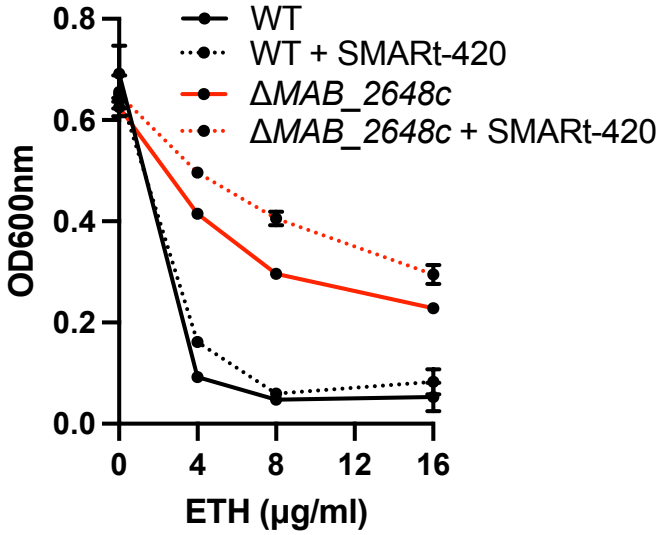

Figure 4.11. SMARt-420 does not reverse ETH resistance in the absence of Mab_2648c. WT and Δ*MAB_2648c Mabs* were exposed to a two-fold dilution series of ETH with and without SMARt-420 (10 μM). Bacterial growth was measured as described in materials and methods.

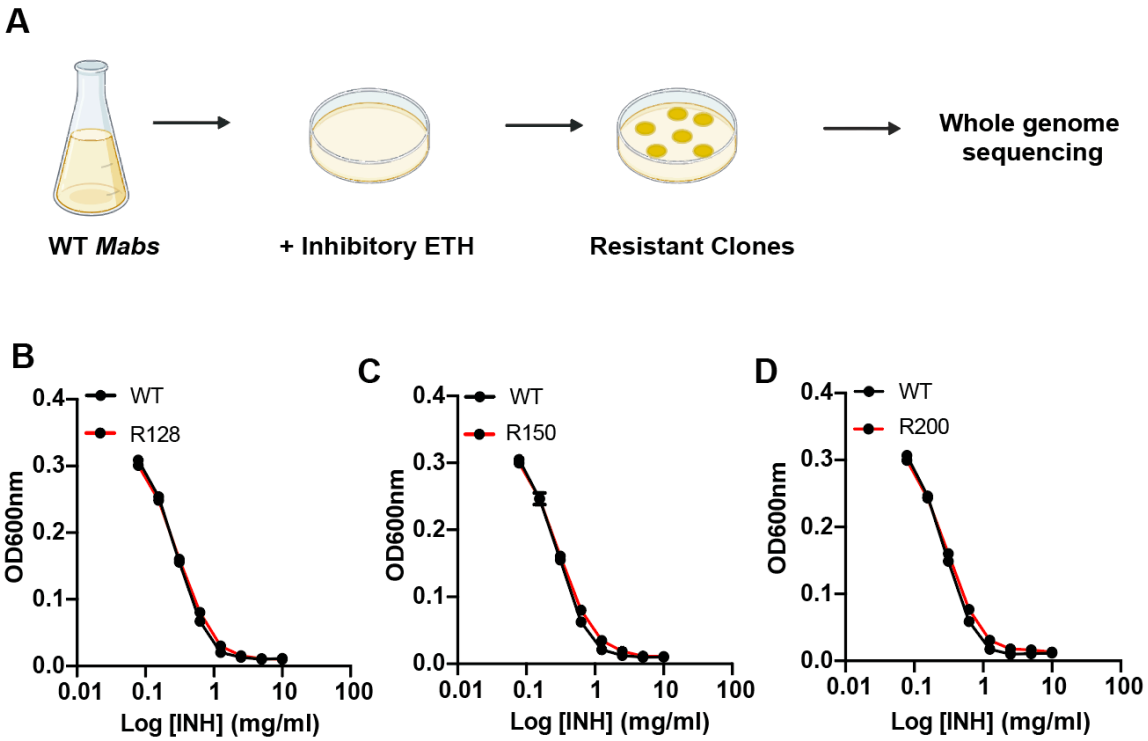

Figure 4.12. Spontaneous ETH resistance does not confer cross-resistance to INH. (A) WT *Mabs* was plated in the presence of inhibitory ETH to generate resistant bacteria, which were then analyzed by whole genome sequencing. (B-D) Isoniazid (INH) dose-response curves generated against isolated ETH-resistant clones (R128, R150, and R200). Experiments are representative of at least two biological replicates. Error bars represent standard deviation.

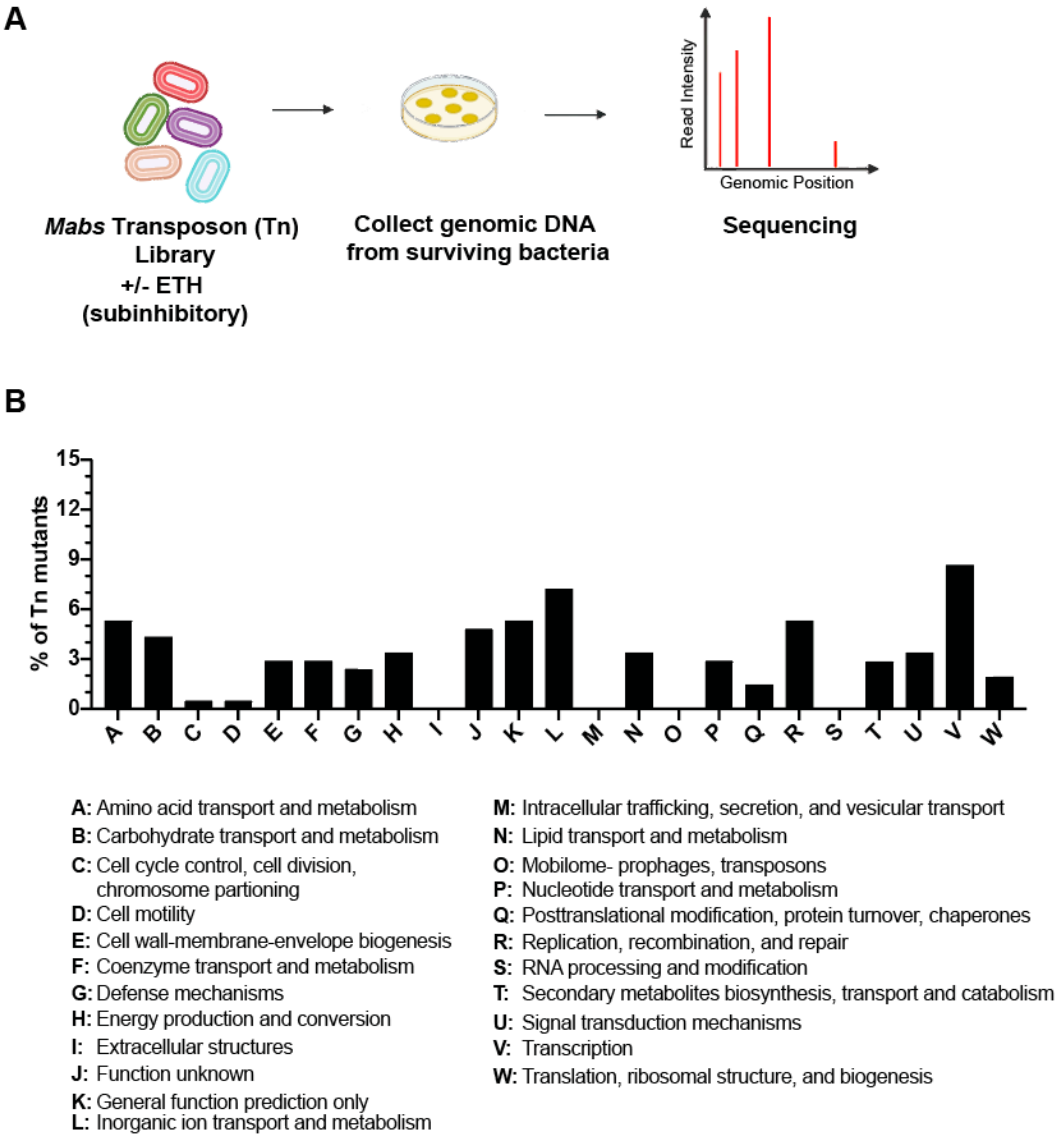

Figure 4.13. Cluster of Orthologous Group (COG) analysis of transposon mutants exposed to ETH. (A) A library of transposon mutants was treated with and without ETH. Surviving bacteria were then plated, genomic DNA collected, and transposon-enriched sequences analyzed by whole genome sequencing. (B) Percentage of transposon mutants represented in the indicated COG categories. Gene hits without any COG annotations are not shown.

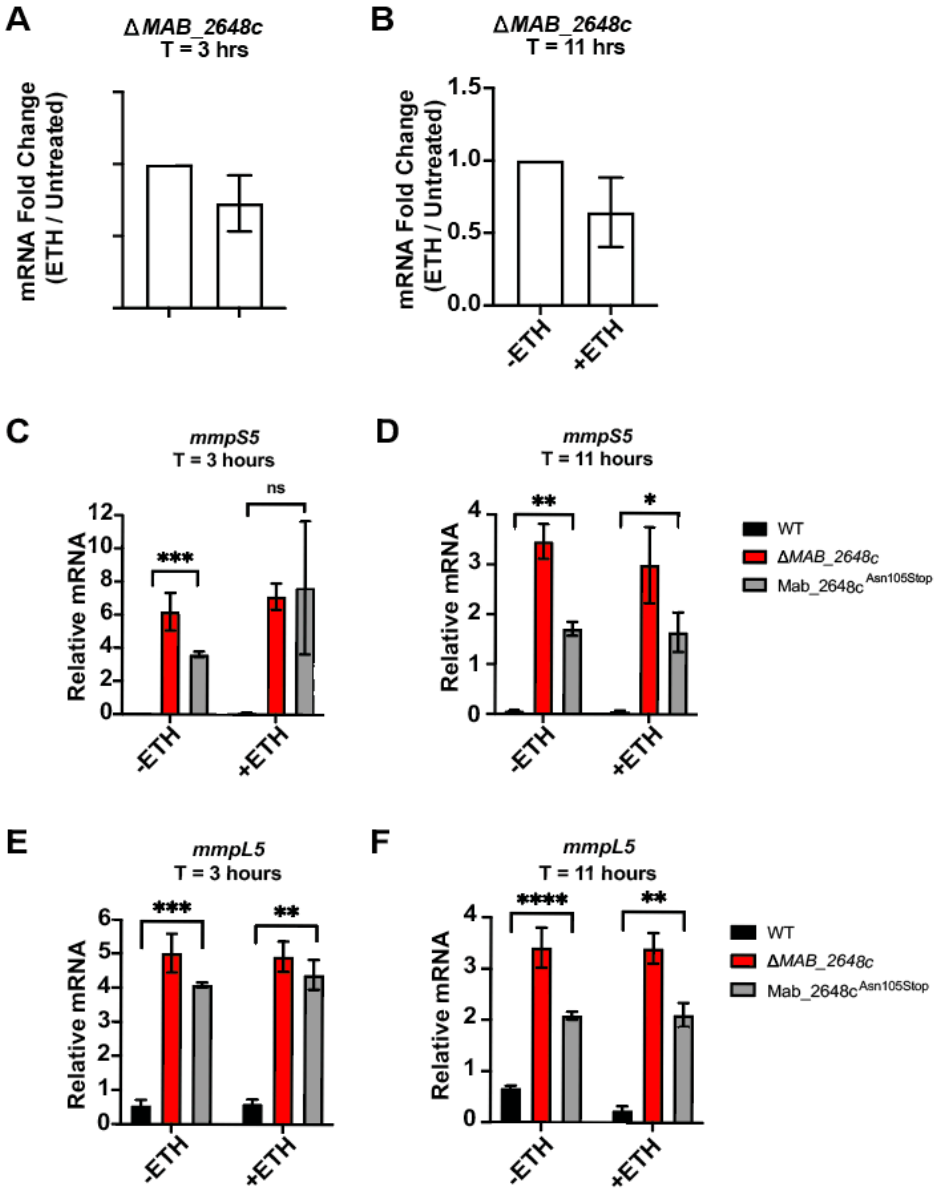

Figure 4.14. *MAB_2648c* is not induced in the presence of ETH. (A-B) Gene expression levels of *MAB_2648c* in WT *Mabs* in the presence and absence of ETH after 3 (A) and 11 hours (B) of exposure. (C-F) Gene expression levels of *mmpS5* and *mmpL5* in WT, Δ*MAB_2648c*, and Mab_2648c^{Asn105Stop} bacteria in the presence and absence of ETH at the indicated time points. Experiments are representative of at least two biological replicates. Error bars represent standard deviation. no significance (ns); $p \leq 0.05$ (*); $p \leq 0.01$ (**); $p \leq 0.001$ (***); $p \leq 0.0001$ (****)

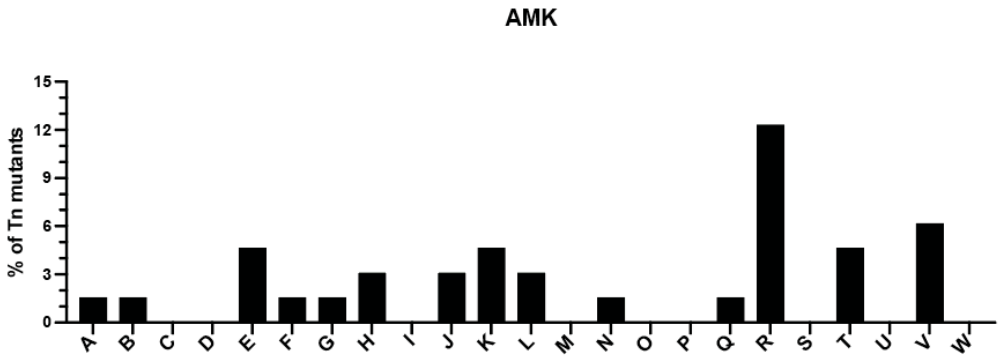

A: Amino acid transport and metabolism

B: Carbohydrate transport and metabolism

C: Cell cycle control, cell division, chromosome partioning

D: Cell motility

E: Cell wall-membrane-envelope biogenesis

F: Coenzyme transport and metabolism

G: Defense mechanisms

H: Energy production and conversion

I: Extracellular structures

J: Function unknown

K: General function prediction only

L: Inorganic ion transport and metabolism

M: Intracellular trafficking, secretion, and vesicular transport

N: Lipid transport and metabolism

O: Mobilome- prophages, transposons

P: Nucleotide transport and metabolism

Q: Posttranslational modification, protein turnover, chaperones

R: Replication, recombination, and repair

S: RNA processing and modification

T: Secondary metabolites biosynthesis, transport and catabolism

U: Signal transduction mechanisms

V: Transcription

W: Translation, ribosomal structure, and biogenesis

Figure 4.15. COG analysis of transposon mutants exposed to AMK. Percentage of transposon mutants exposed to AMK represented in the indicated COG categories. Gene hits without any COG annotations are not shown.

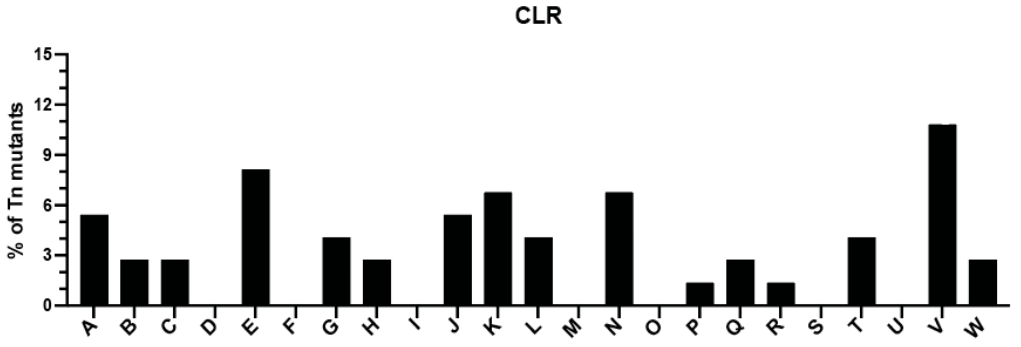

A: Amino acid transport and metabolism

B: Carbohydrate transport and metabolism

C: Cell cycle control, cell division, chromosome partioning

D: Cell motility

E: Cell wall-membrane-envelope biogenesis

F: Coenzyme transport and metabolism

G: Defense mechanisms

H: Energy production and conversion

I: Extracellular structures

J: Function unknown

K: General function prediction only

L: Inorganic ion transport and metabolism

M: Intracellular trafficking, secretion, and vesicular transport

N: Lipid transport and metabolism

O: Mobilome- prophages, transposons

P: Nucleotide transport and metabolism

Q: Posttranslational modification, protein turnover, chaperones

R: Replication, recombination, and repair

S: RNA processing and modification

T: Secondary metabolites biosynthesis, transport and catabolism

U: Signal transduction mechanisms

V: Transcription

W: Translation, ribosomal structure, and biogenesis

Figure 4.16. COG analysis of transposon mutants exposed to CLR. Percentage of transposon mutants exposed to CLR represented in the indicated COG categories. Gene hits without any COG annotations are not shown.

Antibiotic	WT MIC (µg/ml)	Δ*MAB_2648c* MIC (µg/ml)
Amikacin	2	2
Bedaquiline	0.25	0.25
Cefoxitin	4	4
Clofazimine	>16	>16
Ethambutol	32	32
Isoniazid	1250	1250
Thiacetazone	> 500	>500
Imipenem	4	4
p-aminosalicylic acid	> 160	> 160
Moxifloxacin	1	1
Doxycycline	> 64	> 64
Clarithromycin	4	4

Table 4.1. Comparison of MIC values in WT and Δ*MAB_2648c Mabs* to functionally diverse antibiotics.

Antibiotic	ETH MIC (µg/ml)
AMK	8
CLR	8
MFX	8
CEF	4
IPM	4

Table 4.2. ETH MIC values in WT *Mabs* in the presence of each indicated antibiotic.
AMK: Amikacin; CLR: Clarithromycin; MFX: Moxifloxacin; CEF: Cefoxitin; IPM: Imipenem

Gene Name	Tb Locus	Essentiality (TB)	Mabs Locus	Essentiality (Mabs)
MmpL3	Rv0206c	ES	MAB_4508	ES
FabH	Rv0533	NE	MAB_1141c	NE
HadA	Rv0635	ES	MAB_3898c	NE
HadB	Rv0636	ES	MAB_3897c	NE
HadC	Rv0637	NE	MAB_3896c	NE
MabA	Rv1483	ES	MAB_2723c	NE
InhA	Rv1484	ES	MAB_2722c	ES
FabD	Rv2243	ES	MAB_1879c	NE
AcpM	Rv2244	ES	MAB_1878c	ES
KasA	Rv2245	ES	MAB_1877c	ES
KasB	Rv2246	NE	MAB_2028	NE
AccD6	Rv2247	GD	MAB_1876c	NE
CmrA	Rv2509	ES	MAB_1537c	NE
FAS-I	Rv2524c	ES	MAB_1512	ES
AccA3	Rv3285	ES	MAB_3643	ES
AccD4	Rv3799c	ES	MAB_0181	ES
Pks13	Rv3800c	ES	MAB_0180	ES
FadD32	Rv3801c	ES	MAB_0179	ES

Fas-II
FAS-I/central carbon metabolism
Mycolate condensation and maturation
Funneling of intermediates to FAS-II

Table 4.3. Most mycolic acid biosynthetic genes are essential in both *Mtb* and *Mabs.* ES, essential; NE; not essential; GD, growth defect

Chapter 5. Identifying potential substrates of MmpSL5 and the ETH mechanism of action against *Mabs*

Abstract

mmpSL genes encode for protein complexes in mycobacterial species associated with the inner membrane, where they are known to transport various lipids and siderophore compounds. Many are known to contribute to mycobacterial virulence, pathogenesis, and drug resistance. There is speculation that they may function as efflux pumps, since *mmpSL* mutants are sensitive to various antibiotics and their overexpression confers drug resistance. The biological role of many MmpSL proteins have been well studies in *Mtb.* The *Mabs* MmpSL5 couple identified in this work is most homologous to MmpS5 (Rv0677c, 38.57%) and MmpL5 (Rv0676c, 48.56%) in *Mtb*, where they have been shown to transport mycobactin and carboxy-mycobactin, the two major iron scavenging siderophores produced in *Mtb*. Furthermore, *Mtb mmpSL5* is under the negative control of a TetR regulator (Rv0678) that contributes to azole resistance. We hypothesized that the MmpSL5 couple identified in this work is either an ETH or iron transporter, possibly both. To address the hypothesis that MmpSL5 in *Mabs* is an ETH transporter, we examined ETH sensitivity in the context of several efflux pump inhibitors (verapamil, reserpine, carbonyl cyanide chlorophenylhydrazone, bedaquiline and ethidium bromide). We did not find any differences in ETH sensitivity with or without efflux pump inhibitors or any dependency on Mab_2648c activity. To determine whether MmpSL5 is iron transporter, we tested the ability of an *mmpSL5* mutant in a Mab_2648c deficient background (Mab_2648c^{Asn105Stop} Δ*mmpSL5*) to grow in an iron-starved environment. Additionally, we measured expression levels of *trpE2*, which encodes for the isochorismate synthase MbtL, associated with mycobactin synthesis, in the presence and absence of ETH. We did not find any growth defects upon iron starvation in Mab_2648c^{Asn105Stop} Δ*mmpSL5* bacteria. Interestingly, we identified that *trpE2* was significantly induced upon ETH exposure in WT bacteria, but not in Δ*MAB_2648c* bacteria in an iron-rich environment. The functional consequence of this upregulation remains unknown. Collectively, these results that MmpSL5 in *Mabs* is not likely to efflux ETH directly, leaving its role in ETH resistance unknown.

Introduction

Efflux pumps are broadly distributed in both gram negative and positive bacteria (258, 259). In gram positive bacteria, efflux pumps localize to the cytoplasmic membrane (258). Although this is also true in gram-negative bacteria, there is an additional mechanism required for export across the outer membrane in these organisms (259). The substrates of these efflux pumps include antibiotics from functionally diverse classes with distinct modes of action and may also include, non-antibiotic compounds, such as bile, heavy metals, and quorum sensing molecules (258–265). Efflux pumps are classified into five major categories that differ in their specificity and energy source required for efflux (258, 259, 265). ABC (ATP Binding Cassette) pumps utilize ATP hydrolysis to efflux substrates out of the bacterial cell. MATE (Multidrug and Toxic Compounds Extrusion), MFS (Major Facilitator Superfamily), SMR (Small Multidrug Resistance), and RND (Resistance

Nodulation and Cell Division) efflux pumps require the use of an electrochemical proton (H^+) gradient. ABC, MATE, MFS, and SMR pumps are predominately founds in gram-positive bacteria whereas RND pumps are predominately present in gram-negative bacteria (258, 259). The MmpSL5 transporter identified in this work is annotated as a member of the RND class (129, 252, 266, 267).

RND pumps have been well studied in several antibiotic resistant bacterial pathogens, including *P. aeruginosa* (MexAB-OprM), *A. baumannii* (AdeABC), and *N. gonorrhoea* (MtrCDE) (268–270). Some antibiotic substrates for RND systems include fluoroquinolones, tetracyclines, and aminoglycosides (271–274). Bacterial mutants lacking these efflux pumps are sensitive to antibiotic treatment (272, 274–276). The activity of these efflux pumps is tightly regulated transcriptionally by TetR regulators that negatively represses transcription of the encoded genes (275, 277, 278). Examples of TetR-dependent transcriptional regulation of RND efflux pump components have been demonstrated for AcrR, MtrR, and MarR (279–281).

MarR is a well-known regulator of efflux pump activity in many bacterial species, including *S. aureus* and *E. coli* (281–284). In *E. coli*, transcriptional activation of the *marRAB* operon can be induced though direct binding of aromatic metabolites to MarR, including salicylate, 2,3-dihydrozybenzoate, and anthranilate (250). 2,3-dihydrobenzoate is associated with enterobactin biosynthesis, an iron-binding siderophore produced by *E. coli* and other gram-negative bacterial pathogens (285–287). It has been proposed that enterobactin biosynthesis and transport requires transcriptional activation of MarR, since MarR negatively regulates expression of the *acrAB* operon, which encodes for the periplasmic (AcrA) and inner membrane (AcrB) protein components that bind to the enterobactin transporter TolC (288–292).

Mycobacteria acquire iron using two major siderophores: the cytoplasmic membrane-bound mycobactin and extracellularly localized exochelin (*M. smegmatis*) or carboxymycobactin (*Mtb*) (293). Although iron uptake mechanisms have not been fully mapped out in mycobacteria, is it generally thought that exochelin and carboxymycobactin bind ferric iron (Fe^{3+}) in the extracellular space and then transfer the bound iron to receptor proteins, possibly porins, across the mycobacterial cell envelope (293). Iron overspill and/or the presence of ferric reductases in the periplasmic space then transfer the bound iron to membrane bound mycobactin (293). Ferric reductases bound to the cytoplasmic membrane reduce the bound iron to ferrous iron (Fe^{2+}) and then transfer Fe^{2+} to iron-storage proteins such as bacterioferritin (293).

In *Mtb*, mutants lacking *mmpSL4* are unable to grow under iron-limiting conditions because they are defective in mycobactin synthesis and transport (254). MmpSL4 interact with MmpL5 and addition of a genetic copy of *mmpL5* rescues the growth defect of a *mmpSL4* mutant under iron starvation (254). Aside from serving a role in growth under low iron and siderophore transport, MmpSL5 also contributes to clofazimine and bedaquiline resistance in *Mtb* (294, 295). Although iron-uptake and transport has not been

well studied in *Mabs*, it has been discovered that the type VII ESX-3 secretion system is required for iron uptake and that ESX-3 secretes a siderophore that is structurally distinct from those in other mycobacterial species (296). The structure of the *Mabs* siderophore resembles those produced in Nocardia species, which represents another class of actinomycete species closely related to mycobacteria (296, 297). This suggest that siderophore biosynthesis and transport may be distinct from what has been observed in other mycobacterial species, including *Mtb* and other NTM.

Results

We examined bacterial growth in the presence of ETH with and without subinhibitory doses of several efflux pump inhibitors: verapamil (VER, 64 μg/ml), reserpine (RES, 10 μg/ml), carbonyl cyanide chlorophenylhydrazone (CCCP, 2 μg/ml) and bedaquiline (BDQ, 30 ng/ml). Reserpine and verapamil have been shown to inhibit the activity of many efflux pumps, with subsequent increases in drug sensitivity in many bacterial pathogens, including *Mtb* (298–309). Verapamil has also been shown to increase membrane permeability in *Mtb* (310). Similar to what has been observed in other studies, the addition of verapamil increases the sensitivity of *Mabs* to various drugs, including bedaquiline and clofazimine (311). CCCP and bedaquiline both inhibit the generation of proton motive forces, which is necessary for the activity of RND and other efflux pumps (308, 312–315). We did not find any differences in ETH sensitivity in the presence of these inhibitors, suggesting that ETH may not be subjected to efflux activity (Fig. 5.1).

We hypothesized that MmpSL5 may function as a transporter that exports ETH, because many membrane transporters function as efflux pumps to export antibiotics (258, 259, 308). To test this hypothesis, we tested whether the Δ*MAB_2648c* mutant strain that expresses *mmpSL5* at high levels displays higher rates of ethidium bromide (EtBr) efflux, an assay commonly used to assay mycobacterial efflux in the context of drug resistance (316). EtBr is capable of directly binding to many efflux pumps, acting a competitive inhibitor for endogenous targets of these pumps (308, 316). Although we observed EtBr accumulating in *Mabs* cells in a dose dependent manner (Fig. 5.2), we did not observe any difference in EtBr levels when comparing WT and the Δ*MAB_2648c* mutant at a single dose. The inability to detect increased EtBr efflux in the Δ*MAB_2648c* mutant does not rule out the hypothesis that *mmpSL5* is a transporter of ETH, but it suggests there may be specificity to the transport that precludes the use of this assay.

We hypothesized that MmpSL5 in *Mabs* is a siderophore transporter and that ETH directly or indirectly targets iron-uptake pathways in *Mabs*. It is possible that Δ*MAB_2648c* bacteria are ETH resistant because the cellular target of ETH is a component of the mycobactin biosynthetic pathway that is being overproduced in Δ*MAB_2648c* bacteria. We observed approximately a 10-fold increase in *trpE2* expression levels in WT bacteria exposed to ETH, but not in the absence of ETH (Fig. 5.3 A-B). This increase is dependent on Mab_2648c activity, since Δ*MAB_2648c* (Fig. 5.3 A) and Mab_2648c^{Asn105Stop} (Fig 5.3 B) bacteria did not display an increase in *trpE2* (*MAB_2245*) levels. This is intriguing, as this elevated expression level suggest that *Mabs* is potentially synthesizing mycobactin,

despite the presence of an iron-rich growth environment (~ 180 mM free iron) (317). It is possible that ETH treatment is directly or indirectly corrupting mycobactin synthesis, free iron uptake, or both. This expression data supports our hypothesis that ETH may target iron metabolism in *Mabs*. If this is the case, then Mab_2648c^{Asn105Stop} Δ*mmpSL5* bacteria should display a growth defect in iron-deficient conditions. We determined whether Δ*MAB_2648c Mabs* may be resistant to *p*-amino salicylic acid (PAS), a clinically relevant anti-tuberculosis agent that is thought to inhibit iron uptake (318–321). We did not find any differences in PAS sensitivity between WT and Δ*MAB_2648c Mabs* (Fig. 5.4 A-B, Table 4.1).

To remove iron from our growth media, we utilized Chelex, a resin that has a high affinity for iron (322–324). To determine whether *mmpSL5* is required for growth under iron-deficient conditions, we incubated WT, Δ*MAB_2648c*, and Mab_2648c^{Asn105Stop} Δ*mmpSL5* bacteria in chelex-treated minimal media containing glycerol as the sole carbon without any exogenous iron supplementation (Fig. 5.4 C) (325). We did not observe any differences in colony forming units (CFU) between the strains at 2- and 5-days post exposure to iron-deficient conditions with and without ETH. (Fig. 5.4 D) These data suggest that *mmpSL*5 is not required for growth under low iron conditions and may not be a siderophore transporter.

Immediately downstream of *MAB_2648c* is *trpE* (*MAB_2647c*), which encodes for anthranilate synthase, an enzyme that participates in the tryptophan biosynthetic pathway, catalyzing the conversion of anthranilate from chorismite (326, 327). The intergenic region between *MAB_2648c* and *trpE* is 65 base pairs, suggesting that the transcriptional regulation of these two genes may be linked (Fig. 5.5 A) (129). In *E. coli*, anthranilate is a transcriptional inducer of the *marRAB* operon (322). Furthermore, MarR ligands that lead to transcriptional de-repression are known to be aromatic compounds (328). Therefore, we hypothesized that anthranilate directly binds MarR, leading to transcriptional de-repression of *mmpSL5* and potentially other target genes (326). This binding may be used to control tryptophan biosynthesis which may then subsequently directly or indirectly influence ETH efficacy.

To determine whether Mab_2648c is a negative regulator of *trpE*, we measured expression levels of *trpE* in WT and Δ*MAB_2648c* bacteria in the presence and absence of ETH at 3- and 11-hours post-treatment by qPCR. We found that at each time point, irrespective of drug treatment, the expression levels were significantly higher in the absence of Mab_2648c, compared to WT bacteria, suggesting Mab_2648c may be a negative regulator of tryptophan metabolism (Fig. 5.5 B). We considered the possibility that this expression change may be attributed to a polar effect, because the genetic approach utilized for the construction of a *MAB_2648c* mutant did not result in an unmarked mutant, but rather introduced a plasmid backbone of approximately 3 kb in place of the *MAB_2648c* coding sequence (328). To address this, we measured *trpE* expression levels under the same conditions in Mab_2648c^{Asn105Stop} bacteria, which does not possess this plasmid backbone. Unfortunately, we did not observe an increase in *trpE*

levels in Mab_2648c^{Asn105Stop} (Fig. 5.5 C), suggesting that the observed phenotype in the absence of *MAB_2648c* is due to a polar effect.

To determine whether tryptophan metabolism is linked to ETH efficacy in *Mabs*, we examined ETH sensitivity in WT and Δ*MAB_2648c* with and without exogenous supplementation of tryptophan and indole, a tryptophan intermediate (326, 327). Unfortunately, we were unable to include anthranilate due to the lack of a researcher Drug Enforcement Administration (DEA) license for working with controlled substances. We did not observe any differences in ETH sensitivity in the presence or absence of tryptophan (Fig. 5.5 D) and indole (Fig. 5.5 E), suggesting that tryptophan metabolism does not influence ETH sensitivity.

Discussion

Although we did not find any differences in ETH sensitivity with or without efflux inhibitor, or any Mab_2648c-dependecy of ethidium bromide efflux, we cannot eliminate the possibility that MmpSL5 is an efflux pump. It is possible that ETH sensitivity may be altered in the presence of other efflux pump inhibitors that were not tested in this study (valinomycin, Phe-Arg-β-napthylamide, and spectinamides) (329). Additional efflux pump inhibitors should be tested in the future. Biochemical approaches can also be utilized to test whether MmpSL5 is an efflux pump. Obtaining a crystal structure of MmpSL5 and aligning it with those of known efflux pumps, such as MexB from *P. aeruginosa* (330), could prove to be valuable. Determining whether ETH is a natural ligand of MmpSL5 using biolayer interferometry and isothermal titration calorimetry would also be beneficial (331).

Although we did not observe a phenotype in Mab_2648c^{Asn105Stop} Δ*mmpSL5* bacteria under iron-deficient conditions, alternative approaches can be utilized to determine whether iron bio-availability influences ETH efficacy. Examining ETH sensitivity using mutants that are unable to synthesize and transport mycobactin is one approach (296). Additionally, examining the transcriptome profiles of mycobactin and iron-uptake genes with and without ETH treatment using RNA-sequencing is an alternative approach (332). The absence of an ETH sensitivity phenotype in mycobactin mutants and the lack of a *mmpSL5* dependency on iron transcription would be consistent with the data reported here.

It remains unknown as to whether tryptophan metabolism influences ETH sensitivity, since tryptophan metabolism is tightly regulated transcriptionally, translationally, and allosterically (326). Mycobacteria are capable of synthesizing tryptophan *de novo*, and exogenous supplementation of these metabolites may alter tryptophan metabolism beyond our experimental control (326, 327). Examining ETH sensitivity in mutants auxotrophic for tryptophan provides a more directed approach for establishing a potential link.

Materials & Methods

Examining ETH sensitivity in the presence of efflux pump inhibitors and tryptophan metabolites

Mabs strains were grown to an OD600nm of 0.2-1.0 in 7H9 and diluted to an OD600nm of 0.01 with and without a two-fold dilution series of antibiotics to be tested in 96 well, TC-treated plates in a final volume of 100 μl. Efflux pump inhibitors were included at the following concentrations: verapamil (VER, 64 μg/ml), reserpine (RES, 10 μg/ml), carbonyl cyanide chlorophenylhydrazone (CCCP, 2 μg/ml) and bedaquiline (BDQ, 30 ng/ml). Tryptophan (2 mM) and Indole (3 μg/ml) were included when necessary. Plates were incubated at 37°C for four days without shaking in tightly sealed, moist Tupperware containers to prevent evaporation. After 4 days, bacteria were fixed with an equal volume of 5% Formalin (Sigma) for safety reasons. Optical densities were then recorded at 600 nm using a SpectraMax M3 Microplate Reader (Molecular Devices). The MIC here is defined as the lowest concentration of antibiotic that inhibits 99% of bacterial growth.

EtBr efflux assays

Mabs strains were grown to a OD600nm of 0.2-1.0. 10 ml of bacteria were harvested at 3500 rpm for 10 minutes and washed twice with 1X Phosphate-buffered-saline (PBS), pH 7.4. The OD600nm of the bacterial cultures was adjusted to 0.4 with 1X PBS supplemented with 0.4% glucose, pH 7.4. 100 μl of bacteria was treated with and without a two-fold dilution series of EtBr (0.25 – 8 μg/ml) in dark, clear bottom 96 well plates (Greiner). EtBr fluorescence (excitation wavelength: 530nm; emission wavelength: 585nm) was measured a SpectraMax M3 Microplate Reader (Molecular Devices) at 37°C for 60 minutes.

Quantitative PCR (qPCR)

Bacteria at an OD600nm of 0.1 were treated with and without ETH (16 μg/ml). At 3- and 11-hours post-treatment, bacteria were harvested at 3500 rpm for 10 minutes and RNA was extracted using TRIzol (Invitrogen) and purified using the RNeasy Mini Kit (Qiagen) following the manufacturer's protocol. Total RNA was reversed transcribed to cDNA using the Superscript™ III First-Strand Synthesis System (Invitrogen) following the manufacturer's protocol. For each primer pair: *MAB_2647c* (*trpE)* and *MAB_2245* (*trpE2*), ten-fold serial dilutions of cDNA were prepared for generation of standard amplification curves on a CFX Connect-Real Time PCR Detection System (Bio-Rad). Fluorescence was detected using the SsoAdvanced Universal SYBR Green Supermix (Bio-Rad). cDNA synthesis reactions without RT were included in parallel to control for genomic DNA contamination. Expression levels were normalized to *sigA* (*MAB_3009*) before calculating relative expression levels using the delta-delta C_T method ($2^{-\Delta\Delta C_T}$).

Iron-deprivation assays

Bacteria were grown in 7H9 overnight and washed twice in chelex-treated minimal media without exogenous iron supplementation (3.6 mM of KH_2PO_4, 6% (v/v) of glycerol, 30 mM of L-asparagine, and 0.05% (v/v) of Tween 80, pH 6.8) (325). 2 μl of washed bacteria was passaged in minimal media without iron before ETH treatment. Minimal media was prepared by treating with Chelex® 100 sodium form (10 g/L, Sigma) and then stirring at

room temperature for 2 days (322). Chelex was removed by filtration and then supplemented with 2.0 mM of $MgSO_4$ $7H_2O$ and 0.006 mM of $ZnSO_4$ $7H_20$ (325). After passaging without iron, bacteria were diluted to an OD600nm of 0.1 with and without ETH (16 μg/ml) in chelex-treated minimal media. After 2- and 5-days post-treatment, 1 ml of bacteria was collected, washed twice, and then serial dilutions were prepared and plated on LB agar. Plates were incubated at 37°C for 5 days before CFU enumeration.

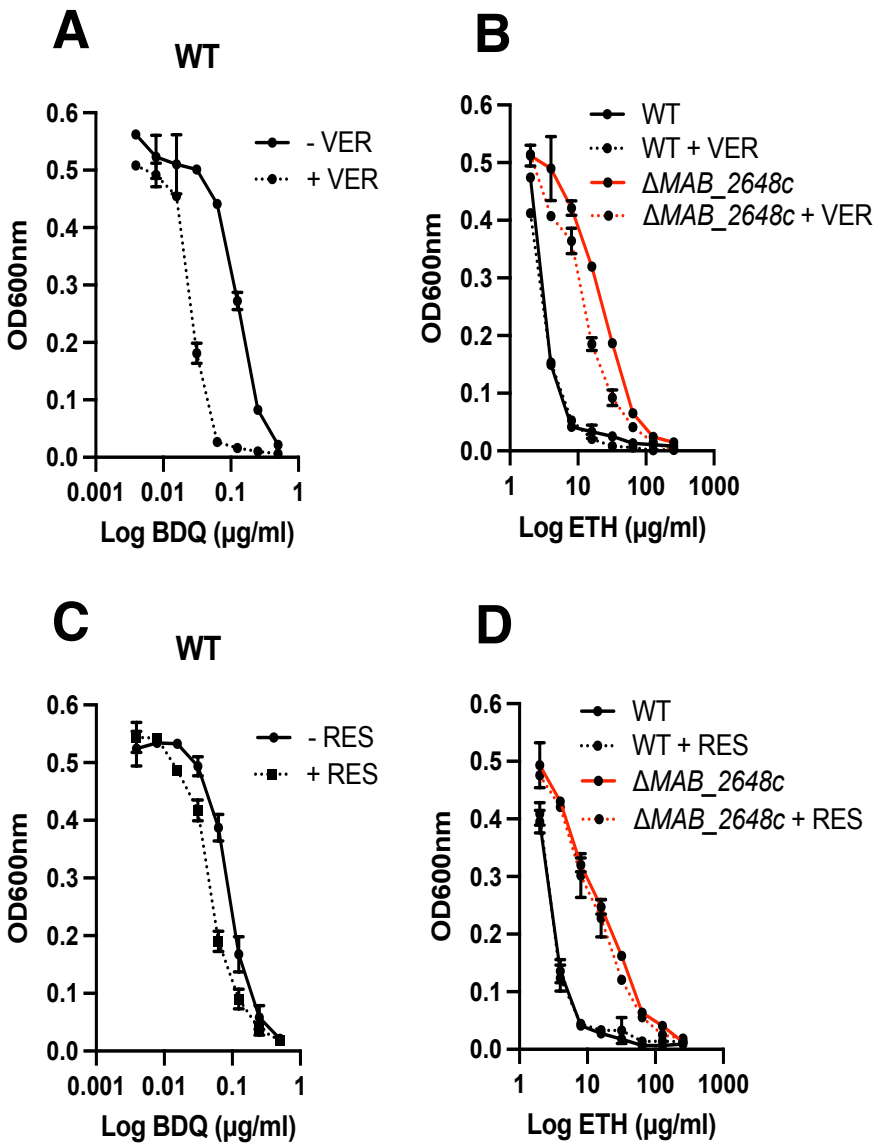
A
WT
OD600nm
0.6
0.5
0.4
0.3
0.2
0.1
0.0
0.001
0.01
0.1
1
Log BDQ (µg/ml)
- VER
+ VER
B
WT
WT + VER
ΔMAB_2648c
ΔMAB_2648c + VER
OD600nm
1
10
100
1000
Log ETH (µg/ml)
C
WT
- RES
+ RES
OD600nm
Log BDQ (µg/ml)
D
WT
WT + RES
ΔMAB_2648c
ΔMAB_2648c + RES
OD600nm
Log ETH (µg/ml)

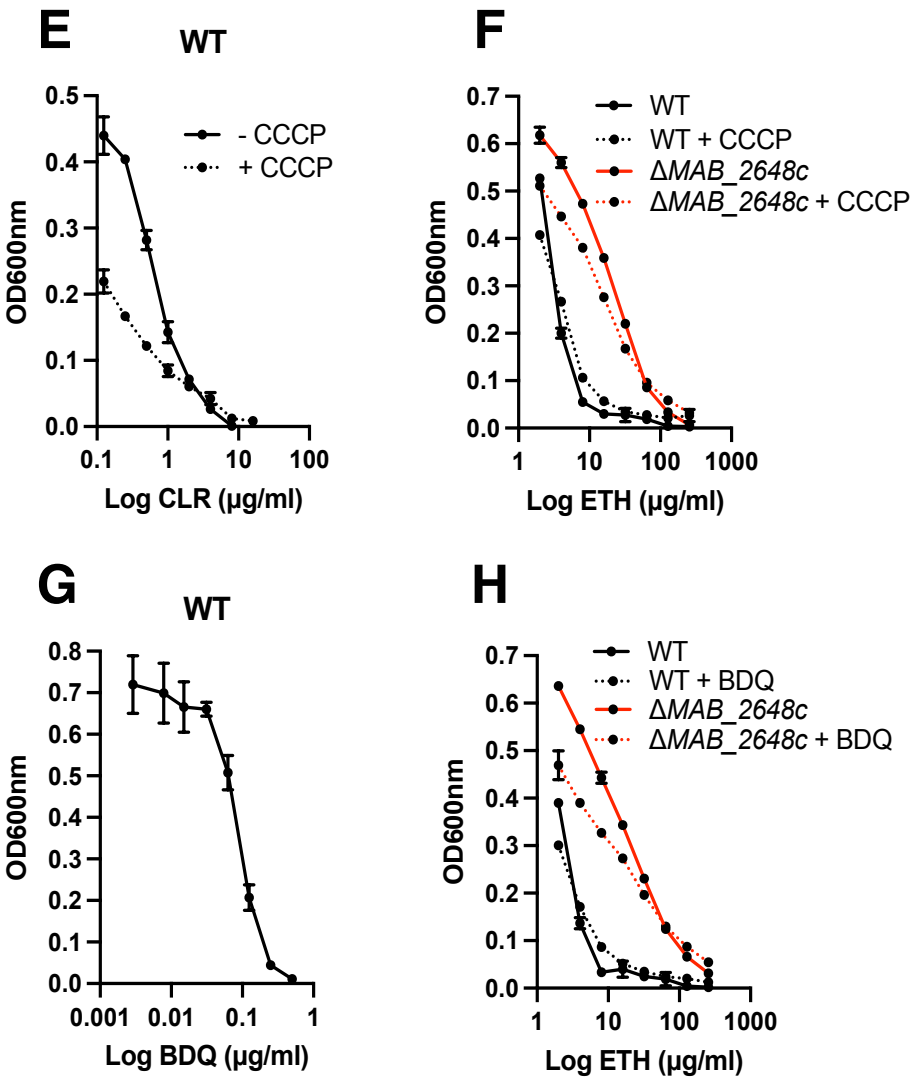

Figure 5.1. ETH sensitivity is not altered in the presence of efflux pump inhibitors and is independent of Mab_2648c activity. WT and Δ*MAB_2648c Mabs* were exposed to a two-fold dilution of ETH with and without subinhibitory concentrations the following efflux pump inhibitors: Verapamil (VER, 64 μg/ml) (A-B), Reserpine (RES, 10 μg/ml) (C-D), Carbonyl Cyanide Chlorophenylhydrazone (CCCP, 2 μg/ml) (E-F), and Bedaquiline (BDQ, 30 ng/ml) (G-H). Panels on the left (A, C, E, and G) represent positive control assays for each inhibitor used. CLR: Clarithromycin. Bacterial growth was measured as described in materials and methods.

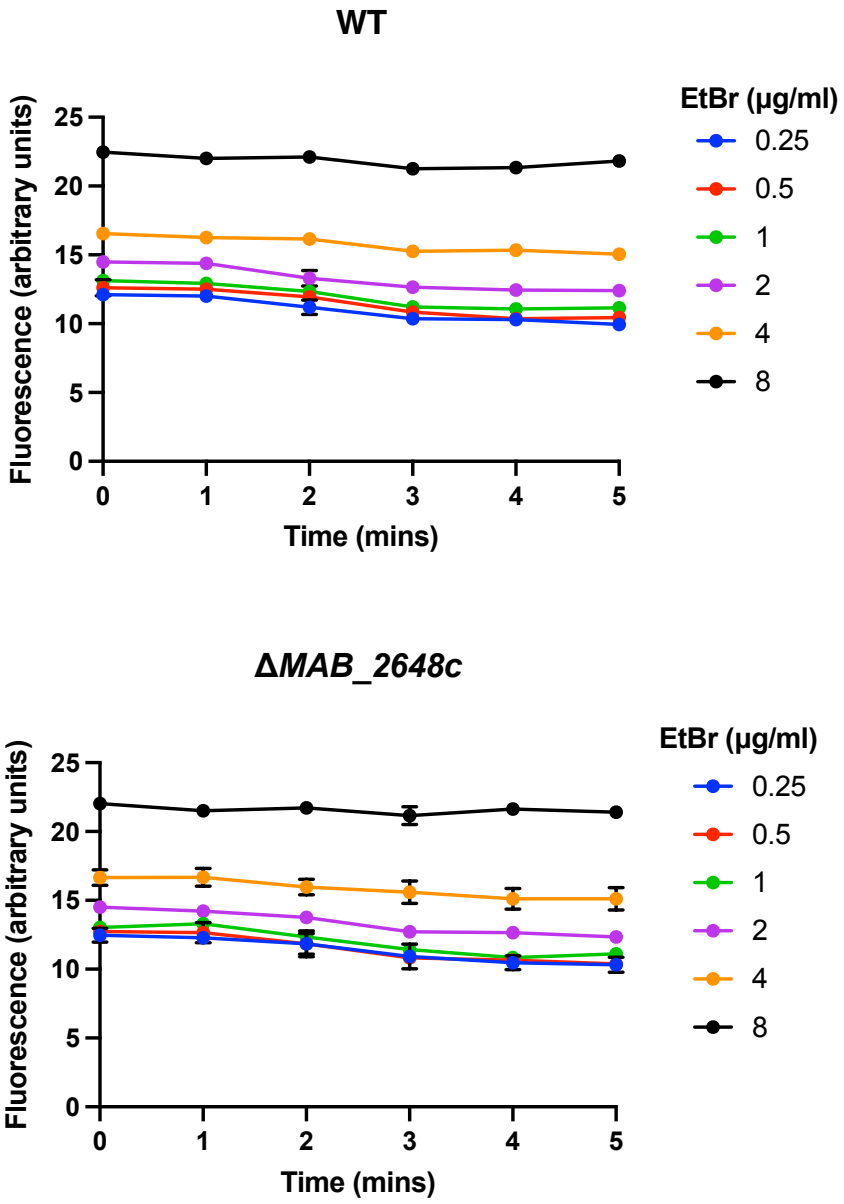

<u>Figure 5.2.</u> Loss of Mab_2648c activity does not lead to changes in Ethidium Bromide (EtBr) accumulation. WT (A) and Δ*MAB_2648c* (B) *Mabs* were treated with two-fold dilutions of EtBr (0.25 – 8 μg/ml) in PBS supplemented with 0.4% glucose (pH 7.4) and EtBr fluorescence measured for 60 minutes at 37°C (excitation wavelength: 530 nm; emission wavelength: 585 nm).

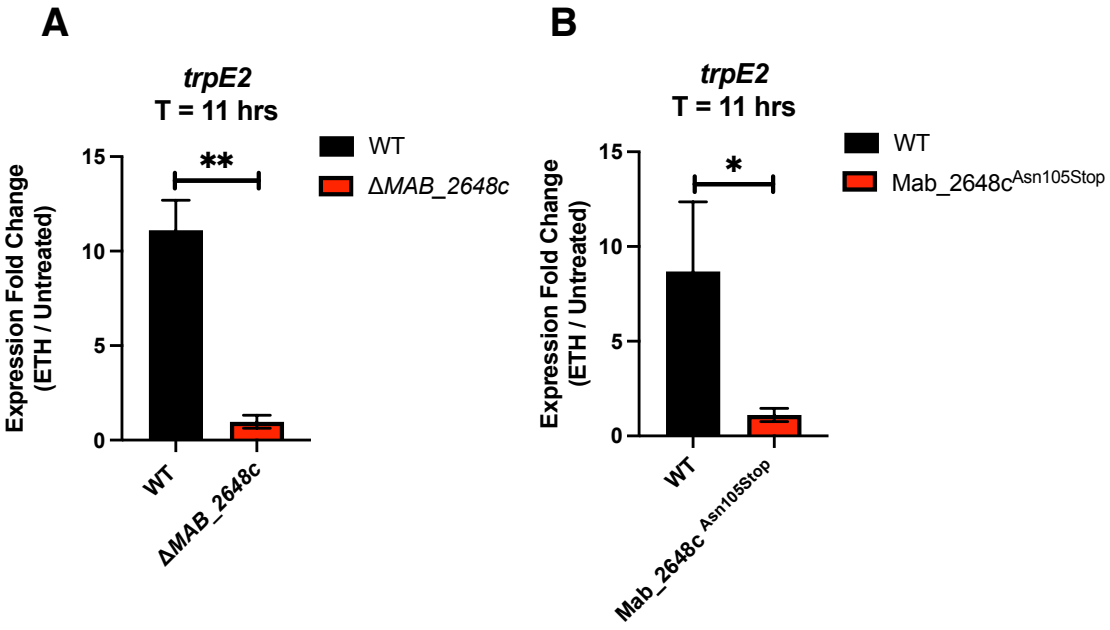

Figure 5.3. ETH exposure leads to *trpE2* induction and is dependent on Mab_2648c activity. WT, Δ*MAB_2648c*, and Mab_2648c^{Asn105Stop} *Mabs* were treated with and without ETH (16 μg/ml) for 11 hours. RNA was collected, reverse transcribed to cDNA, and then *trpE2* expression levels were measured by qPCR.

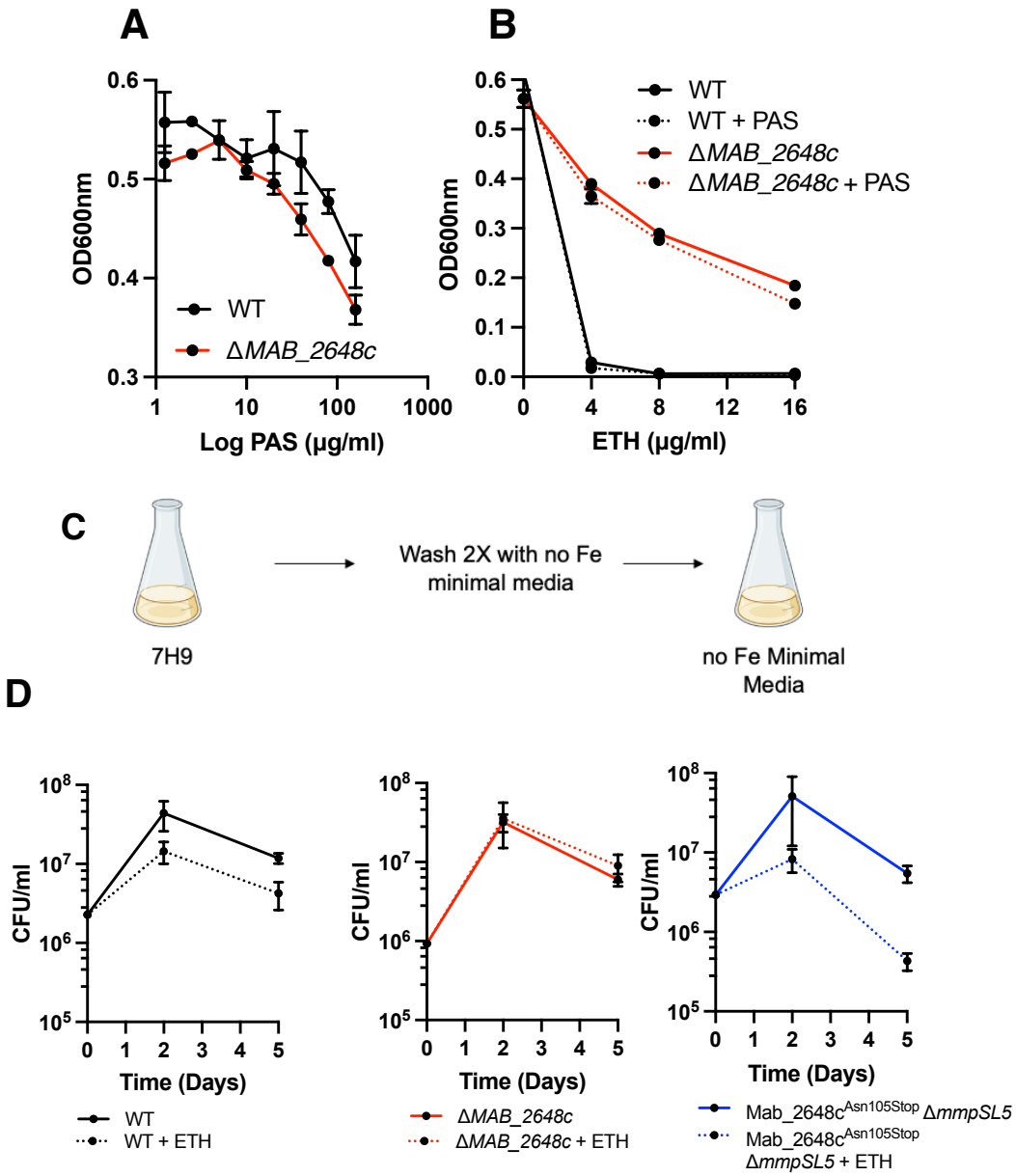

Figure 5.4. Bacterial growth under iron deprivation is independent of Mab_2648c. (A) WT and Δ*MAB_2648c Mabs* were treated with and without a two-fold dilution series of PAS. (B) WT and Δ*MAB_2648c Mabs* were treated with a two-fold dilution series of ETH with and without a subinhibitory concentration of PAS (1.25 µg/ml). Bacterial growth was examined as described in materials and methods. (C) Schematic representation of growth conditions established to achieve iron depletion. (D) The indicated bacterial strains adapted to iron-deprived growth conditions were cultured without iron and growth examined by plating for CFU with and without ETH at the indicated time points (8 µg/ml).

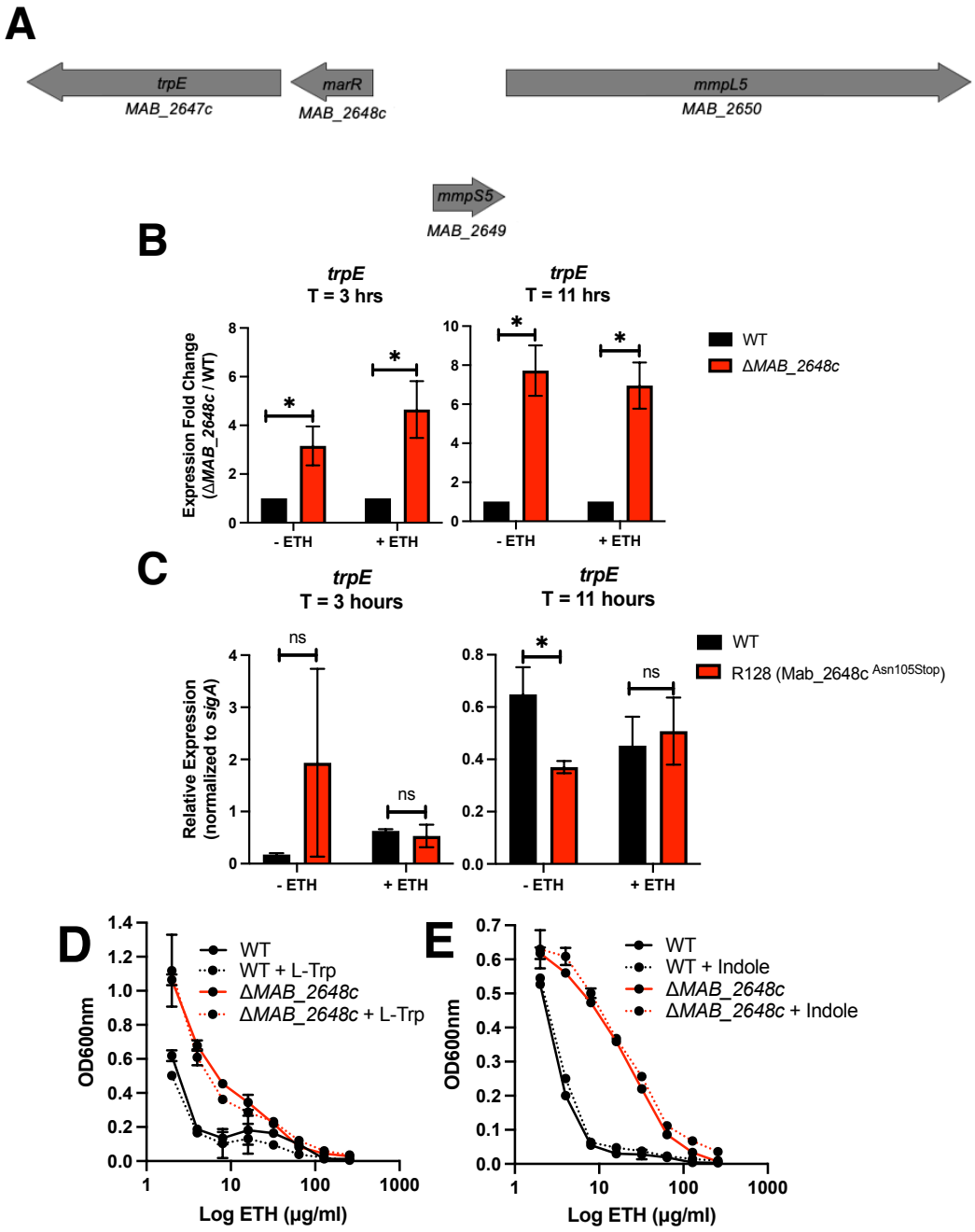

Figure 5.5. Transcriptional regulation of *trpE* is independent of Mab_2648c. (A) Schematic representation of the genomic organization of *trpE* relative to *MAB_2648c*. (B and C) WT, Δ*MAB_2648c* (B), and Mab_2648c^{Asn105Stop} (C) *Mabs* were treated with and without ETH (16 μg/ml) for 3 and 11 hours. RNA was collected, reverse transcribed to cDNA, and then *trpE* expression levels were measured by qPCR. (D and E) The indicated bacterial strains were treated with a two-fold dilution series of ETH with and without L-Tryptophan (L-Trp, 2 mM) (D) and Indole (3 μg/ml) (E). Bacterial growth was measured as described in materials and methods.

Future Directions

Identifying the substrate of the MmpSL5 transporter

MmpSL transporters in other mycobacteria are known to transport lipids into the extracellular space to assist with mycomembrane biogenesis (128). It is possible that the MmpSL5 transporter identified in this work is a lipid transporter, since ETH is a known inhibitor of lipid metabolism in *Mtb* (184, 333, 334), although it is currently unknown if this is also true for *Mabs*. Upregulation in MmpSL5 activity may result in more lipids being transported across the inner membrane, which may result in a less permeable mycomembrane. Reduced permeability may explain why the loss of *MAB_2648c* increases ETH resistance. To address these hypothesis, future work examining the permeability of the mycomembrane using fluorescence-based assays and lipid transport using thin-layer chromatography should be considered (335, 336).

High-throughput chemical screening assays to identify compounds that synergize with ETH

Several studies have identified many non-antibiotic, FDA approved compounds that are active against *Mabs* (125–127). Since we were unable to identify antibiotics and other compounds that synergize with ETH (Fig. 4.11; Table 4.2; Fig 5.1; & Fig 5.4 A-B), a high-throughput chemical screening approach should be considered in the future. Promising compounds would augment the clinical relevance of ETH against *Mabs*. It is possible that synergistic candidates can reduce the concentration of ETH needed to achieve a bactericidal effect to levels that are therapeutically achievable and tolerable to the host. Furthermore, potential candidates may have the ability to reverse ETH resistance (249). Such compounds should be examined in combination with ETH using mouse models of infection.

Identifying binding ligands and biological conditions associated with Mab_2648c transcriptional de-repression

It remains unknown what biological conditions lead to transcriptional de-repression of Mab_2648c and subsequent upregulation of *mmpSL5* and other potential, target genes. Future work should involve screening a chemical library of aromatic compounds for their ability to bind to purified Mab_2648c using biochemical approaches. Potential candidates should then be screened for their ability to induce transcriptional de-repression of Mab_2648c using RNA seq and chromatin immunoprecipitation followed by sequencing (ChIP-Seq) (243). Identifying natural ligands of Mab_2648c may prove useful in determining the biological function of Mab_2648c unrelated to ETH resistance and/or the ETH mechanism of action.

Conclusions

ETH displays mild bactericidal activity against *Mabs in vitro* and possibly *in vivo*, suggesting that ETH may have repurposing potential against *Mabs*. Importantly, we did not observe any antagonistic interactions with ETH when combined with some clinically relevant, functionally distinct antibiotics currently utilized to treat *Mabs* infections. It is worth noting that despite the lack of growth observed in bacteria treated with ETH/AMK and ETH/CLR 2-days post treatment, they were equally resistant to all drugs within this time interval, suggesting that this lack of growth may not be attributed to drug sensitivity, but possibly antibiotic persistence or tolerance.

We have identified an ETH resistance mechanism that requires the activity of an MmpSL5 transporter and is mediated by the MarR homolog Mab_2648c. In addition, we have identified potentially novel genetic determinants of drug sensitivity to AMK, CLR, and ETH using Tn-Seq that require further evaluation in future studies. For the clinically relevant antibiotics AMK and CLR, many of our TnSeq hits have not been previously reported to be important for growth on these antibiotics. Overlap in specific gene hits in our CLR and ETH dataset suggest there may be shared mechanisms of drug resistance among both drugs. The transport mechanism associated with MmpSL5 identified in this work remains unknown, but our findings rule out drug efflux and iron transport as potential mechanisms.

References

1. Griffith DE. 2019. Nontuberculous Mycobacterial Disease: An Introduction and Historical Perspective, p. 1–14. *In* Nontuberculous Mycobacterial Disease. Springer International Publishing, Cham.
2. Lopeman RC, Harrison J, Desai M, Cox JAG. 2019. Mycobacterium abscessus: Environmental Bacterium Turned Clinical Nightmare. Microorganisms 7:90.
3. Philley JV, Griffith DE. 2019. Disease Caused by Mycobacterium Abscessus and Other Rapidly Growing Mycobacteria (RGM), p. 369–399. *In* Nontuberculous Mycobacterial Disease. Springer International Publishing, Cham.
4. Sarma S, Sharma S, Baweja UK, Mehta Y. 2011. Mycobacterium abscessus bacteremia in an immunocompetent patient following a coronary artery bypass graft. J Cardiovasc Dis Res 2:80–82.
5. Lee M-R, Cheng A, Lee Y-C, Yang C-Y, Lai C-C, Huang Y-T, Ho C-C, Wang H-C, Yu C-J, Hsueh P-R. 2012. CNS infections caused by Mycobacterium abscessus complex: clinical features and antimicrobial susceptibilities of isolates. J Antimicrob Chemother 67:222–225.
6. Griffith DE, Girard WM, Wallace RJ Jr. 1993. Clinical features of pulmonary disease caused by rapidly growing mycobacteria. An analysis of 154 patients. Am Rev Respir Dis 147:1271–1278.
7. Lee M-R, Sheng W-H, Hung C-C, Yu C-J, Lee L-N, Hsueh P-R. 2015. Mycobacterium abscessus Complex Infections in Humans. Emerg Infect Dis 21:1638–1646.
8. Abdelaal HFM, Chan ED, Young L, Baldwin SL, Coler RN. 2022. Mycobacterium abscessus: It's complex. Microorganisms 10:1454.
9. Wagner D, Lipman M, Cooray S, Ringshausen FC, Morimoto K, Koh W-J, Thomson R. 2019. Global epidemiology of NTM disease (except northern America), p. 163–260. *In* Nontuberculous Mycobacterial Disease. Springer International Publishing, Cham.
10. Brown-Elliott BA, Wallace RJ Jr. 2002. Clinical and taxonomic status of pathogenic nonpigmented or late-pigmenting rapidly growing mycobacteria. Clin Microbiol Rev 15:716–746.
11. Falkinham JO. 2003. The changing pattern of nontuberculous mycobacterial disease. Can J Infect Dis 14:281–286.
12. Donohue MJ, Wymer L. 2016. Increasing prevalence rate of nontuberculous mycobacteria infections in five states, 2008–2013. Ann Am Thorac Soc 13:2143–2150.
13. Kothavade RJ, Dhurat RS, Mishra SN, Kothavade UR. 2013. Clinical and laboratory aspects of the diagnosis and management of cutaneous and subcutaneous infections caused by rapidly growing mycobacteria. Eur J Clin Microbiol Infect Dis 32:161–188.
14. Johnson MM, Odell JA. 2014. Nontuberculous mycobacterial pulmonary infections. J Thorac Dis 6:210–220.
15. Wang L, Ding W, Mo Y, Shi D, Zhang S, Zhong L, Wang K, Wang J, Huang C, Zhang S, Ye Z, Shen J, Xing Z. 2021. Distinguishing nontuberculous mycobacteria from

Mycobacterium tuberculosis lung disease from CT images using a deep learning framework. Eur J Nucl Med Mol Imaging 48:4293–4306.
16. 2000. Management of opportunist mycobacterial infections: Joint Tuberculosis Committee Guidelines 1999. Subcommittee of the Joint Tuberculosis Committee of the British Thoracic Society. Thorax 55:210–218.
17. Kwak N, Lee CH, Lee H-J, Kang YA, Lee JH, Han SK, Yim J-J. 2016. Non-tuberculous mycobacterial lung disease: diagnosis based on computed tomography of the chest. Eur Radiol 26:4449–4456.
18. Bernut A, Dupont C, Ogryzko NV, Neyret A, Herrmann J-L, Floto RA, Renshaw SA, Kremer L. 2019. CFTR protects against Mycobacterium abscessus infection by fine-tuning host oxidative defenses. Cell Rep 26:1828-1840.e4.
19. Gadsby DC, Vergani P, Csanády L. 2006. The ABC protein turned chloride channel whose failure causes cystic fibrosis. Nature 440:477–483.
20. Donaldson SH, Boucher RC. 2003. Update on pathogenesis of cystic fibrosis lung disease. Curr Opin Pulm Med 9:486–491.
21. Gardner AI, McClenaghan E, Saint G, McNamara PS, Brodlie M, Thomas MF. 2019. Epidemiology of nontuberculous mycobacteria infection in children and young people with cystic fibrosis: Analysis of UK cystic fibrosis Registry. Clin Infect Dis 68:731–737.
22. D. Grogono, J. Bryant, D. Rodriguez-Rincon, I. Everall, K. Brown, P. Moreno, D. Verma, E. Hill, J. Drijkoningen, C. Haworth, S. Harris, D. Ordway, J. Parkhill, R. Floto. 2017. Whole-Genome Sequencing Reveals Global Spread of Mycobacterium abscessus Clones Amongst Patients with Cystic Fibrosis. C25 NON-TUBERCULOUS MYCOBACTERIA: FROM BENCH TO CLINIC A7650.
23. Ruis C, Bryant JM, Bell SC, Thomson R, Davidson RM, Hasan NA, van Ingen J, Strong M, Floto RA, Parkhill J. 2021. Dissemination of Mycobacterium abscessus via global transmission networks. Nat Microbiol 6:1279–1288.
24. Bryant JM, Brown KP, Burbaud S, Everall I, Belardinelli JM, Rodriguez-Rincon D, Grogono DM, Peterson CM, Verma D, Evans IE, Ruis C, Weimann A, Arora D, Malhotra S, Bannerman B, Passemar C, Templeton K, MacGregor G, Jiwa K, Fisher AJ, Blundell TL, Ordway DJ, Jackson M, Parkhill J, Floto RA. 2021. Stepwise pathogenic evolution of Mycobacterium abscessus. Science 372:eabb8699.
25. Yoshida M, Chien J-Y, Morimoto K, Kinjo T, Aono A, Murase Y, Fujiwara K, Morishige Y, Nagano H, Jou R, Hasegawa N, Ato M, Hoshino Y, Hsueh P-R, Mitarai S. 2022. Molecular epidemiological characteristics of Mycobacterium abscessus complex derived from non-cystic fibrosis patients in Japan and Taiwan. Microbiol Spectr 10:e0057122.
26. Davidson RM, Hasan NA, de Moura VCN, Duarte RS, Jackson M, Strong M. 2013. Phylogenomics of Brazilian epidemic isolates of Mycobacterium abscessus subsp. bolletii reveals relationships of global outbreak strains. Infect Genet Evol 20:292–297.
27. Yan J, Kevat A, Martinez E, Teese N, Johnson K, Ranganathan S, Harrison J, Massie J, Daley A. 2020. Investigating transmission of Mycobacterium abscessus amongst children in an Australian cystic fibrosis centre. J Cyst Fibros 19:219–224.

28. Fujiwara K, Yoshida M, Murase Y, Aono A, Furuuchi K, Tanaka Y, Ohta K, Ato M, Mitarai S, Morimoto K. 2022. Potential cross-transmission of Mycobacterium abscessus among non-cystic fibrosis patients at a tertiary hospital in Japan. Microbiol Spectr 10:e0009722.
29. Chew KL, Octavia S, Jureen R, Ng OT, Marimuthu K, Lin RTP, Teo JWP. 2021. Molecular epidemiology and phylogenomic analysis of Mycobacterium abscessus clinical isolates in an Asian population. Microb Genom 7.
30. Wetzstein N, Diricks M, Kohl TA, Wichelhaus TA, Andres S, Paulowski L, Schwarz C, Lewin A, Kehrmann J, Kahl BC, Dichtl K, Hügel C, Eickmeier O, Smaczny C, Schmidt A, Zimmermann S, Nährlich L, Hafkemeyer S, Niemann S, Maurer FP, Hogardt M. 2022. Molecular epidemiology of Mycobacterium abscessus isolates recovered from German cystic fibrosis patients. Microbiol Spectr 10:e0171422.
31. Harris KA, Underwood A, Kenna DTD, Brooks A, Kavaliunaite E, Kapatai G, Tewolde R, Aurora P, Dixon G. 2015. Whole-genome sequencing and epidemiological analysis do not provide evidence for cross-transmission of mycobacterium abscessus in a cohort of pediatric cystic fibrosis patients. Clin Infect Dis 60:1007–1016.
32. Yoon J-K, Kim TS, Kim J-I, Yim J-J. 2020. Whole genome sequencing of Nontuberculous Mycobacterium (NTM) isolates from sputum specimens of co-habiting patients with NTM pulmonary disease and NTM isolates from their environment. BMC Genomics 21:322.
33. Thomson R, Donnan E, Konstantinos A. 2017. Notification of nontuberculous mycobacteria: An Australian perspective. Ann Am Thorac Soc 14:318–323.
34. Nie W, Duan H, Huang H, Lu Y, Bi D, Chu N. 2014. Species identification of Mycobacterium abscessus subsp. abscessus and Mycobacterium abscessus subsp. bolletii using rpoB and hsp65, and susceptibility testing to eight antibiotics. Int J Infect Dis 25:170–174.
35. Li G, Lian L-L, Wan L, Zhang J, Zhao X, Jiang Y, Zhao L-L, Liu H, Wan K. 2013. Antimicrobial susceptibility of standard strains of nontuberculous mycobacteria by microplate Alamar Blue assay. PLoS One 8:e84065.
36. Luthra S, Rominski A, Sander P. 2018. The role of antibiotic-target-modifying and antibiotic-modifying enzymes in Mycobacterium abscessus drug resistance. Front Microbiol 9:2179.
37. Nessar R, Cambau E, Reyrat JM, Murray A, Gicquel B. 2012. Mycobacterium abscessus: a new antibiotic nightmare. J Antimicrob Chemother 67:810–818.
38. Griffith DE, Brown-Elliott BA, Benwill JL, Wallace RJ Jr. 2015. Mycobacterium abscessus. “Pleased to meet you, hope you guess my name...” Ann Am Thorac Soc 12:436–439.
39. Griffith DE, Aksamit T, Brown-Elliott BA, Catanzaro A, Daley C, Gordin F, Holland SM, Horsburgh R, Huitt G, Iademarco MF, Iseman M, Olivier K, Ruoss S, von Reyn CF, Wallace RJ Jr, Winthrop K, ATS Mycobacterial Diseases Subcommittee, American Thoracic Society, Infectious Disease Society of America. 2007. An official ATS/IDSA statement: diagnosis, treatment, and prevention of nontuberculous mycobacterial diseases. Am J Respir Crit Care Med 175:367–416.

40. Haworth CS, Banks J, Capstick T, Fisher AJ, Gorsuch T, Laurenson IF, Leitch A, Loebinger MR, Milburn HJ, Nightingale M, Ormerod P, Shingadia D, Smith D, Whitehead N, Wilson R, Floto RA. 2017. British Thoracic Society guidelines for the management of non-tuberculous mycobacterial pulmonary disease (NTM-PD). Thorax 72:ii1–ii64.
41. Harada T, Akiyama Y, Kurashima A, Nagai H, Tsuyuguchi K, Fujii T, Yano S, Shigeto E, Kuraoka T, Kajiki A, Kobashi Y, Kokubu F, Sato A, Yoshida S, Iwamoto T, Saito H. 2013. Clinical and Microbiological Differences between Mycobacterium abscessus and Mycobacterium massiliense Lung Diseases. J Clin Microbiol 51:1061–1061.
42. Weng Y-W, Huang C-K, Sy C-L, Wu K-S, Tsai H-C, Lee SS-J. 2020. Treatment for Mycobacterium abscessus complex-lung disease. J Formos Med Assoc 119 Suppl 1:S58–S66.
43. Park YE, Jo K-W, Chong YP, Shim TS. 2020. Spontaneous sputum conversion and reversion in Mycobacterium abscessus complex lung diseaseB106. BREAKTHROUGHS IN NTM DIAGNOSIS AND TREATMENT. American Thoracic Society.
44. Cheng L-P, Chen S-H, Lou H, Gui X-W, Shen X-N, Cao J, Sha W, Sun Q. 2022. Factors associated with treatment outcome in patients with nontuberculous Mycobacterial pulmonary disease: A large population-based retrospective cohort study in Shanghai. Trop Med Infect Dis 7.
45. Chandrashekaran S, Escalante P, Kennedy CC. 2017. Mycobacterium abscessus disease in lung transplant recipients: Diagnosis and management. J Clin Tuberc Other Mycobact Dis 9:10–18.
46. Broncano-Lavado A, Senhaji-Kacha A, Santamaría-Corral G, Esteban J, García-Quintanilla M. 2022. Alternatives to antibiotics against Mycobacterium abscessus. Antibiotics (Basel) 11:1322.
47. Smibert O, Snell GI, Bills H, Westall GP, Morrissey CO. 2016. Mycobacterium abscessus complex - a particular challenge in the setting of lung transplantation. Expert Rev Anti Infect Ther 14:325–333.
48. Garrison AP, Morris MI, Doblecki Lewis S, Smith L, Cleary TJ, Procop GW, Vincek V, Rosa-Cunha I, Alfonso B, Burke GW, Tzakis A, Hartstein AI. 2009. Mycobacterium abscessus infection in solid organ transplant recipients: report of three cases and review of the literature. Transpl Infect Dis 11:541–548.
49. Vongthilath R, Richaud Thiriez B, Dehillotte C, Lemonnier L, Guillien A, Degano B, Dalphin M-L, Dalphin J-C, Plésiat P. 2019. Clinical and microbiological characteristics of cystic fibrosis adults never colonized by Pseudomonas aeruginosa: Analysis of the French CF registry. PLoS One 14:e0210201.
50. Kramer R, Sauer-Heilborn A, Welte T, Guzman CA, Abraham W-R, Höfle MG. 2015. Cohort study of airway mycobiome in adult cystic fibrosis patients: Differences in community structure between fungi and bacteria reveal predominance of transient fungal elements. J Clin Microbiol 53:2900–2907.
51. Esposito A, Pompilio A, Bettua C, Crocetta V, Giacobazzi E, Fiscarelli E, Jousson O, Di Bonaventura G. 2017. Evolution of Stenotrophomonas maltophilia in cystic fibrosis

lung over chronic infection: A genomic and phenotypic population study. Front Microbiol 8:1590.
52. Chernenko SM, Humar A, Hutcheon M, Chow C-W, Chaparro C, Keshavjee S, Singer LG. 2006. Mycobacterium abscessus infections in lung transplant recipients: the international experience. J Heart Lung Transplant 25:1447–1455.
53. Longworth SA, Vinnard C, Lee I, Sims KD, Barton TD, Blumberg EA. 2014. Risk factors for nontuberculous mycobacterial infections in solid organ transplant recipients: a case-control study. Transpl Infect Dis 16:76–83.
54. Misch EA, Saddler C, Davis JM. 2018. Skin and soft tissue infections due to nontuberculous mycobacteria. Curr Infect Dis Rep 20:6.
55. Moreno-Izquierdo C, Zurita J, Contreras-Yametti FI, Jara-Palacios MA. 2020. Mycobacterium abscessus subspecies abscessus infection associated with cosmetic surgical procedures: Cases series. IDCases 22:e00992.
56. Toporek A, Lechtzin N. 2022. Viruses to the rescue-Use of bacteriophage to treat resistant pulmonary infections. Cell. Elsevier BV.
57. Dedrick RM, Smith BE, Cristinziano M, Freeman KG, Jacobs-Sera D, Belessis Y, Whitney Brown A, Cohen KA, Davidson RM, van Duin D, Gainey A, Garcia CB, Robert George CR, Haidar G, Ip W, Iredell J, Khatami A, Little JS, Malmivaara K, McMullan BJ, Michalik DE, Moscatelli A, Nick JA, Tupayachi Ortiz MG, Polenakovik HM, Robinson PD, Skurnik M, Solomon DA, Soothill J, Spencer H, Wark P, Worth A, Schooley RT, Benson CA, Hatfull GF. 2022. Phage therapy of Mycobacterium infections: Compassionate-use of phages in twenty patients with drug-resistant Mycobacterial disease. Clin Infect Dis https://doi.org/10.1093/cid/ciac453.
58. Nick JA, Dedrick RM, Gray AL, Vladar EK, Smith BE, Freeman KG, Malcolm KC, Epperson LE, Hasan NA, Hendrix J, Callahan K, Walton K, Vestal B, Wheeler E, Rysavy NM, Poch K, Caceres S, Lovell VK, Hisert KB, de Moura VC, Chatterjee D, De P, Weakly N, Martiniano SL, Lynch DA, Daley CL, Strong M, Jia F, Hatfull GF, Davidson RM. 2022. Host and pathogen response to bacteriophage engineered against Mycobacterium abscessus lung infection. Cell 185:1860-1874.e12.
59. Dedrick RM, Freeman KG, Nguyen JA, Bahadirli-Talbott A, Cardin ME, Cristinziano M, Smith BE, Jeong S, Ignatius EH, Lin CT, Cohen KA, Hatfull GF. 2022. Nebulized bacteriophage in a patient with refractory Mycobacterium abscessus lung disease. Open Forum Infect Dis 9:ofac194.
60. Dedrick RM, Freeman KG, Nguyen JA, Bahadirli-Talbott A, Smith BE, Wu AE, Ong AS, Lin CT, Ruppel LC, Parrish NM, Hatfull GF, Cohen KA. 2021. Potent antibody-mediated neutralization limits bacteriophage treatment of a pulmonary Mycobacterium abscessus infection. Nat Med 27:1357–1361.
61. Dedrick RM, Guerrero-Bustamante CA, Garlena RA, Russell DA, Ford K, Harris K, Gilmour KC, Soothill J, Jacobs-Sera D, Schooley RT, Hatfull GF, Spencer H. 2019. Engineered bacteriophages for treatment of a patient with a disseminated drug-resistant Mycobacterium abscessus. Nat Med 25:730–733.
62. Phage Therapy of Mycobacterium Infections: Compassionate-use of Phages in Twenty Patients 1 with Drug-Resistant Mycobacterial Disease.

63. Wright RCT, Friman V-P, Smith MCM, Brockhurst MA. 2019. Resistance evolution against phage combinations depends on the timing and order of exposure. MBio 10.
64. Moller AG, Lindsay JA, Read TD. 2019. Determinants of phage host range in Staphylococcus species. Appl Environ Microbiol 85.
65. Qvist T, Eickhardt S, Kragh KN, Andersen CB, Iversen M, Høiby N, Bjarnsholt T. 2015. Chronic pulmonary disease with Mycobacterium abscessus complex is a biofilm infection. Eur Respir J 46:1823–1826.
66. Kim B-R, Kim B-J, Kook Y-H, Kim B-J. 2019. Phagosome escape of rough Mycobacterium abscessus strains in Murine macrophage via phagosomal rupture can lead to type I interferon production and their cell-to-cell spread. Front Immunol 10:125.
67. Lara-Reyna S, Scambler T, Holbrook J, Wong C, Jarosz-Griffiths HH, Martinon F, Savic S, Peckham D, McDermott MF. 2019. Metabolic reprograming of cystic fibrosis macrophages via the IRE1α arm of the unfolded protein response results in exacerbated inflammation. Front Immunol 10:1789.
68. Lara-Reyna S, Holbrook J, Jarosz-Griffiths HH, Peckham D, McDermott MF. 2020. Dysregulated signalling pathways in innate immune cells with cystic fibrosis mutations. Cell Mol Life Sci 77:4485–4503.
69. Wakao H, Yoshikiyo K, Koshimizu U, Furukawa T, Enomoto K, Matsunaga T, Tanaka T, Yasutomi Y, Yamada T, Minakami H, Tanaka J, Oda A, Sasaki T, Wakao R, Lantz O, Udagawa T, Sekiya Y, Higuchi K, Harada N, Nishimura K, Ohtaka M, Nakanishi M, Fujita H. 2013. Expansion of functional human mucosal-associated invariant T cells via reprogramming to pluripotency and redifferentiation. Cell Stem Cell 12:546–558.
70. Kim J-S, Cha S-H, Kim WS, Han SJ, Cha SB, Kim HM, Kwon KW, Kim SJ, Choi H-H, Lee J, Cho S-N, Koh W-J, Park Y-M, Shin SJ. 2016. A novel therapeutic approach using mesenchymal stem cells to protect against Mycobacterium abscessus. Stem Cells 34:1957–1970.
71. Ricotta EE, Prevots DR, Olivier KN. 2022. CFTR modulator use and risk of nontuberculous mycobacteria positivity in cystic fibrosis, 2011-2018. ERJ Open Res 8:00724–02021.
72. Elson EC, Capel P, Haynes J, Duehlmeyer S, Fischer M, Escobar H. 2022. CFTR modulator therapy in an individual with cystic fibrosis caused by a N1303K CFTR variant and infected with Mycobacterium abscessus. J Pediatr Pharmacol Ther 27:396–399.
73. Goetz DM, Savant AP. 2021. Review of CFTR modulators 2020. Pediatr Pulmonol 56:3595–3606.
74. Zhang S, Zou Y, Guo Q, Chen J, Xu L, Wan X, Zhang Z, Li B, Chu H. 2020. AR-12 exhibits direct and host-targeted antibacterial activity toward Mycobacterium abscessus. Antimicrob Agents Chemother 64.
75. Kim YS, Kim JK, Hanh BTB, Kim SY, Kim HJ, Kim YJ, Jeon SM, Park CR, Oh GT, Park J-W, Kim J-M, Jang J, Jo E-K. 2020. The peroxisome proliferator-activated receptor α- agonist gemfibrozil promotes defense against Mycobacterium abscessus infections. Cells 9:648.

76. Poerio N, Riva C, Olimpieri T, Rossi M, Lorè NI, De Santis F, Henrici De Angelis L, Ciciriello F, D'Andrea MM, Lucidi V, Cirillo DM, Fraziano M. 2022. Combined host- and pathogen-directed therapy for the control of Mycobacterium abscessus infection. Microbiol Spectr 10:e0254621.
77. Ferrell KC, Johansen MD, Triccas JA, Counoupas C. 2022. Virulence mechanisms of Mycobacterium abscessus: Current knowledge and implications for vaccine design. Front Microbiol 13:842017.
78. Johnson MM, Collier MA, Hoang KV, Pino EN, Graham-Gurysh EG, Gallovic MD, Zahid MSH, Chen N, Schlesinger L, Gunn JS, Bachelder EM, Ainslie KM. 2018. In vivo and cellular trafficking of acetalated dextran microparticles for delivery of a host-directed therapy for salmonella enterica serovar typhi infection. Mol Pharm 15:5336–5348.
79. Hoang KV, Curry H, Collier MA, Borteh H, Bachelder EM, Schlesinger LS, Gunn JS, Ainslie KM. 2016. Needle-free delivery of acetalated dextran-encapsulated AR-12 protects mice from Francisella tularensis lethal challenge. Antimicrob Agents Chemother 60:2052–2062.
80. Molina-Torres CA, Tamez-Peña L, Castro-Garza J, Ocampo-Candiani J, Vera-Cabrera L. 2018. Evaluation of the intracellular activity of drugs against Mycobacterium abscessus using a THP-1 macrophage model. J Microbiol Methods 148:29–32.
81. Gugliandolo E, Fusco R, Ginestra G, D'amico R, Bisignano C, Mandalari G, Cuzzocrea S, Di Paola R. 2019. Involvement of TLR4 and PPAR-α receptors in host response and NLRP3 inflammasome activation, against pulmonary infection with Pseudomonas aeruginosa. Shock 51:221–227.
82. Kim YS, Lee H-M, Kim JK, Yang C-S, Kim TS, Jung M, Jin HS, Kim S, Jang J, Oh GT, Kim J-M, Jo E-K. 2017. PPAR-α activation mediates innate host defense through induction of TFEB and lipid catabolism. J Immunol 198:3283–3295.
83. Asayama K, Sandhir R, Sheikh FG, Hayashibe H, Nakane T, Singh I. 1999. Increased peroxisomal fatty acid beta-oxidation and enhanced expression of peroxisome proliferator-activated receptor-alpha in diabetic rat liver. Mol Cell Biochem 194:227–234.
84. Watson K, Russell CD, Baillie JK, Dhaliwal K, Fitzgerald JR, Mitchell TJ, Simpson AJ, Renshaw SA, Dockrell DH. 2020. Developing novel host-based therapies targeting microbicidal responses in macrophages and neutrophils to combat bacterial antimicrobial resistance. Front Immunol 11:786.
85. Chung Y-SA, Kocks C. 2012. Phagocytosis of bacterial pathogens. Fly (Austin) 6:21–25.
86. Steinberg BE, Grinstein S. 2008. Pathogen destruction versus intracellular survival: the role of lipids as phagosomal fate determinants. J Clin Invest 118:2002–2011.
87. Yeung T, Grinstein S. 2007. Lipid signaling and the modulation of surface charge during phagocytosis. Immunol Rev 219:17–36.
88. Wu M-L, Aziz DB, Dartois V, Dick T. 2018. NTM drug discovery: status, gaps and the way forward. Drug Discov Today 23:1502–1519.
89. Falkinham JO III. 2018. Challenges of NTM drug development. Front Microbiol 9.

90. Soni I, De Groote MA, Dasgupta A, Chopra S. 2016. Challenges facing the drug discovery pipeline for non-tuberculous mycobacteria. J Med Microbiol 65:1–8.
91. Gumbo T, Cirrincione K, Srivastava S. 2020. Repurposing drugs for treatment of Mycobacterium abscessus: a view to a kill. J Antimicrob Chemother 75:1212–1217.
92. Lee SFK, Laughon BE, McHugh TD, Lipman M. 2019. New drugs to treat difficult tuberculous and nontuberculous mycobacterial pulmonary disease. Curr Opin Pulm Med 25:271–280.
93. DiMasi JA, Grabowski HG, Hansen RW. 2016. Innovation in the pharmaceutical industry: New estimates of R&D costs. J Health Econ 47:20–33.
94. 2020. Tracking the global pipeline of antibiotics in developmentThe Pew Charitable Trusts.
95. Beyer P, Paulin S. 2020. The antibacterial research and development pipeline needs urgent solutions. ACS Infect Dis 6:1289–1291.
96. 2019. 2019 antibacterial agents in clinical development: an analysis of the antibacterial clinical development pipeline. World Health Organization.
97. Iannaccone M, Boattini M, Bianco G, Cavallo R, Costa C. 2022. Evaluation of synergistic activity of plazomicin-based combinations against KPC-producing Klebsiella pneumoniae with complex multidrug resistance phenotypes. J Chemother 34:71–72.
98. Farha MA, Brown ED. 2019. Drug repurposing for antimicrobial discovery. Nat Microbiol 4:565–577.
99. Ashburn TT, Thor KB. 2004. Drug repositioning: identifying and developing new uses for existing drugs. Nat Rev Drug Discov 3:673–683.
100. Egorova A, Jackson M, Gavrilyuk V, Makarov V. 2021. Pipeline of anti-Mycobacterium abscessus small molecules: Repurposable drugs and promising novel chemical entities. Med Res Rev 41:2350–2387.
101. Dupont C, Viljoen A, Thomas S, Roquet-Banères F, Herrmann J-L, Pethe K, Kremer L. 2017. Bedaquiline inhibits the ATP synthase in Mycobacterium abscessus and is effective in infected zebrafish. Antimicrob Agents Chemother 61.
102. Tang YW, Cheng B, Yeoh SF, Lin RTP, Teo JWP. 2018. Tedizolid Activity Against Clinical Mycobacterium abscessus Complex Isolates-An in vitro Characterization Study. Front Microbiol 9:2095.
103. Compain F, Soroka D, Heym B, Gaillard J-L, Herrmann J-L, Dorchène D, Arthur M, Dubée V. 2018. In vitro activity of tedizolid against the Mycobacterium abscessus complex. Diagn Microbiol Infect Dis 90:186–189.
104. Taramona-Espinoza C, Church LWP, Steed L. 2015. In vitro tedizolid minimum inhibitory concentration (MIC) against clinical isolates of Mycobacterium abscessus. Open Forum Infect Dis 2.
105. Lefebvre A-L, Le Moigne V, Bernut A, Veckerlé C, Compain F, Herrmann J-L, Kremer L, Arthur M, Mainardi J-L. 2017. Inhibition of the β-lactamase BlaMab by avibactam improves the in vitro and in vivo efficacy of imipenem against Mycobacterium abscessus. Antimicrob Agents Chemother 61.
106. Dubée V, Bernut A, Cortes M, Lesne T, Dorchene D, Lefebvre A-L, Hugonnet J-E, Gutmann L, Mainardi J-L, Herrmann J-L, Gaillard J-L, Kremer L, Arthur M. 2015. β-

Lactamase inhibition by avibactam in Mycobacterium abscessus. J Antimicrob Chemother 70:1051–1058.
107. Kaushik A, Gupta C, Fisher S, Story-Roller E, Galanis C, Parrish N, Lamichhane G. 2017. Combinations of avibactam and carbapenems exhibit enhanced potencies against drug-resistant Mycobacterium abscessus. Future Microbiol 12:473–480.
108. Meir M, Bifani P, Barkan D. 2018. The addition of avibactam renders piperacillin an effective treatment for Mycobacterium abscessus infection in an in vivo model. Antimicrob Resist Infect Control 7:151.
109. Le Run E, Arthur M, Mainardi J-L. 2019. In vitro and intracellular activity of imipenem combined with tedizolid, rifabutin, and avibactam against Mycobacterium abscessus. Antimicrob Agents Chemother 63.
110. Pryjma M, Burian J, Thompson CJ. 2018. Rifabutin acts in synergy and is bactericidal with frontline Mycobacterium abscessus antibiotics clarithromycin and tigecycline, suggesting a potent treatment combination. Antimicrob Agents Chemother 62.
111. Ganapathy US, Dartois V, Dick T. 2019. Repositioning rifamycins for Mycobacterium abscessus lung disease. Expert Opin Drug Discov 14:867–878.
112. Aziz DB, Low JL, Wu M-L, Gengenbacher M, Teo JWP, Dartois V, Dick T. 2017. Rifabutin Is Active against Mycobacterium abscessus Complex. Antimicrob Agents Chemother 61.
113. Le Run E, Arthur M, Mainardi J-L. 2018. In vitro and intracellular activity of imipenem combined with rifabutin and avibactam against Mycobacterium abscessus. Antimicrob Agents Chemother 62.
114. Halloum I, Viljoen A, Khanna V, Craig D, Bouchier C, Brosch R, Coxon G, Kremer L. 2017. Resistance to thiacetazone derivatives active against Mycobacterium abscessus involves mutations in the MmpL5 transcriptional repressor MAB_4384. Antimicrob Agents Chemother 61.
115. Calvori C, Frontali L, Leoni L, Tecce G. 1965. Effect of rifamycin on protein synthesis. Nature 207:417–418.
116. Hartmann G, Honikel KO, Knüsel F, Nüesch J. 1967. The specific inhibition of the DNA-directed RNA synthesis by rifamycin. Biochim Biophys Acta 145:843–844.
117. Pang H, Li G, Zhao X, Liu H, Wan K, Yu P. 2015. Drug susceptibility testing of 31 antimicrobial agents on rapidly growing mycobacteria isolates from China. Biomed Res Int 2015:419392.
118. Sha W, Weng X-H, Xiao H-P, He G-J. 2003. Investigation of drug-resistance to rifampin and rpoB gene sequence analysis of Mycobacterium abscessus. Zhonghua Jie He He Hu Xi Za Zhi 26:544–547.
119. Cheng A, Tsai Y-T, Chang S-Y, Sun H-Y, Wu U-I, Sheng W-H, Chen Y-C, Chang S-C. 2019. In vitro synergism of rifabutin with clarithromycin, imipenem, and tigecycline against the Mycobacterium abscessus complex. Antimicrob Agents Chemother 63.
120. Story-Roller E, Maggioncalda EC, Lamichhane G. 2019. Select β-lactam combinations exhibit synergy against Mycobacterium abscessus in vitro. Antimicrob Agents Chemother 63.

121. Davidson PT, Le HQ. 1992. Drug treatment of tuberculosis--1992. Drugs 43:651–673.
122. Nunn P, Porter J, Winstanley P. 1993. Thiacetazone--avoid like poison or use with care? Trans R Soc Trop Med Hyg 87:578–582.
123. Watkins WM, Mungai M, Muhia DK, Mberu EK, Gathua S, Winstanley PA, Gilks CF, Nunn P. 1996. Cutaneous hypersensitivity reactions to thiacetazone, HIV infection and thiacetazone concentrations in plasma. Br J Clin Pharmacol 41:160–162.
124. Grzegorzewicz AE, Eynard N, Quémard A, North EJ, Margolis A, Lindenberger JJ, Jones V, Korduláková J, Brennan PJ, Lee RE, Ronning DR, McNeil MR, Jackson M. 2015. Covalent modification of the Mycobacterium tuberculosis FAS-II dehydratase by Isoxyl and Thiacetazone. ACS Infect Dis 1:91–97.
125. Richter A, Strauch A, Chao J, Ko M, Av-Gay Y. 2018. Screening of preselected libraries targeting Mycobacterium abscessus for drug discovery. Antimicrob Agents Chemother 62:AAC.00828-18.
126. Gupta R, Netherton M, Byrd TF, Rohde KH. 2017. Reporter-Based Assays for High-Throughput Drug Screening against Mycobacterium abscessus. Front Microbiol 8.
127. Chopra S, Matsuyama K, Hutson C, Madrid P. 2011. Identification of antimicrobial activity among FDA-approved drugs for combating Mycobacterium abscessus and Mycobacterium chelonae. J Antimicrob Chemother 66:1533–1536.
128. Viljoen A, Dubois V, Girard-Misguich F, Blaise M, Herrmann J-L, Kremer L. 2017. The diverse family of MmpL transporters in mycobacteria: from regulation to antimicrobial developments. Mol Microbiol 104:889–904.
129. Kapopoulou A, Lew JM, Cole ST. 2011. The MycoBrowser portal: a comprehensive and manually annotated resource for mycobacterial genomes. Tuberculosis (Edinb) 91:8–13.
130. Ripoll F, Pasek S, Schenowitz C, Dossat C, Barbe V, Rottman M, Macheras E, Heym B, Herrmann J-L, Daffé M, Brosch R, Risler J-L, Gaillard J-L. 2009. Non mycobacterial virulence genes in the genome of the emerging pathogen Mycobacterium abscessus. PLoS One 4:e5660.
131. Kim S-Y, Kim DH, Moon SM, Song JY, Huh HJ, Lee NY, Shin SJ, Koh W-J, Jhun BW. 2021. Association between 16S rRNA gene mutations and susceptibility to amikacin in Mycobacterium avium Complex and Mycobacterium abscessus clinical isolates. Sci Rep 11:6108.
132. Mougari F, Bouziane F, Crockett F, Nessar R, Chau F, Veziris N, Sapriel G, Raskine L, Cambau E. 2017. Selection of Resistance to Clarithromycin in Mycobacterium abscessus Subspecies. Antimicrob Agents Chemother 61.
133. Rominski A, Selchow P, Becker K, Brülle JK, Dal Molin M, Sander P. 2017. Elucidation of Mycobacterium abscessus aminoglycoside and capreomycin resistance by targeted deletion of three putative resistance genes. J Antimicrob Chemother 72:2191–2200.
134. Aínsa JA, Pérez E, Pelicic V, Berthet FX, Gicquel B, Martín C. 1997. Aminoglycoside 2'-N-acetyltransferase genes are universally present in

mycobacteria: characterization of the aac(2')-Ic gene from Mycobacterium tuberculosis and the aac(2')-Id gene from Mycobacterium smegmatis. Mol Microbiol 24:431–441.
135. Pricer RE, Houghton JL, Green KD, Mayhoub AS, Garneau-Tsodikova S. 2012. Biochemical and structural analysis of aminoglycoside acetyltransferase Eis from Anabaena variabilis. Mol Biosyst 8:3305–3313.
136. Ung KL, Alsarraf HMAB, Olieric V, Kremer L, Blaise M. 2019. Crystal structure of the aminoglycosides N-acetyltransferase Eis2 from Mycobacterium abscessus. FEBS J 286:4342–4355.
137. Hurst-Hess K, Rudra P, Ghosh P. 2017. Mycobacterium abscessus WhiB7 regulates a species-specific repertoire of genes to confer extreme antibiotic resistance. Antimicrob Agents Chemother 61.
138. Rodriguez R, Campbell-Kruger N, Gonzalez Camba J, Berude J, Fetterman R, Stanley SA. 2022. MarR-Dependent Transcriptional Regulation of mmpSL5 induces Ethionamide Resistance in Mycobacterium abscessus. BioRxiv. University of California, Berkeley.
139. Kertesz MA. 2001. Bacterial transporters for sulfate and organosulfur compounds. Res Microbiol 152:279–290.
140. Gangadharam PR, Cohn ML, Middlebrook G. 1963. Infectivity, pathogenicity and sulpholipid fraction of some Indian and British strains of tubercle bacilli. Tubercle 44:452–455.
141. Mougous JD, Senaratne RH, Petzold CJ, Jain M, Lee DH, Schelle MW, Leavell MD, Cox JS, Leary JA, Riley LW, Bertozzi CR. 2006. A sulfated metabolite produced by stf3 negatively regulates the virulence of Mycobacterium tuberculosis. Proc Natl Acad Sci U S A 103:4258–4263.
142. Gilleron M, Stenger S, Mazorra Z, Wittke F, Mariotti S, Böhmer G, Prandi J, Mori L, Puzo G, De Libero G. 2004. Diacylated sulfoglycolipids are novel mycobacterial antigens stimulating CD1-restricted T cells during infection with Mycobacterium tuberculosis. J Exp Med 199:649–659.
143. Schelle MW, Bertozzi CR. 2006. Sulfate metabolism in mycobacteria. ChemInform 37.
144. Ramón-García S, Ng C, Jensen PR, Dosanjh M, Burian J, Morris RP, Folcher M, Eltis LD, Grzesiek S, Nguyen L, Thompson CJ. 2013. WhiB7, an Fe-S-dependent transcription factor that activates species-specific repertoires of drug resistance determinants in actinobacteria. J Biol Chem 288:34514–34528.
145. Barquist L, Boinett CJ, Cain AK. 2013. Approaches to querying bacterial genomes with transposon-insertion sequencing. RNA Biol 10:1161–1169.
146. Koh W-J, Jeon K, Lee NY, Kim B-J, Kook Y-H, Lee S-H, Park YK, Kim CK, Shin SJ, Huitt GA, Daley CL, Kwon OJ. 2011. Clinical significance of differentiation of Mycobacterium massiliense from Mycobacterium abscessus. Am J Respir Crit Care Med 183:405–410.
147. Adékambi T, Berger P, Raoult D, Drancourt M. 2006. rpoB gene sequence-based characterization of emerging non-tuberculous mycobacteria with descriptions of

Mycobacterium bolletii sp. nov., Mycobacterium phocaicum sp. nov. and Mycobacterium aubagnense sp. nov. Int J Syst Evol Microbiol 56:133–143.
148. Adékambi T, Reynaud-Gaubert M, Greub G, Gevaudan M-J, La Scola B, Raoult D, Drancourt M. 2004. Amoebal coculture of “Mycobacterium massiliense” sp. nov. from the sputum of a patient with hemoptoic pneumonia. J Clin Microbiol 42:5493–5501.
149. Bastian S, Veziris N, Roux A-L, Brossier F, Gaillard J-L, Jarlier V, Cambau E. 2011. Assessment of clarithromycin susceptibility in strains belonging to the Mycobacterium abscessus group by erm(41) and rrl sequencing. Antimicrob Agents Chemother 55:775–781.
150. Nash KA, Brown-Elliott BA, Wallace RJ Jr. 2009. A novel gene, erm(41), confers inducible macrolide resistance to clinical isolates of Mycobacterium abscessus but is absent from Mycobacterium chelonae. Antimicrob Agents Chemother 53:1367–1376.
151. Goh BC, Xiang X, Lescar J, Dedon PC. 2022. Crystal structure and functional analysis of mycobacterial erythromycin resistance methyltransferase Erm38 reveals its RNA-binding site. J Biol Chem 298:101571.
152. Roux A-L, Catherinot E, Soismier N, Heym B, Bellis G, Lemonnier L, Chiron R, Fauroux B, Le Bourgeois M, Munck A, Pin I, Sermet I, Gutierrez C, Véziris N, Jarlier V, Cambau E, Herrmann J-L, Guillemot D, Gaillard J-L, OMA group. 2015. Comparing Mycobacterium massiliense and Mycobacterium abscessus lung infections in cystic fibrosis patients. J Cyst Fibros 14:63–69.
153. Zelazny AM, Root JM, Shea YR, Colombo RE, Shamputa IC, Stock F, Conlan S, McNulty S, Brown-Elliott BA, Wallace RJ Jr, Olivier KN, Holland SM, Sampaio EP. 2009. Cohort study of molecular identification and typing of Mycobacterium abscessus, Mycobacterium massiliense, and Mycobacterium bolletii. J Clin Microbiol 47:1985–1995.
154. Choi G-E, Shin SJ, Won C-J, Min K-N, Oh T, Hahn M-Y, Lee K, Lee SH, Daley CL, Kim S, Jeong B-H, Jeon K, Koh W-J. 2012. Macrolide treatment for Mycobacterium abscessus and Mycobacterium massiliense infection and inducible resistance. Am J Respir Crit Care Med 186:917–925.
155. Pryjma M, Burian J, Kuchinski K, Thompson CJ. 2017. Antagonism between front-line antibiotics clarithromycin and amikacin in the treatment of Mycobacterium abscessus infections is mediated by the whiB7 gene. Antimicrob Agents Chemother 61.
156. Soroka D, Dubée V, Soulier-Escrihuela O, Cuinet G, Hugonnet J-E, Gutmann L, Mainardi J-L, Arthur M. 2014. Characterization of broad-spectrum Mycobacterium abscessus class A β-lactamase. J Antimicrob Chemother 69:691–696.
157. Kohanski MA, Dwyer DJ, Collins JJ. 2010. How antibiotics kill bacteria: from targets to networks. Nat Rev Microbiol 8:423–435.
158. Lavollay M, Fourgeaud M, Herrmann J-L, Dubost L, Marie A, Gutmann L, Arthur M, Mainardi J-L. 2011. The peptidoglycan of Mycobacterium abscessus is predominantly cross-linked by L,D-transpeptidases. J Bacteriol 193:778–782.

159. Kumar P, Chauhan V, Silva JRA, Lameira J, d'Andrea FB, Li S-G, Ginell SL, Freundlich JS, Alves CN, Bailey S, Cohen KA, Lamichhane G. 2017. Mycobacterium abscessus l,d-transpeptidases are susceptible to inactivation by carbapenems and cephalosporins but not penicillins. Antimicrob Agents Chemother 61.
160. Dubée V, Triboulet S, Mainardi J-L, Ethève-Quelquejeu M, Gutmann L, Marie A, Dubost L, Hugonnet J-E, Arthur M. 2012. Inactivation of Mycobacterium tuberculosis l,d-transpeptidase $LdtMt_1$ by carbapenems and cephalosporins. Antimicrob Agents Chemother 56:4189–4195.
161. Kumar P, Kaushik A, Lloyd EP, Li S-G, Mattoo R, Ammerman NC, Bell DT, Perryman AL, Zandi TA, Ekins S, Ginell SL, Townsend CA, Freundlich JS, Lamichhane G. 2017. Non-classical transpeptidases yield insight into new antibacterials. Nat Chem Biol 13:54–61.
162. van Ingen J, Boeree MJ, van Soolingen D, Mouton JW. 2012. Resistance mechanisms and drug susceptibility testing of nontuberculous mycobacteria. Drug Resist Updat 15:149–161.
163. Nguyen L, Thompson CJ. 2006. Foundations of antibiotic resistance in bacterial physiology: the mycobacterial paradigm. Trends Microbiol 14:304–312.
164. Dubée V, Soroka D, Cortes M, Lefebvre A-L, Gutmann L, Hugonnet J-E, Arthur M, Mainardi J-L. 2015. Impact of β-lactamase inhibition on the activity of ceftaroline against Mycobacterium tuberculosis and Mycobacterium abscessus. Antimicrob Agents Chemother 59:2938–2941.
165. Rudra P, Hurst-Hess K, Lappierre P, Ghosh P. 2018. High levels of intrinsic tetracycline resistance in Mycobacterium abscessus are conferred by a tetracycline-modifying monooxygenase. Antimicrob Agents Chemother 62.
166. Cummings MP, Segal MR. 2004. Few amino acid positions in rpoB are associated with most of the rifampin resistance in Mycobacterium tuberculosis. BMC Bioinformatics 5:137.
167. Goldstein BP. 2014. Resistance to rifampicin: a review. J Antibiot (Tokyo) 67:625–630.
168. Rominski A, Roditscheff A, Selchow P, Böttger EC, Sander P. 2017. Intrinsic rifamycin resistance of Mycobacterium abscessus is mediated by ADP-ribosyltransferase MAB_0591. J Antimicrob Chemother 72:376–384.
169. Baysarowich J, Koteva K, Hughes DW, Ejim L, Griffiths E, Zhang K, Junop M, Wright GD. 2008. Rifamycin antibiotic resistance by ADP-ribosylation: Structure and diversity of Arr. Proc Natl Acad Sci U S A 105:4886–4891.
170. Surette MG. 2014. The cystic fibrosis lung microbiome. Ann Am Thorac Soc 11 Suppl 1:S61-5.
171. Rodríguez-Sevilla G, Crabbé A, García-Coca M, Aguilera-Correa JJ, Esteban J, Pérez-Jorge C. 2019. Antimicrobial Treatment Provides a Competitive Advantage to Mycobacterium abscessus in a Dual-Species Biofilm with Pseudomonas aeruginosa. Antimicrob Agents Chemother 63.
172. Layeux B, Taccone FS, Fagnoul D, Vincent J-L, Jacobs F. 2010. Amikacin monotherapy for sepsis caused by panresistant Pseudomonas aeruginosa. Antimicrob Agents Chemother 54:4939–4941.

173. Zhang H, Jia P, Zhu Y, Zhang G, Zhang J, Kang W, Duan S, Zhang W, Yang Q, Xu Y. 2021. Susceptibility to Imipenem/Relebactam of Pseudomonas aeruginosa and Acinetobacter baumannii Isolates from Chinese Intra-Abdominal, Respiratory and Urinary Tract Infections: SMART 2015 to 2018. Infect Drug Resist 14:3509–3518.
174. Melander RJ, Zurawski DV, Melander C. 2018. Narrow-spectrum antibacterial agents. Medchemcomm 9:12–21.
175. Obregón-Henao A, Arnett KA, Henao-Tamayo M, Massoudi L, Creissen E, Andries K, Lenaerts AJ, Ordway DJ. 2015. Susceptibility of Mycobacterium abscessus to antimycobacterial drugs in preclinical models. Antimicrob Agents Chemother 59:6904–6912.
176. Ruth MM, Sangen JJN, Remmers K, Pennings LJ, Svensson E, Aarnoutse RE, Zweijpfenning SMH, Hoefsloot W, Kuipers S, Magis-Escurra C, Wertheim HFL, van Ingen J. 2019. A bedaquiline/clofazimine combination regimen might add activity to the treatment of clinically relevant non-tuberculous mycobacteria. J Antimicrob Chemother 74:935–943.
177. Viljoen A, Raynaud C, Johansen MD, Roquet-Banères F, Herrmann J-L, Daher W, Kremer L. 2019. Verapamil improves the activity of bedaquiline against Mycobacterium abscessus in vitro and in macrophages. Antimicrob Agents Chemother 63.
178. van Ingen J, Totten SE, Helstrom NK, Heifets LB, Boeree MJ, Daley CL. 2012. In vitro synergy between clofazimine and amikacin in treatment of nontuberculous mycobacterial disease. Antimicrob Agents Chemother 56:6324–6327.
179. Yano T, Kassovska-Bratinova S, Teh JS, Winkler J, Sullivan K, Isaacs A, Schechter NM, Rubin H. 2011. Reduction of clofazimine by Mycobacterial type 2 NADH:Quinone oxidoreductase. J Biol Chem 286:10276–10287.
180. Vesenbeckh S, Schönfeld N, Roth A, Bettermann G, Krieger D, Bauer TT, Rüssmann H, Mauch H. 2017. Bedaquiline as a potential agent in the treatment of Mycobacterium abscessus infections. Eur Respir J 49:1700083.
181. Daley CL, Iaccarino JM, Lange C, Cambau E, Wallace RJ, Andrejak C, Böttger EC, Brozek J, Griffith DE, Guglielmetti L, Huitt GA, Knight SL, Leitman P, Marras TK, Olivier KN, Santin M, Stout JE, Tortoli E, van Ingen J, Wagner D, Winthrop KL. 2020. Treatment of nontuberculous Mycobacterial pulmonary disease: An official ATS/ERS/ESCMID/IDSA clinical practice guideline. Clin Infect Dis 71:905–913.
182. Zhao J, Siddiqui S, Shang S, Bian Y, Bagchi S, He Y, Wang C-R. 2015. Mycolic acid-specific T cells protect against Mycobacterium tuberculosis infection in a humanized transgenic mouse model. Elife 4.
183. Kalscheuer R, Weinrick B, Veeraraghavan U, Besra GS, Jacobs WR Jr. 2010. Trehalose-recycling ABC transporter LpqY-SugA-SugB-SugC is essential for virulence of Mycobacterium tuberculosis. Proc Natl Acad Sci U S A 107:21761–21766.
184. Marrakchi H, Lanéelle M-A, Daffé M. 2014. Mycolic acids: structures, biosynthesis, and beyond. Chem Biol 21:67–85.

185. Sani M, Houben ENG, Geurtsen J, Pierson J, de Punder K, van Zon M, Wever B, Piersma SR, Jiménez CR, Daffé M, Appelmelk BJ, Bitter W, van der Wel N, Peters PJ. 2010. Direct visualization by cryo-EM of the mycobacterial capsular layer: a labile structure containing ESX-1-secreted proteins. PLoS Pathog 6:e1000794.
186. Barry CE 3rd, Lee RE, Mdluli K, Sampson AE, Schroeder BG, Slayden RA, Yuan Y. 1998. Mycolic acids: structure, biosynthesis and physiological functions. Prog Lipid Res 37:143–179.
187. Gao L-Y, Laval F, Lawson EH, Groger RK, Woodruff A, Morisaki JH, Cox JS, Daffe M, Brown EJ. 2003. Requirement for kasB in Mycobacterium mycolic acid biosynthesis, cell wall impermeability and intracellular survival: implications for therapy. Mol Microbiol 49:1547–1563.
188. Barkan D, Liu Z, Sacchettini JC, Glickman MS. 2009. Mycolic acid cyclopropanation is essential for viability, drug resistance, and cell wall integrity of Mycobacterium tuberculosis. Chem Biol 16:499–509.
189. Lefebvre C, Boulon R, Ducoux M, Gavalda S, Laval F, Jamet S, Eynard N, Lemassu A, Cam K, Bousquet M-P, Bardou F, Burlet-Schiltz O, Daffé M, Quémard A. 2018. HadD, a novel fatty acid synthase type II protein, is essential for alpha- and epoxy-mycolic acid biosynthesis and mycobacterial fitness. Sci Rep 8.
190. Lefebvre C, Frigui W, Slama N, Lauzeral-Vizcaino F, Constant P, Lemassu A, Parish T, Eynard N, Daffé M, Brosch R, Quémard A. 2020. Discovery of a novel dehydratase of the fatty acid synthase type II critical for ketomycolic acid biosynthesis and virulence of Mycobacterium tuberculosis. Sci Rep 10:2112.
191. Halloum I, Carrère-Kremer S, Blaise M, Viljoen A, Bernut A, Le Moigne V, Vilchèze C, Guérardel Y, Lutfalla G, Herrmann J-L, Jacobs WR Jr, Kremer L. 2016. Deletion of a dehydratase important for intracellular growth and cording renders rough Mycobacterium abscessus avirulent. Proc Natl Acad Sci U S A 113:E4228-37.
192. Bloch K, Vance D. 1977. Control mechanisms in the synthesis of saturated fatty acids. Annu Rev Biochem 46:263–298.
193. Fernandes ND, Kolattukudy PE. 1996. Cloning, sequencing and characterization of a fatty acid synthase-encoding gene from Mycobacterium tuberculosis var. bovis BCG. Gene 170:95–99.
194. Gago G, Diacovich L, Arabolaza A, Tsai S-C, Gramajo H. 2011. Fatty acid biosynthesis in actinomycetes. FEMS Microbiol Rev 35:475–497.
195. Tropis M, Meniche X, Wolf A, Gebhardt H, Strelkov S, Chami M, Schomburg D, Krämer R, Morbach S, Daffé M. 2005. The crucial role of trehalose and structurally related oligosaccharides in the biosynthesis and transfer of mycolic acids in Corynebacterineae. J Biol Chem 280:26573–26585.
196. Grzegorzewicz AE, Pham H, Gundi VAKB, Scherman MS, North EJ, Hess T, Jones V, Gruppo V, Born SEM, Korduláková J, Chavadi SS, Morisseau C, Lenaerts AJ, Lee RE, McNeil MR, Jackson M. 2012. Inhibition of mycolic acid transport across the Mycobacterium tuberculosis plasma membrane. Nat Chem Biol 8:334–341.
197. Puech V, Bayan N, Salim K, Leblon G, Daffé M. 2000. Characterization of the in vivo acceptors of the mycoloyl residues transferred by the corynebacterial PS1 and the related mycobacterial antigens 85. Mol Microbiol 35:1026–1041.

198. Franz ND, Belardinelli JM, Kaminski MA, Dunn LC, Calado Nogueira de Moura V, Blaha MA, Truong DD, Li W, Jackson M, North EJ. 2017. Design, synthesis and evaluation of indole-2-carboxamides with pan anti-mycobacterial activity. Bioorg Med Chem 25:3746–3755.
199. Kozikowski AP, Onajole OK, Stec J, Dupont C, Viljoen A, Richard M, Chaira T, Lun S, Bishai W, Raj VS, Ordway D, Kremer L. 2017. Targeting mycolic acid transport by indole-2-carboxamides for the treatment of Mycobacterium abscessus infections. J Med Chem 60:5876–5888.
200. Lun S, Guo H, Onajole OK, Pieroni M, Gunosewoyo H, Chen G, Tipparaju SK, Ammerman NC, Kozikowski AP, Bishai WR. 2013. Indoleamides are active against drug-resistant Mycobacterium tuberculosis. Nat Commun 4:2907.
201. Rao SPS, Lakshminarayana SB, Kondreddi RR, Herve M, Camacho LR, Bifani P, Kalapala SK, Jiricek J, Ma NL, Tan BH, Ng SH, Nanjundappa M, Ravindran S, Seah PG, Thayalan P, Lim SH, Lee BH, Goh A, Barnes WS, Chen Z, Gagaring K, Chatterjee AK, Pethe K, Kuhen K, Walker J, Feng G, Babu S, Zhang L, Blasco F, Beer D, Weaver M, Dartois V, Glynne R, Dick T, Smith PW, Diagana TT, Manjunatha UH. 2013. Indolcarboxamide is a preclinical candidate for treating multidrug-resistant tuberculosis. Sci Transl Med 5:214ra168.
202. Li W, Yazidi A, Pandya AN, Hegde P, Tong W, Calado Nogueira de Moura V, North EJ, Sygusch J, Jackson M. 2018. MmpL3 as a target for the treatment of drug-resistant nontuberculous Mycobacterial infections. Front Microbiol 9.
203. Pandya AN, Prathipati PK, Hegde P, Li W, Graham KF, Mandal S, Drescher KM, Destache CJ, Ordway D, Jackson M, North EJ. 2019. Indole-2-carboxamides are active against Mycobacterium abscessus in a mouse model of acute infection. Antimicrob Agents Chemother 63.
204. Dupont C, Viljoen A, Dubar F, Blaise M, Bernut A, Pawlik A, Bouchier C, Brosch R, Guérardel Y, Lelièvre J, Ballell L, Herrmann J-L, Biot C, Kremer L. 2016. A new piperidinol derivative targeting mycolic acid transport in Mycobacterium abscessus. Mol Microbiol 101:515–529.
205. Costa-Gouveia J, Pancani E, Jouny S, Machelart A, Delorme V, Salzano G, Iantomasi R, Piveteau C, Queval CJ, Song O-R, Flipo M, Deprez B, Saint-André J-P, Hureaux J, Majlessi L, Willand N, Baulard A, Brodin P, Gref R. 2017. Combination therapy for tuberculosis treatment: pulmonary administration of ethionamide and booster co-loaded nanoparticles. Sci Rep 7.
206. Vilchèze C, Jacobs WR Jr. 2014. Resistance to Isoniazid and Ethionamide in Mycobacterium tuberculosis: Genes, Mutations, and Causalities. Microbiol Spectr 2:MGM2-0014–2013.
207. Baulard AR, Betts JC, Engohang-Ndong J, Quan S, McAdam RA, Brennan PJ, Locht C, Besra GS. 2000. Activation of the pro-drug ethionamide is regulated in mycobacteria. J Biol Chem 275:28326–28331.
208. Wang F, Langley R, Gulten G, Dover LG, Besra GS, Jacobs WR Jr, Sacchettini JC. 2007. Mechanism of thioamide drug action against tuberculosis and leprosy. J Exp Med 204:73–78.

209. Ushtanit A, Kulagina E, Mikhailova Y, Makarova M, Safonova S, Zimenkov D. 2022. Molecular determinants of ethionamide resistance in clinical isolates of Mycobacterium tuberculosis. Antibiotics (Basel) 11:133.
210. Chen I-MA, Chu K, Palaniappan K, Ratner A, Huang J, Huntemann M, Hajek P, Ritter SJ, Webb C, Wu D, Varghese NJ, Reddy TBK, Mukherjee S, Ovchinnikova G, Nolan M, Seshadri R, Roux S, Visel A, Woyke T, Eloe-Fadrosh EA, Kyrpides NC, Ivanova NN. 2022. The IMG/M data management and analysis system v.7: content updates and new features. Nucleic Acids Res https://doi.org/10.1093/nar/gkac976.
211. Mukherjee S, Stamatis D, Li CT, Ovchinnikova G, Bertsch J, Sundaramurthi JC, Kandimalla M, Nicolopoulos PA, Favognano A, Chen I-MA, Kyrpides NC, Reddy TBK. 2022. Twenty-five years of Genomes OnLine Database (GOLD): data updates and new features in v.9. Nucleic Acids Res https://doi.org/10.1093/nar/gkac974.
212. Cain AK, Barquist L, Goodman AL, Paulsen IT, Parkhill J, van Opijnen T. 2020. A decade of advances in transposon-insertion sequencing. Nat Rev Genet 21:526–540.
213. van Opijnen T, Bodi KL, Camilli A. 2009. Tn-seq: high-throughput parallel sequencing for fitness and genetic interaction studies in microorganisms. Nat Methods 6:767–772.
214. Chao MC, Abel S, Davis BM, Waldor MK. 2016. The design and analysis of transposon insertion sequencing experiments. Nat Rev Microbiol 14:119–128.
215. van Opijnen T, Camilli A. 2013. Transposon insertion sequencing: a new tool for systems-level analysis of microorganisms. Nat Rev Microbiol 11:435–442.
216. Gallagher LA, Shendure J, Manoil C. 2011. Genome-scale identification of resistance functions in Pseudomonas aeruginosa using Tn-seq. MBio 2:e00315-10.
217. Rajagopal M, Martin MJ, Santiago M, Lee W, Kos VN, Meredith T, Gilmore MS, Walker S. 2016. Multidrug intrinsic resistance factors in Staphylococcus aureus identified by profiling fitness within high-diversity transposon libraries. MBio 7.
218. Philalay JS, Palermo CO, Hauge KA, Rustad TR, Cangelosi GA. 2004. Genes Required for Intrinsic Multidrug Resistance in Mycobacterium avium. Antimicrob Agents Chemother 48:3412–3418.
219. Foreman M, Gershoni M, Barkan D. 2020. A simplified and efficient method for Himar-1 transposon sequencing in bacteria, demonstrated by creation and analysis of a saturated transposon-mutant library in Mycobacterium abscessus. mSystems 5.
220. Akusobi C, Benghomari BS, Zhu J, Wolf ID, Singhvi S, Dulberger CL, Ioerger TR, Rubin EJ. 2022. Transposon mutagenesis in Mycobacterium abscessus identifies an essential penicillin-binding protein involved in septal peptidoglycan synthesis and antibiotic sensitivity. Elife 11.
221. Rifat D, Chen L, Kreiswirth BN, Nuermberger EL. 2021. Genome-wide essentiality analysis of Mycobacterium abscessus by saturated transposon Mutagenesis and deep sequencing. MBio 12:e0104921.
222. Sullivan MR, McGowen K, Liu Q, Akusobi C. 2022. Cell envelope remodeling requires high concentrations of biotin during Mycobacterium abscessus model lung infection. bioRxiv.

223. Köser CU, Ellington MJ, Peacock SJ. 2014. Whole-genome sequencing to control antimicrobial resistance. Trends Genet 30:401–407.
224. Metcalf BJ, Chochua S, Gertz RE Jr, Li Z, Walker H, Tran T, Hawkins PA, Glennen A, Lynfield R, Li Y, McGee L, Beall B, Active Bacterial Core surveillance team. 2016. Using whole genome sequencing to identify resistance determinants and predict antimicrobial resistance phenotypes for year 2015 invasive pneumococcal disease isolates recovered in the United States. Clin Microbiol Infect 22:1002.e1-1002.e8.
225. Mouftah SF, Cobo-Díaz JF, Álvarez-Ordóñez A, Elserafy M, Saif NA, Sadat A, El-Shibiny A, Elhadidy M. 2021. High-throughput sequencing reveals genetic determinants associated with antibiotic resistance in Campylobacter spp. from farm-to-fork. PLoS One 16:e0253797.
226. Richard M, Gutiérrez AV, Viljoen A, Rodriguez-Rincon D, Roquet-Baneres F, Blaise M, Everall I, Parkhill J, Floto RA, Kremer L. 2019. Mutations in the MAB_2299c TetR regulator confer cross-resistance to clofazimine and bedaquiline in Mycobacterium abscessus. Antimicrob Agents Chemother 63.
227. Sassetti CM, Boyd DH, Rubin EJ. 2001. Comprehensive identification of conditionally essential genes in mycobacteria. Proc Natl Acad Sci U S A 98:12712–12717.
228. Medjahed H, Singh AK. 2010. Genetic manipulation of Mycobacterium abscessus. Curr Protoc Microbiol Chapter 10:Unit 10D.2.
229. Long JE, DeJesus M, Ward D, Baker RE, Ioerger T, Sassetti CM. 2015. Identifying essential genes in Mycobacterium tuberculosis by global phenotypic profiling. Methods Mol Biol 1279:79–95.
230. DeJesus MA, Ambadipudi C, Baker R, Sassetti C, Ioerger TR. 2015. TRANSIT--A software tool for Himar1 TnSeq analysis. PLoS Comput Biol 11:e1004401.
231. Nolan CM. 2003. Isoniazid for latent tuberculosis infection: approaching 40 and reaching its prime. Am J Respir Crit Care Med. American Thoracic Society.
232. Vilchèze C, Wang F, Arai M, Hazbón MH, Colangeli R, Kremer L, Weisbrod TR, Alland D, Sacchettini JC, Jacobs WR Jr. 2006. Transfer of a point mutation in Mycobacterium tuberculosis inhA resolves the target of isoniazid. Nat Med 12:1027–1029.
233. Heysell SK, Pholwat S, Mpagama SG, Pazia SJ, Kumburu H, Ndusilo N, Gratz J, Houpt ER, Kibiki GS. 2015. Sensititre MycoTB plate compared to Bactec MGIT 960 for first- and second-line antituberculosis drug susceptibility testing in Tanzania: a call to operationalize MICs. Antimicrob Agents Chemother 59:7104–7108.
234. Wallace RJ, Philley JV, & Griffith D. E. 2015. 38 - Antimycobacterial Agents, p. 463–478. *In* Bennett, JE, Dolin, R, & Blaser, MJ (eds.), Mandell, Douglas, and Bennett's Principles and Practice of Infectious Diseases.
235. Agarwal A, Maloney RW. 2011. Mycobacterium abscessus outbreak after rhytidectomies performed in an outpatient surgery center. Plast Reconstr Surg 128:85e–86e.
236. Gonzalez-Juarrero M, Hattle JM, Izzo A, Junqueira-Kipnis AP, Shim TS, Trapnell BC, Cooper AM, Orme IM. 2005. Disruption of granulocyte macrophage-colony

stimulating factor production in the lungs severely affects the ability of mice to control Mycobacterium tuberculosis infection. J Leukoc Biol 77:914–922.
237. De Groote MA, Johnson L, Podell B, Brooks E, Basaraba R, Gonzalez-Juarrero M. 2014. GM-CSF knockout mice for preclinical testing of agents with antimicrobial activity against Mycobacterium abscessus. J Antimicrob Chemother 69:1057–1064.
238. Shen Y, Wang X, Jin J, Wu J, Zhang X, Chen J, Zhang W. 2018. In Vitro Susceptibility of Mycobacterium abscessus and Mycobacterium fortuitum Isolates to 30 Antibiotics. Biomed Res Int 2018:4902941.
239. Wankar J, Salzano G, Pancani E, Benkovics G, Malanga M, Manoli F, Gref R, Fenyvesi E, Manet I. 2017. Efficient loading of ethionamide in cyclodextrin-based carriers offers enhanced solubility and inhibition of drug crystallization. Int J Pharm 531:568–576.
240. Cuthbertson L, Nodwell JR. 2013. The TetR family of regulators. Microbiol Mol Biol Rev 77:440–475.
241. Morlock GP, Metchock B, Sikes D, Crawford JT, Cooksey RC. 2003. ethA, inhA, and katG loci of ethionamide-resistant clinical Mycobacterium tuberculosis isolates. Antimicrob Agents Chemother 47:3799–3805.
242. Cohen SP, McMurry LM, Hooper DC, Wolfson JS, Levy SB. 1989. Cross-resistance to fluoroquinolones in multiple-antibiotic-resistant (Mar) Escherichia coli selected by tetracycline or chloramphenicol: decreased drug accumulation associated with membrane changes in addition to OmpF reduction. Antimicrob Agents Chemother 33:1318–1325.
243. Kotecka K, Kawalek A, Kobylecki K, Bartosik AA. 2021. The MarR-type regulator PA3458 is involved in osmoadaptation control in Pseudomonas aeruginosa. Int J Mol Sci 22:3982.
244. Ziha-Zarifi I, Llanes C, Köhler T, Pechere J-C, Plesiat P. 1999. In vivo emergence of multidrug-resistant mutants of Pseudomonas aeruginosa overexpressing the active efflux system MexA-MexB-OprM. Antimicrob Agents Chemother 43:287–291.
245. Ehrt S, Guo XV, Hickey CM, Ryou M, Monteleone M, Riley LW, Schnappinger D. 2005. Controlling gene expression in mycobacteria with anhydrotetracycline and Tet repressor. Nucleic Acids Res 33:e21.
246. Sadeghi K, Hamishehkar H, Najmeddin F, Ahmadi A, Hazrati E, Honarmand H, Mojtahedzadeh M. 2018. High-dose amikacin for achieving serum target levels in critically ill elderly patients. Infect Drug Resist 11:223–228.
247. Rodvold KA. 1999. Clinical pharmacokinetics of clarithromycin. Clin Pharmacokinet 37:385–398.
248. Heinrichs MT, Vashakidze S, Nikolaishvili K, Sabulua I, Tukvadze N, Bablishvili N, Gogishvili S, Little BP, Bernheim A, Guarner J, Peloquin CA, Blumberg HM, Derendorf H, Kempker RR. 2018. Moxifloxacin target site concentrations in patients with pulmonary TB utilizing microdialysis: a clinical pharmacokinetic study. J Antimicrob Chemother 73:477–483.
249. Blondiaux N, Moune M, Desroses M, Frita R, Flipo M, Mathys V, Soetaert K, Kiass M, Delorme V, Djaout K, Trebosc V, Kemmer C, Wintjens R, Wohlkönig A, Antoine R, Huot L, Hot D, Coscolla M, Feldmann J, Gagneux S, Locht C, Brodin P, Gitzinger

M, Déprez B, Willand N, Baulard AR. 2017. Reversion of antibiotic resistance in Mycobacterium tuberculosis by spiroisoxazoline SMARt-420. Science 355:1206–1211.
250. Chubiz LM, Rao CV. 2010. Aromatic acid metabolites of Escherichia coli K-12 can induce the marRAB operon. J Bacteriol 192:4786–4789.
251. Sharma P, Haycocks JRJ, Middlemiss AD, Kettles RA, Sellars LE, Ricci V, Piddock LJV, Grainger DC. 2017. The multiple antibiotic resistance operon of enteric bacteria controls DNA repair and outer membrane integrity. Nat Commun 8:1444.
252. Altschul SF, Gish W, Miller W, Myers EW, Lipman DJ. 1990. Basic local alignment search tool. J Mol Biol 215:403–410.
253. Melly G, Purdy GE. 2019. MmpL Proteins in Physiology and Pathogenesis of M. tuberculosis. Microorganisms 7:70.
254. Wells RM, Jones CM, Xi Z, Speer A, Danilchanka O, Doornbos KS, Sun P, Wu F, Tian C, Niederweis M. 2013. Discovery of a siderophore export system essential for virulence of Mycobacterium tuberculosis. PLoS Pathog 9:e1003120.
255. Mukherjee D, Wu M-L, Teo JWP, Dick T. 2017. Vancomycin and clarithromycin show synergy against Mycobacterium abscessus in vitro. Antimicrob Agents Chemother 61.
256. Murphy KC, Nelson SJ, Nambi S, Papavinasasundaram K, Baer CE, Sassetti CM. 2018. ORBIT: A new paradigm for genetic engineering of Mycobacterial chromosomes. MBio 9.
257. Andreu N, Zelmer A, Fletcher T, Elkington PT, Ward TH, Ripoll J, Parish T, Bancroft GJ, Schaible U, Robertson BD, Wiles S. 2010. Optimisation of bioluminescent reporters for use with mycobacteria. PLoS One 5:e10777.
258. Schindler BD, Kaatz GW. 2016. Multidrug efflux pumps of Gram-positive bacteria. Drug Resist Updat 27:1–13.
259. Blair JMA, Richmond GE, Piddock LJV. 2014. Multidrug efflux pumps in Gram-negative bacteria and their role in antibiotic resistance. Future Microbiol 9:1165–1177.
260. Yamasaki S, Wang L-Y, Hirata T, Hayashi-Nishino M, Nishino K. 2015. Multidrug efflux pumps contribute to Escherichia coli biofilm maintenance. Int J Antimicrob Agents 45:439–441.
261. Bay DC, Stremick CA, Slipski CJ, Turner RJ. 2017. Secondary multidrug efflux pump mutants alter Escherichia coli biofilm growth in the presence of cationic antimicrobial compounds. Res Microbiol 168:208–221.
262. Nies DH. 2003. Efflux-mediated heavy metal resistance in prokaryotes. FEMS Microbiol Rev 27:313–339.
263. Conroy O, Kim E-H, McEvoy MM, Rensing C. 2010. Differing ability to transport nonmetal substrates by two RND-type metal exporters. FEMS Microbiol Lett 308:115–122.
264. Yang S, Lopez CR, Zechiedrich EL. 2006. Quorum sensing and multidrug transporters in Escherichia coli. Proc Natl Acad Sci U S A 103:2386–2391.
265. Alav I, Sutton JM, Rahman KM. 2018. Role of bacterial efflux pumps in biofilm formation. J Antimicrob Chemother 73:2003–2020.

266. Venter H, Mowla R, Ohene-Agyei T, Ma S. 2015. RND-type drug efflux pumps from Gram-negative bacteria: molecular mechanism and inhibition. Front Microbiol 6:377.
267. UniProt Consortium. 2022. UniProt: The universal protein knowledgebase in 2023. Nucleic Acids Res https://doi.org/10.1093/nar/gkac1052.
268. Masuda N, Sakagawa E, Ohya S, Gotoh N, Tsujimoto H, Nishino T. 2000. Substrate specificities of MexAB-OprM, MexCD-OprJ, and MexXY-oprM efflux pumps in Pseudomonas aeruginosa. Antimicrob Agents Chemother 44:3322–3327.
269. Xu C, Bilya SR, Xu W. 2019. adeABC efflux gene in Acinetobacter baumannii. New Microbes New Infect 30:100549.
270. Ohneck EA, Zalucki YM, Johnson PJT, Dhulipala V, Golparian D, Unemo M, Jerse AE, Shafer WM. 2011. A novel mechanism of High-Level, broad-spectrum antibiotic resistance caused by a single base pair change in Neisseria gonorrhoeae. MBio 2.
271. Aires JR, Nikaido H. 2005. Aminoglycosides are captured from both periplasm and cytoplasm by the AcrD multidrug efflux transporter of Escherichia coli. J Bacteriol 187:1923–1929.
272. Masuda N, Gotoh N, Ohya S, Nishino T. 1996. Quantitative correlation between susceptibility and OprJ production in NfxB mutants of Pseudomonas aeruginosa. Antimicrob Agents Chemother 40:909–913.
273. Sobel ML, Neshat S, Poole K. 2005. Mutations in PA2491 (mexS) promote MexT-dependent mexEF-oprN expression and multidrug resistance in a clinical strain of Pseudomonas aeruginosa. J Bacteriol 187:1246–1253.
274. Köhler T, Michéa-Hamzehpour M, Henze U, Gotoh N, Curty LK, Pechère JC. 1997. Characterization of MexE-MexF-OprN, a positively regulated multidrug efflux system of Pseudomonas aeruginosa. Mol Microbiol 23:345–354.
275. Lin C-W, Huang Y-W, Hu R-M, Yang T-C. 2014. SmeOP-TolCSm efflux pump contributes to the multidrug resistance of Stenotrophomonas maltophilia. Antimicrob Agents Chemother 58:2405–2408.
276. Chan BK, Sistrom M, Wertz JE, Kortright KE, Narayan D, Turner PE. 2016. Phage selection restores antibiotic sensitivity in MDR Pseudomonas aeruginosa. Sci Rep 6:26717.
277. Bador J, Neuwirth C, Grangier N, Muniz M, Germé L, Bonnet J, Pillay V-G, Llanes C, de Curraize C, Amoureux L. 2017. Role of AxyZ transcriptional regulator in overproduction of AxyXY-OprZ multidrug efflux system in Achromobacter species mutants selected by tobramycin. Antimicrob Agents Chemother 61.
278. Blanco P, Corona F, Martínez JL. 2019. Involvement of the RND efflux pump transporter SmeH in the acquisition of resistance to ceftazidime in Stenotrophomonas maltophilia. Sci Rep 9:4917.
279. Ma D, Alberti M, Lynch C, Nikaido H, Hearst JE. 1996. The local repressor AcrR plays a modulating role in the regulation of acrAB genes of Escherichia coli by global stress signals. Mol Microbiol 19:101–112.
280. Lucas CE, Balthazar JT, Hagman KE, Shafer WM. 1997. The MtrR repressor binds the DNA sequence between the mtrR and mtrC genes of Neisseria gonorrhoeae. J Bacteriol 179:4123–4128.

281. Beggs GA, Brennan RG, Arshad M. 2020. MarR family proteins are important regulators of clinically relevant antibiotic resistance. Protein Sci 29:647–653.
282. Dabul ANG, Avaca-Crusca JS, Van Tyne D, Gilmore MS, Camargo ILBC. 2018. Resistance in in vitro selected tigecycline-resistant methicillin-resistant Staphylococcus aureus Sequence Type 5 is driven by mutations in mepR and mepA genes. Microb Drug Resist 24:519–526.
283. McAleese F, Petersen P, Ruzin A, Dunman PM, Murphy E, Projan SJ, Bradford PA. 2005. A novel MATE family efflux pump contributes to the reduced susceptibility of laboratory-derived Staphylococcus aureus mutants to tigecycline. Antimicrob Agents Chemother 49:1865–1871.
284. Okusu H, Ma D, Nikaido H. 1996. AcrAB efflux pump plays a major role in the antibiotic resistance phenotype of Escherichia coli multiple-antibiotic-resistance (Mar) mutants. J Bacteriol 178:306–308.
285. Luke RK, Gibson F. 1971. Location of three genes concerned with the conversion of 2,3-dihydroxybenzoate into enterochelin in Escherichia coli K-12. J Bacteriol 107:557–562.
286. Young IG, Langman L, Luke RK, Gibson F. 1971. Biosynthesis of the iron-transport compound enterochelin: mutants of Escherichia coli unable to synthesize 2,3-dihydroxybenzoate. J Bacteriol 106:51–57.
287. Raymond KN, Dertz EA, Kim SS. 2003. Enterobactin: an archetype for microbial iron transport. Proc Natl Acad Sci U S A 100:3584–3588.
288. Ruiz C, Levy SB. 2014. Regulation of acrAB expression by cellular metabolites in Escherichia coli. J Antimicrob Chemother 69:390–399.
289. Li X-Z, Nikaido H. 2004. Efflux-mediated drug resistance in bacteria. Drugs 64:159–204.
290. Blair JMA, Piddock LJV. 2009. Structure, function and inhibition of RND efflux pumps in Gram-negative bacteria: an update. Curr Opin Microbiol 12:512–519.
291. Sulavik MC, Houseweart C, Cramer C, Jiwani N, Murgolo N, Greene J, DiDomenico B, Shaw KJ, Miller GH, Hare R, Shimer G. 2001. Antibiotic susceptibility profiles of Escherichia coli strains lacking multidrug efflux pump genes. Antimicrob Agents Chemother 45:1126–1136.
292. Nishino K, Yamaguchi A. 2001. Analysis of a complete library of putative drug transporter genes in Escherichia coli. J Bacteriol 183:5803–5812.
293. Shyam M, Shilkar D, Verma H, Dev A, Sinha BN, Brucoli F, Bhakta S, Jayaprakash V. 2021. The mycobactin biosynthesis pathway: A prospective therapeutic target in the battle against tuberculosis. J Med Chem 64:71–100.
294. Andries K, Villellas C, Coeck N, Thys K, Gevers T, Vranckx L, Lounis N, de Jong BC, Koul A. 2014. Acquired resistance of Mycobacterium tuberculosis to bedaquiline. PLoS One 9:e102135.
295. Hartkoorn RC, Uplekar S, Cole ST. 2014. Cross-resistance between clofazimine and bedaquiline through upregulation of MmpL5 in Mycobacterium tuberculosis. Antimicrob Agents Chemother 58:2979–2981.
296. Bythrow GV, Farhat MF, Levendosky K, Mohandas P, Germain GA, Yoo B, Quadri LEN. 2022. Mycobacterium abscessus mutants with a compromised functional link

between the type VII ESX-3 system and an iron uptake mechanism reliant on an unusual mycobactin siderophore. Pathogens 11:953.
297. Chun J, Goodfellow M. 1995. A phylogenetic analysis of the genus Nocardia with 16S rRNA gene sequences. Int J Syst Bacteriol 45:240–245.
298. Poelarends GJ, Mazurkiewicz P, Konings WN. 2002. Multidrug transporters and antibiotic resistance in Lactococcus lactis. Biochim Biophys Acta Bioenerg 1555:1–7.
299. Rodrigues L, Machado D, Couto I, Amaral L, Viveiros M. 2012. Contribution of efflux activity to isoniazid resistance in the Mycobacterium tuberculosis complex. Infect Genet Evol 12:695–700.
300. Gibbons S, Udo EE. 2000. The effect of reserpine, a modulator of multidrug efflux pumps, on the in vitro activity of tetracycline against clinical isolates of methicillin resistant Staphylococcus aureus (MRSA) possessing the tet(K) determinant. Phytother Res 14:139–140.
301. Colangeli R, Helb D, Sridharan S, Sun J, Varma-Basil M, Hazbón MH, Harbacheuski R, Megjugorac NJ, Jacobs WR Jr, Holzenburg A, Sacchettini JC, Alland D. 2005. The Mycobacterium tuberculosis iniA gene is essential for activity of an efflux pump that confers drug tolerance to both isoniazid and ethambutol. Mol Microbiol 55:1829–1840.
302. Viveiros M, Portugal I, Bettencourt R, Victor TC, Jordaan AM, Leandro C, Ordway D, Amaral L. 2002. Isoniazid-induced transient high-level resistance in Mycobacterium tuberculosis. Antimicrob Agents Chemother 46:2804–2810.
303. Louw GE, Warren RM, Gey van Pittius NC, Leon R, Jimenez A, Hernandez-Pando R, McEvoy CRE, Grobbelaar M, Murray M, van Helden PD, Victor TC. 2011. Rifampicin reduces susceptibility to ofloxacin in rifampicin-resistant Mycobacterium tuberculosis through efflux. Am J Respir Crit Care Med 184:269–276.
304. Zhang Y, Scorpio A, Nikaido H, Sun Z. 1999. Role of acid pH and deficient efflux of pyrazinoic acid in unique susceptibility of Mycobacterium tuberculosis to pyrazinamide. J Bacteriol 181:2044–2049.
305. Zhang Y, Permar S, Sun Z. 2002. Conditions that may affect the results of susceptibility testing of Mycobacterium tuberculosis to pyrazinamide. J Med Microbiol 51:42–49.
306. Gupta S, Tyagi S, Almeida DV, Maiga MC, Ammerman NC, Bishai WR. 2013. Acceleration of tuberculosis treatment by adjunctive therapy with verapamil as an efflux inhibitor. Am J Respir Crit Care Med 188:600–607.
307. Rodrigues L, Villellas C, Bailo R, Viveiros M, Aínsa JA. 2013. Role of the Mmr efflux pump in drug resistance in Mycobacterium tuberculosis. Antimicrob Agents Chemother 57:751–757.
308. Pule CM, Sampson SL, Warren RM, Black PA, van Helden PD, Victor TC, Louw GE. 2016. Efflux pump inhibitors: targeting mycobacterial efflux systems to enhance TB therapy. J Antimicrob Chemother 71:17–26.
309. Ahmed M, Borsch CM, Neyfakh AA, Schuldiner S. 1993. Mutants of the Bacillus subtilis multidrug transporter Bmr with altered sensitivity to the antihypertensive alkaloid reserpine. J Biol Chem 268:11086–11089.

310. Chen C, Gardete S, Jansen RS, Shetty A, Dick T, Rhee KY, Dartois V. 2018. Verapamil Targets Membrane Energetics in Mycobacterium tuberculosis. Antimicrob Agents Chemother 62.
311. Gupta S, Cohen KA, Winglee K, Maiga M, Diarra B, Bishai WR. 2014. Efflux inhibition with verapamil potentiates bedaquiline in Mycobacterium tuberculosis. Antimicrob Agents Chemother 58:574–576.
312. Ramón-García S, Martín C, Aínsa JA, De Rossi E. 2006. Characterization of tetracycline resistance mediated by the efflux pump Tap from Mycobacterium fortuitum. J Antimicrob Chemother 57:252–259.
313. Pasca MR, Guglierame P, Arcesi F, Bellinzoni M, De Rossi E, Riccardi G. 2004. Rv2686c-Rv2687c-Rv2688c, an ABC Fluoroquinolone Efflux Pump in Mycobacterium tuberculosis. Antimicrob Agents Chemother 48:3175–3178.
314. Van Bambeke F, Pagès J-M, Lee VJ. 2006. Inhibitors of bacterial efflux pumps as adjuvants in antibiotic treatments and diagnostic tools for detection of resistance by efflux. Recent Pat Antiinfect Drug Discov 1:157–175.
315. Kundu S, Biukovic G, Grüber G, Dick T. 2016. Bedaquiline targets the ε subunit of Mycobacterial F-ATP synthase. Antimicrob Agents Chemother 60:6977–6979.
316. Rodrigues L, Ramos J, Couto I, Amaral L, Viveiros M. 2011. Ethidium bromide transport across Mycobacterium smegmatis cell-wall: correlation with antibiotic resistance. BMC Microbiol 11:35.
317. Cortes MAM, Nessar R, Singh AK. 2010. Laboratory maintenance of Mycobacterium abscessus. Curr Protoc Microbiol Chapter 10:Unit 10D.1.
318. Zhang T, Jiang G, Wen S, Huo F, Wang F, Huang H, Pang Y. 2019. Para-aminosalicylic acid increases the susceptibility to isoniazid in clinical isolates of Mycobacterium tuberculosis. Infect Drug Resist 12:825–829.
319. Nagachar N, Ratledge C. 2010. Knocking out salicylate biosynthesis genes in Mycobacterium smegmatis induces hypersensitivity to p-aminosalicylate (PAS). FEMS Microbiol Lett 311:193–199.
320. Ratledge C, Brown KA. 1972. Inhibition of mycobactin formation in Mycobacterium smegmatis by p-aminosalicylate. A new proposal for the mode of action of p-aminosalicylate. Am Rev Respir Dis 106:774–776.
321. Adilakshmi T, Ayling PD, Ratledge C. 2000. Mutational analysis of a role for salicylic acid in iron metabolism of Mycobacterium smegmatis. J Bacteriol 182:264–271.
322. Siegrist MS, Unnikrishnan M, McConnell MJ, Borowsky M, Cheng T-Y, Siddiqi N, Fortune SM, Moody DB, Rubin EJ. 2009. Mycobacterial Esx-3 is required for mycobactin-mediated iron acquisition. Proc Natl Acad Sci U S A 106:18792–18797.
323. Kingston H, Pella PA. 1981. Preconcentration of trace metals in environmental and biological samples by cation exchange resin filters for X-ray spectrometry. Anal Chem 53:223–227.
324. 2012. Characterization of the Chesapeake bay systematic analysis of toxic trace elements. Bibliogov.
325. Oliveira FM, Da Costa AC, Procopio VO, Garcia W, Araújo JN, Da Silva RA, Junqueira-Kipnis AP, Kipnis A. 2018. Mycobacterium abscessus subsp. massiliense

mycma_0076 and mycma_0077 Genes Code for Ferritins That Are Modulated by Iron Concentration. Front Microbiol 9:1072.
326. Merino E, Jensen RA, Yanofsky C. 2008. Evolution of bacterial trp operons and their regulation. Curr Opin Microbiol 11:78–86.
327. Libardo MDJ, Duncombe CJ, Green SR, Wyatt PG, Thompson S, Ray PC, Ioerger TR, Oh S, Goodwin MB, Boshoff HIM, Barry CE 3rd. 2021. Resistance of Mycobacterium tuberculosis to indole 4-carboxamides occurs through alterations in drug metabolism and tryptophan biosynthesis. Cell Chem Biol 28:1180-1191.e20.
328. Perera IC, Grove A. 2010. Molecular mechanisms of ligand-mediated attenuation of DNA binding by MarR family transcriptional regulators. J Mol Cell Biol 2:243–254.
329. Sharma A, Gupta VK, Pathania R. 2019. Efflux pump inhibitors for bacterial pathogens: From bench to bedside. Indian J Med Res 149:129–145.
330. Sennhauser G, Bukowska MA, Briand C, Grütter MG. 2009. Crystal structure of the multidrug exporter MexB from Pseudomonas aeruginosa. J Mol Biol 389:134–145.
331. Hu H, Wang L, Wang W, Wu G, Tao F, Xu P, Deng Z, Tang H. 2019. Regulatory Mechanism of Nicotine Degradation in Pseudomonas putida. MBio 10.
332. Vatlin AA, Shitikov EA, Shahbaaz M, Bespiatykh DA, Klimina KM, Christoffels A, Danilenko VN, Maslov DA. 2021. Transcriptomic profile of Mycobacterium smegmatis in response to an imidazo[1,2-b][1,2,4,5]tetrazine reveals its possible impact on iron metabolism. Front Microbiol 12:724042.
333. Banerjee A, Dubnau E, Quemard A, Balasubramanian V, Um KS, Wilson T, Collins D, de Lisle G, Jacobs WR Jr. 1994. inhA, a gene encoding a target for isoniazid and ethionamide in Mycobacterium tuberculosis. Science 263:227–230.
334. Kruh NA, Rawat R, Ruzsicska BP, Tonge PJ. 2007. Probing mechanisms of resistance to the tuberculosis drug isoniazid: Conformational changes caused by inhibition of InhA, the enoyl reductase from Mycobacterium tuberculosis. Protein Sci 16:1617–1627.
335. Slayden RA, Barry CE 3rd. 2001. Analysis of the lipids of Mycobacterium tuberculosis. Methods Mol Med 54:229–245.
336. Fiolek TJ, Banahene N, Kavunja HW, Holmes NJ, Rylski AK, Pohane AA, Siegrist MS, Swarts BM. 2019. Engineering the mycomembrane of live mycobacteria with an expanded set of trehalose monomycolate analogues. Chembiochem 20:1282–1291.